Examining Regional Differences in the Gut Microbiota and Their Effects on *Clostridioides difficile* Colonization Resistance

by

Matthew K. Schnizlein

A dissertation submitted in partial fulfillment
of the requirements for the degree of
Doctor of Philosophy
(Microbiology and Immunology)
in the University of Michigan
2022

Doctoral Committee:

Professor Vincent B. Young, Chair
Professor Mary X. O'Riordan
Professor Thomas Schmidt
Assistant Professor Evan Snitkin
Professor Duxin Sun

Matthew K. Schnizlein

mschnizl@umich.edu

ORCID iD: 0000-0002-0797-8357

Dedication

For my family and friends,

you have helped make this dissertation possible

Acknowledgements

I would like to thank the many people who have invested in my life up until this point to make me the person and scientist that I am. I have been blessed to have folks pour into my life throughout its many stages. At Northern Illinois University, Dr. Wesley Swingley first inspired my interest in microbial ecology (and increased that already present for board games). Dr. Jozef Bujarski, Ola Bujarska as well as Drs. Nipin Shrestha and Philipp Weber walked with me as I first began to explore research on a regular basis as we grew plants and infected them with viruses.

I treasure the many outstanding scientists with whom I had the privilege to interact with during my research summers. Drs. Scott Weaver, Rose Langsjoen and Nick Bergren at the University of Texas Medical Branch-Galveston gave me my first taste of the research lab and Drs. David Fredricks and Sujatha Srinivasan as well as Christina Kohler, at the Fred Hutchinson Cancer Research Center, my first taste of what it is like working in the realm of the human microbiome. These individuals have played a large role in figuring out what area of research I wanted to pursue and ultimately my decision to attend the University of Michigan-Ann Arbor for my Ph.D.

Many thanks to my committee members, Drs. Mary O'Riordan, Tom Schmidt, Evan Snitkin and Duxin Sun, who have helped me think creatively about my thesis project over the years. I would like to especially thank Tom and Duxin as my project has intersected more specifically with the work of your labs and have found those interactions stimulating

and helpful. Collaborating with your lab members has been very influential in bringing my thesis to where it is today. I would like to specifically thank Austin Campbell, Kwi Kim, Steve Stoddard, Ruiting Li, Bo Wen and Praveen Kumar.

Vincent Young has been an outstanding advisor whose guidance took me from the uncertainties of my first year to the confidence on my sixth. When I first met Vince, I was immediately impressed by the nature of the questions he would ask during our conversations. While these were at times the bane of my existence, they challenged me to think more deeply about my research and approach questions from new angles. The support and connections he has offered to me as I pursue a non-R1 institution academic path has been very valuable. If it weren't for him, I would not be the scientist I am today.

All my colleagues in the Young Lab have made my Ph.D. a pleasure, particularly when experiments weren't treating me kindly. Krishna Rao and Jonathan Golob, your grasp of statistics and data analysis methods is stunning, having your input on aspects of my project have been quite valuable over the years. Kim Vendrov, thank you for all the advice on mouse handling and being there to answer the random questions that come up due to being my officemate for the last few years. Alex Standke, it has truly been great working with you on the bioreactors. When things leak and make huge messes, it made things a bit better to have someone with whom to laugh about it as we cleaned things up. Summer Edwards and Mark Garmo, I very much enjoyed the opportunity to mentor you during your stints in the Young Lab and wish you all the best as you continue on towards your career goals! Anna Seekatz, your guidance as I navigated the postdoc search and as I published my first first-author paper was invaluable. Maddie Barron, commiserating

with you as we each wrote our dissertations has made this a much more palatable process.

The 2016 Microbiology and Immunology Ph.D. cohort: Anna-Lisa Lawrence, Austin Campbell, Yolanda Rivera-Cuevas, Stephanie Thiede and Edmond Atindaana as well as honorary members Zack Mendel and Zena Lapp. Whether it be playing ping pong, going camping/hiking or finding an ice cream spot (i.e., Blank Slate), it has been wonderful getting to know you all over the last six years. I remember the collective fear in our eyes as we prepared for our preliminary exam together. I wouldn't have been able to predict what the following years would hold, but I have very much enjoyed our friendship.

Lastly, I would like to thank my family and friends who have walked alongside me during my Ph.D. Mom, Dad, Tim and Katie, your continued and unwavering support has meant so much to me over the years. There are so many friends that I've come to value over the last few years that I can't name all of you, but a few who have had a particular impact are as follows: Ryan H., Deanna M., Joe I., Emily M., Micah K., Richard & Lydia F., George & Mary L., Aaron K., Christy K. and Josh B. Without all of you, I would not be where I stand today. A special thanks goes to Anna-Lisa, Deanna, Emily and Maddie for offering critical feedback on chapters of this dissertation.

Table of Contents

List of Tables

List of Figures

Figures:

Supplemental Figures:

Abstract

The mammalian gut is home to a vibrant community of microbes. The ecological interactions that shape this environment are distinct across gut locations. As host and microbial community co-evolved, they formed a complex yet stable relationship that prevents invading microorganisms, such as the spore-forming bacterium, *Clostridioides difficile*, from establishing within the gut. Great strides have been made over the past several years in characterizing *C. difficile* infection physiology, particularly in how gut microbes and their host work together to provide colonization resistance. I designed the work in this thesis to characterize how the mammalian small and large intestines shape *C. difficile* germination and outgrowth. Using observational and experimental approaches, I used human, murine and bioreactor models of the gut microbiota to study varying levels of ecological complexity.

I show that the small intestinal microbiota is predominated by Firmicutes and that fluctuations in the microbiota are associated with changes in pH and bile acids. The bile acid population from the duodenum to the mid jejunum consists mainly of conjugated primary and secondary bile acids, with little microbial metabolism of these compounds occurring across the proximal small intestine. Since conjugated bile acids tend to promote *C. difficile* germination, this environment supports *C. difficile*'s transition from spore to vegetative cell at high efficiencies, suggesting that colonization resistance is tied to preventing the establishment of vegetative cells later in the gut. I also present work

characterizing the effect of dietary xanthan gum on *C. difficile* colonization in a murine model of infection. Xanthan gum administration modified the microbiota and led to increased production of short chain fatty acids. However, it also interfered with the activity of the orally administered antibiotics used to render mice susceptible to *C. difficile* colonization. As a result, *C. difficile* colonization resistance was maintained in mice fed xanthan gum. Finally, I use a bioreactor model to characterize how founder effects shape microbial community establishment and influence *C. difficile* colonization resistance. Dilution increases the variability of the microbiota and abrogates its ability to resist invasion by a non-indigenous microbe. Additionally, we provided some reactor communities with additional concentrations of the dietary polysaccharide inulin. While some communities responded to inulin by producing additional butyrate, more dilute communities concurrently lost their ability to produce additional butyrate and resist *C. difficile* colonization. These data demonstrate that a particular level of microbiota cohesiveness is required to produce both functions and suggests that metabolic activity of butyrate-producing microbes is tied to colonization resistance.

Together, my work demonstrates the importance of understanding the environmental interactions that shape microbial physiology, particularly that of *C. difficile*, in both the small and large intestines. In the small intestine, a variable microbiota with low biomass is shaped by host-driven processes, such as bile acid secretion. However, in the large intestine, a high biomass microbiota shapes the environment by metabolizing complex nutrients and preventing invasive taxa, such as *C. difficile*, from becoming established. Future work can leverage these findings to develop treatment methods that incorporate the dynamics of the intestinal environment to improve efficacy.

Chapter 1: Introduction

A version of this chapter was published as:

Schnizlein MK & Young VB. Capturing the environment of the *Clostridioides difficile* infection cycle. Nature Reviews: Gastroenterology & Hepatology. 2022. *Accepted*.

1.1 *C. difficile* as a member of the gut microbiota

Clostridioides difficile (formerly *Clostridium difficile*) is a Gram-positive, spore-forming bacterium that colonizes individuals whose microbiota is perturbed in structure and function such that colonization resistance to non-indigenous microorganisms is lost (1-3). Understanding the latest advances in *C. difficile* physiology and what constitutes colonization resistance is required before we can develop precision medicine-based treatments for *C. difficile* infection (CDI). *C. difficile* can be successful as a pathogen owing to its ability to adapt to unique environments, particularly those created by antibiotic disruption in the gut (4). This adaptability is largely due to the diversity of its genome (5). *C. difficile*'s genomic and strain diversity, which is well-reviewed elsewhere (5-7), is distributed across 6 phylogenetic clades. Only a small percentage of its genes are present across all sequenced isolates (~16–19%), a number likely to go down as more strains are sequenced (8, 9). This finding reflects the evolution of *C. difficile* to fit unique environmental circumstances.

CDI is usually acquired within clinical settings, in part due to an increased prevalence of *C. difficile* that leads to more exposures, but also due to the increased use

of antibiotics (10, 11). However, the bacterium is also abundant in the environment. Certain strains of *C. difficile* have been well-documented in animals, including bats, dogs and horses (12, 13). *C. difficile* spores are also commonly found in soil (14). These environments can serve as transmission sources for community-acquired infections (15).

The *C. difficile* infection cycle begins when spores are introduced into the gut via the oral route (Fig. 1.1). These spores germinate in response to bile acids and co-germinants, and then grow into vegetative cells (16). To survive in the gut, vegetative *C. difficile* cells utilize several factors to overcome competition from the host as well as other microorganisms (17). Colonization of the gut most often follows antibiotic treatment, which removes many of the microbial competition barriers that block colonization (18, 19). Upon sufficient cellular stress, *C. difficile* initiates two processes that either disrupt the environment to facilitate more favorable conditions, as is the case with the production of toxin, or form a protective coat through sporulation to facilitate exit from or persist in the gut (20-23).

The purpose of this Review is to frame the clinical aspects of *C. difficile* infection within the context of bacterial physiology and gut ecology. *C. difficile* has evolved to thrive in the gut due to substantial antagonistic pressures from indigenous microorganisms and the host. These systems biology perspectives will help inform treatment options as well as future research into lingering questions regarding pathogen physiology. We will accomplish these goals by exploring: clinical relevance of *C. difficile*; *C. difficile* physiology in the gut, including germination, survival mechanisms, toxin production and sporulation; and finally mechanisms by which *C. difficile* is suppressed in the gut,

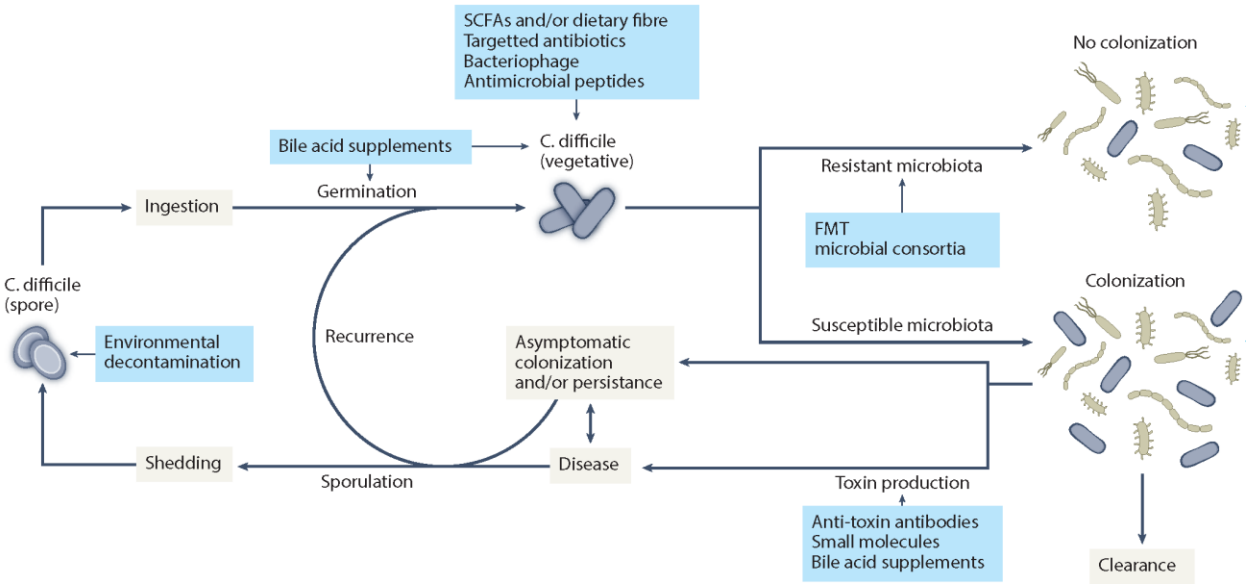

Figure 1.1 Leveraging the environment to interrupt the *C. difficile* infection cycle
The gut contains a number of mechanisms to prevent *Clostridioides difficile* infections, which can be enhanced by targeted treatment. *C. difficile* spores are ingested orally and enter the gut where they germinate in response to bile acids (e.g., taurocholate). The quantity of viable spores that germinate can be reduced by environmental decontamination and germination inhibitors (for example, bile acid analogues or supplements) (24-29). Following germination, the resulting vegetative cells will either proliferate, if the microbiota is susceptible, or be excluded, if the microbiota is resistant. Increasing the resistance of the gut to vegetative *C. difficile* could be facilitated by dietary fiber (that is, short-chain fatty acids (SCFAs); (30, 31), targeted antibiotics (32), bacteriophage (33-35) or antimicrobial peptides (36, 37). Fecal microbiota transplantation (FMT) (38-44) and defined microbial consortia (23) can shift a number of factors influencing vegetative *C. difficile*, including microbial metabolism and host immune responses. After colonization of the gut, *C. difficile* can clear spontaneously, enter a phase of asymptomatic colonization (that is, persistence) or produce toxin to cause disease. The effects of toxins could be ameliorated through anti-toxin antibodies (45), small molecule inhibitors (46, 47) and bile supplementation (48). Sporulation facilitates further persistence in the gut as well as transmission to new hosts through shedding. Following treatment, individuals will clear *C. difficile* or experience recurrence to become re-colonized.

including antimicrobials, bacteriophages, bile acid metabolism, short-chain fatty acids (SCFAs), as well as nutrient competition and nutritional immunity; concluding with a brief summary about how these mechanisms are being leveraged for *C. difficile* treatment.

1.2 Clinical relevance of the environmental paradigm

C. difficile is a pressing health concern that results in a substantial morbidity and mortality. In the USA and Europe, *C. difficile* represents a major health and economic burden (49-52). In the USA alone, *C. difficile* annually infects approximately 0.5 million people and accumulating healthcare costs of about US$5 billion each year (53, 54). Although *C. difficile* infects individuals worldwide, comprehensive studies on *C. difficile* burden in Africa and Asia are limited (55). Infected patients can develop diarrhea and severe gut inflammation, leading to several additional outcomes, including pseudomembranous colitis and toxic megacolon (56). Approximately 70% of infections occur during or immediately following a visit to a healthcare center (49, 57). The remaining 30% of infections are acquired through reservoirs outside the clinic, which include several animal species and the soil (49, 57). Regardless of the location of exposure, individuals that become infected have a 30-day all-cause mortality risk of 15-20% (58, 59).

Although of proven utility for treating infections, antibiotics also alter the gut environment. Several pathogens are known to coopt these disruptions of the microbial community to establish themselves in the gut environment, including vancomycin-resistant enterococci, *Escherichia coli* and *Salmonella Typhimurium* (60-62). *C. difficile* also takes advantage of perturbed gut states to colonize the gut, which is why antibiotic use is the leading risk factor for acquiring an infection (11, 18). Being

immunocompromised or having increased age also lead to microbial community alterations that predispose individuals to CDI. These disruptions of the gut microbial community change the flow of nutrients in the ecosystem, making it easier for non-indigenous microorganisms to establish. First-line treatments for *C. difficile* are antibiotics with activity against the pathogen, including fidaxomicin or vancomycin (63, 64). Problematically, these agents have collateral activity against indigenous microorganisms and further disrupt the gut environment, which leads to a higher risk of becoming reinfected.

After primary infection, up to 30% of individuals develop recurrent *C. difficile* infection (65). The risk of recurrent disease worsens as individuals are treated for each successive infection, increasing up to 40% following the second incident and 65% following the third, suggesting that as the gut environment struggles to recover after successive disturbances and *C. difficile* has greater opportunities for re-establishing itself (65). It is unclear whether *C. difficile* persists in the gut below the limit of detection or persists in the external environment to re-enter the gut following the end of antibiotic treatment. Interestingly, 20-50% of recurrences are the result of a new strain re-infecting the gut (66). Although a number of studies have suggested that up to 10% of patients with CDI are infected with multiple strains, little is known about how multi-strain colonization affects infection outcomes (67, 68). The presence of more than one strain can change important aspects of infection dynamics, such as by protecting against subsequent exposure or shifting immune responses due to multiple sources of *C. difficile* antigens (69, 70).

Fecal microbiota transplantation (FMT) is a treatment option geared towards leveraging mechanisms of gut colonization resistance to fight off *C. difficile* and restore the gut community, including both its bacterial and fungal components, to a state of healthier equilibrium (71). The efficacy of FMT in treating CDI has been well covered in other primary research and review articles (38-44). However, as we learn more about how *C. difficile* interacts with the gut environment, specific pathogen–environment interactions can be leveraged to develop alternative treatment options. As such, treatment guidelines continue to be updated as additional discoveries are made about *C. difficile* and how this pathogen interacts with the gut environment (32, 63). Here, we will discuss discoveries regarding *C. difficile* physiology and how these microorganism–environment interactions are essential for developing targeted non-antibiotic-based means of preventing CDI.

1.3 Physiology of *C. difficile* in the gut environment

1.3.1 Germination

The *C. difficile* lifecycle in human hosts begins as orally ingested spores, which possess several layers to protect cells from hostile environments in and outside of the gut. These layers, including the exosporium, cortex and cell wall, shelter the genetic material and cellular machinery required to restart metabolism (16). Whether or not *C. difficile* germinates and emerges from this protective coat depends on environmental signals, including temperature, pH, bile acids, amino acids and divalent cations, as well as the spore's sensitivity to those signals (72-75). Spores sense germinant through the putative receptors CspC and CspA, after which the signal is transduced through a series of pseudo-proteases resulting in spore cortex hydrolysis (76-78). The relative and

absolute concentrations of germinant signals determine whether the overall signal points towards higher or lower germination efficiency.

The ability of *C. difficile* to germinate is tied to the metabolism of microorganisms in its surroundings (Fig. 1.2) (69, 79, 80). Bile acids are key regulators of *C. difficile* germination. Their primary roles in the gut are to assist in the breakdown of lipid micelles and to modulate the gut microbiota, either through cellular toxicity or as potential carbon sources (81). Thus, indigenous gut microorganisms have evolved diverse mechanisms to detoxify these molecules and scavenge potential energy. These metabolic processes transform primary, conjugated bile acids (e.g., taurocholic acid), which promote *C. difficile* germination, into unconjugated primary and secondary bile acids (e.g., cholic, chenodeoxycholic and deoxycholic acids) that are either less effective germinants or even inhibit this process (82). *C. difficile* is one of the few, if not the only, microorganisms characterized as having evolved a germination receptor that senses bile acids (83). Preliminary work suggests that bile acids do aid in the germination of other microorganisms (e.g., *Clostridium innocuum* and *Clostridium hathewayi*), but it is unclear whether bile acids act through a specific mechanism as is the case with *C. difficile* or if bile acids act through general properties (e.g., their detergent-like nature) to promote germination (84). Host proteases, such as plasminogen, also have a role in promoting germination. However, as a toxin-damaged gut triggers plasminogen release, their role likely is only important in recurrent disease rather than initial infection (85).

One area that merits further study is how physiological levels of germinants interact to promote *C. difficile* germination. Kochan et al. was one of the first to demonstrate *in vitro* that physiologically relevant levels of germinants work in synergy to enable

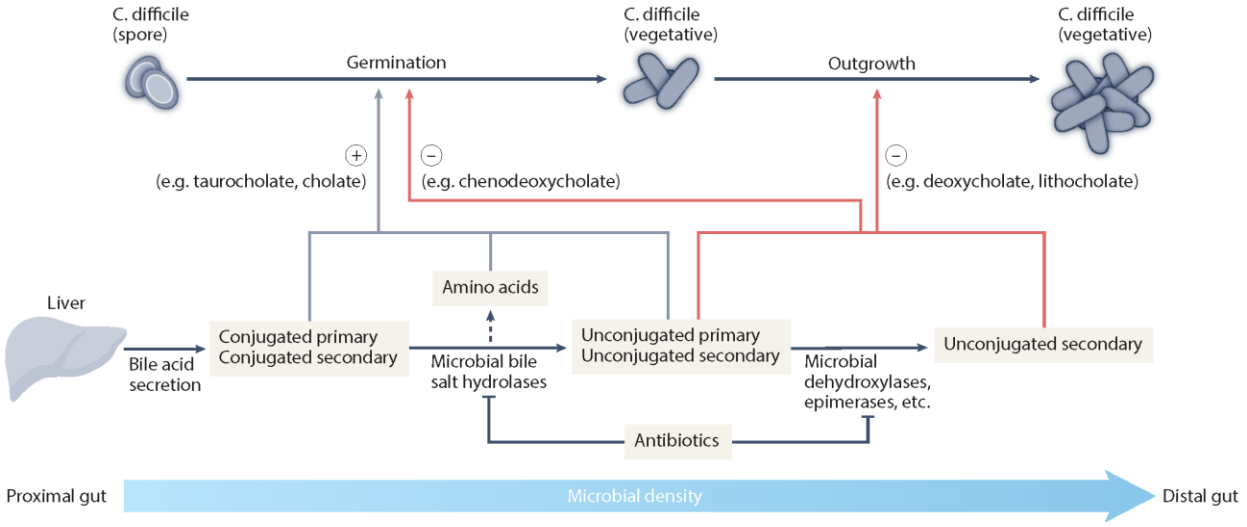

Figure 1.2 Bile acid metabolism and *C. difficile* physiology
Primary (that is, host-synthesized) and secondary (that is, microbially-modified) bile acids are conjugated to amino acids in the liver and secreted into the proximal gut, where they encounter a microbiota that uses a variety of enzymes to modify these compounds. Conjugated primary bile acids, particularly taurocholate (the amino acid taurine conjugated to the bile acid cholate), promote germination. Upon deconjugation by microbial bile salt hydrolases, the germinant potency of taurocholate is greatly reduced in its deconjugated form cholate. Chenodeoxycholate, another primary bile acid competitively inhibits germination. Further processing of bile acids as microorganisms increase in abundance transforms the bile acid pool into mostly secondary acids, which overall inhibit *Clostridioides difficile* germination. These secondary bile acids also are inhibitors of vegetative cell outgrowth. Bile acids are reabsorbed by the host and transported back to the liver where they are conjugated and re-secreted. In a perturbed gut (for example, antibiotic-treated), microbial community metabolism is impaired, which limits bile acid transformations, resulting in an environment that overall leads to higher germination efficiencies and outgrowth.

germination (86). A limitation of many *in vitro* studies is the use of higher than physiological concentrations of germinant to induce robust germination. Germinant synergy is required to understand the complex ecosystem of the gut. Hypothetically in the gut, lower concentrations of germinant might maintain the dormancy of some spores and protect the population from unexpected shifts in hospitability. On the other hand, as certain germinants drop below sufficient levels to induce germination, other compounds might work together to stimulate a response from spores.

Although a great deal of work has been done to identify what machinery *C. difficile* uses to sense germinant signals, much remains to be discovered regarding how individual strains respond to these signals. Some work suggested that some *C. difficile* strains germinate without taurocholate, a key promoter of germination (87). Further research showed that these strains still responded to taurocholate but with increased sensitivity *in vitro* (88). This finding raised interesting questions about why sensitivity to germinant varies from strain to strain, and what implications this has for *C. difficile* evolution and clinical epidemiology. Interestingly, *C. difficile* strains modulate germinant sensitivity by altering the ratios of signaling proteins in mature spores (88). Often, one thinks of varying exterior conditions to modulate germination. However, *C. difficile* strains have developed their own mechanisms to determine what conditions are optimal for ‘dropping their protective shield.’ By modulating signaling protein abundance and thereby their sensitivity to germinant, spores might select for an appropriate environment in the gut to germinate.

Together, germinant synergy and strain-specific germinant sensitivity complicates the prospects of developing germination inhibitors as a potential treatment option for CDI. Such treatments could reduce the infectious dose by decreasing germination efficiency

(26). However, it is unclear how many 'live' *C. difficile* cells are required to colonize and cause disease and whether an inhibitor could sufficiently reduce germination efficiency *in vivo* across an entire population of spores. Similarly, efforts to decrease environmental *C. difficile* reservoirs have been developed. However, the effect of specific methods (for example, ultraviolet light) over standard decontamination methods on transmission rates are not well understood (24, 25).

1.3.2 Adapting to survive: C. difficile *mechanisms for thriving in the gut*

After emerging from its protective shell, *C. difficile* enters the fiercely competitive environment of the mammalian gut. Humans harbor over 1000 unique bacterial, fungal, and protist species that fight over nutrients to occupy niches in the gut (89). Microorganisms not normally present in the human gut, such as *C. difficile*, are at a disadvantage as many of its nutrient and spatial niches are likely already occupied (90). Antibiotic use opens many of those niches for *C. difficile* to occupy (18). However, as gut microorganisms recover from extreme perturbations, *C. difficile* maintains a competitive edge by deploying a variety of factors that ease its ability to persist, such as toxins (discussed in the next section), adhesins, pili, flagella, and biofilms (17). While commonly called virulence factors, these protein complexes are produced by bacteria not always known to cause disease (91). Thus, it might be better to think of these as mechanisms of survival (that is, survival factors) rather than those associated specifically with disease-causing ability. Further research is required to understand the regulatory signals that govern whether *C. difficile* becomes motile or seeks to attach to surfaces, such as the intestinal epithelium (Fig. 1.3A).

Not surprisingly, expressing all survival factors simultaneously in the gut would overtax the bacteria's metabolic potential. Thus, the importance of regulation cannot be overstressed. Although *C. difficile* uses a complex system of transcription factors to transduce environmental signals and regulate expression, it also employs a process of gene inversion, called phase variation, to selectively turn off and on specific genes (92). This process creates multiple distinct subpopulations within a clonal genetic lineage. As Garrett et al. showed, phase variation of genetic regulators leads to unique cellular morphologies and motility patterns depending on environmental selective pressures (92). Selective pressure did not universally induce phase variation but rather created phenotypic heterogeneity during *in vitro* experiments (93). *In vivo*, these adaptations would facilitate increased survival during bottleneck events and other evolutionary pressures amidst a changing environment as *C. difficile* subpopulations express unique assemblies of traits (Fig. 1.3A).

An often-understudied part of the *C. difficile* lifecycle in the gut environment is how the pathogen can persist in the gut environment without causing disease. Increasingly, *C. difficile* is being identified and isolated from the gut of asymptomatic individuals (4-15% of healthy adults in a meta-analysis of 20,334 individuals) (94, 95). A small human study suggested this phenomenon could in part be associated with the mycobiota (N=118) (96). In 2019, Dubois et al. hinted at another phase of *C. difficile* lifecycle characterized by persistence and the production of biofilms, which are induced by deoxycholate *in vitro* (Fig. 1.3A) (97). Although the biofilm-forming abilities of *C. difficile* are certainly not robust, this study suggests *C. difficile* capitalizes on phases of life that do not depend on

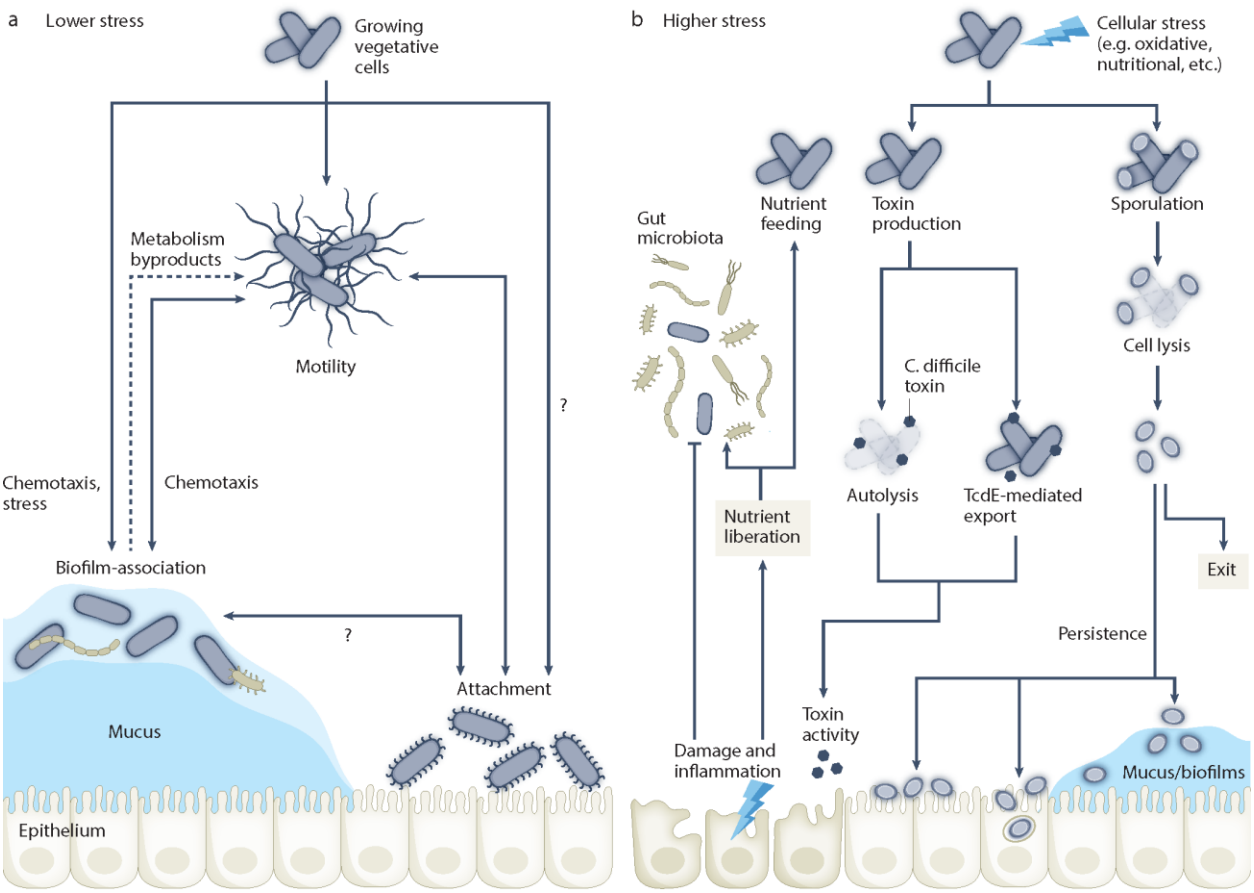

Figure 1.3 Differential stress adaptations of *C. difficile* in the gut environment
Depending on external signals in the gut environment, *Clostridioides difficile* adopts several different cellular pathways including survival mechanism differentiation, toxin production and sporulation. Each of these cellular options can be expressed simultaneously within different parts of *C. difficile* populations. **A)** Under lower stress and/or nutrient replete conditions, growing vegetative cells transition between several phases of life. Some might produce flagella to seek out nutrients. Biofilm- association assists *C. difficile* in joining microbial consortia and provides an environmental shield. Adhesins facilitate attachment to epithelial cells or other surfaces in the gut. **B)** Under higher cellular stress, *C. difficile* will induce toxin production and/or sporulation. Following toxin release through autolysis or TcdE-mediated export, toxin activity on the *C. difficile* spores can persist in the gut by adhering to biofilms or the intestinal epithelium as well as being internalized within the epithelium itself. Finally, spores can exit the gut altogether.

disrupting the environment through toxin production (98). Induction of biofilms accompanies the repression of flagella and toxins as well as sporulation. The ability to produce different biofilm structures characterized by unique metabolism types, each with reduced sporulation and toxin production, suggests that *C. difficile* adapts to changing nutrient availability during its persistent lifestyle *in vivo* (99). Furthermore, *C. difficile* might favor persistence when nutrients are plentiful to avoid activating a disruptive lifestyle (that is, toxin production) or attempting to escape the gut entirely (that is, sporulation). Further research is needed to understand the clinical significance of *C. difficile* biofilm formation, particularly in the context of recurrent infections.

1.3.3 Toxin production and sporulation

Toxin production and sporulation are induced upon sufficient cellular stress and thought to be co-regulated (20, 100-103). However, it is unclear how populations of *C. difficile* cells balance these two processes. Although sporulation results in cell lysis, toxin release might occur through lytic and/or non-lytic pathways (104-108). This process leads to several hypotheses: sporulation and toxin production tend to occur within a single cell, where lysis of the mother cell releases the spore and toxins at the same time and/or toxin is released gradually through non-lytic pathways prior to spore release; sporulation and toxin production tend to occur in separate cell populations with each adopting processes maximized to their particular goal. The latter might be better supported by literature but has not been conclusively shown (109). Either way, *C. difficile* begins these pathways to either perturb the environment, liberating nutrients to prolong the current iteration of the

cycle, or to escape and bide its time until favorable conditions return to reinitiate the infection cycle.

1.3.3.1 Toxins: remodeling the gut environment

C. difficile strains have been demonstrated to produce at least three toxins that mediate *C. difficile*-associated disease called TcdA (Toxin A), TcdB (Toxin B), and CDT (also known as binary toxin) (110). Production is induced when nutrients, such as glucose and amino acids, are limiting and when there are inhibitory microbial metabolites, such as bile acids or short chain fatty acids (Fig. 1.3B) (111). Interestingly, there a several non-toxigenic strains that, although they do not cause disease, still colonize and persist in the gut (112). A strain's ability to encode zero, one or all of the known toxins suggests that toxin production is only one of the many survival mechanisms *C. difficile* uses and that causing disease is not always evolutionarily advantageous (113). Toxins are released from *C. difficile* cells by either autolysis or TcdE-dependent secretion (104, 105, 107, 108). Although both pathways might be used by a given strain, certain strains might rely on one more than the other. This aspect is particularly clear in strains with high toxin production, which require TcdE for normal toxin release (106). Both TcdA and TcdB have multiple receptors that either facilitate cellular toxin adherence or promote their endocytosis (114-117). The specific mechanism of endocytosis uptake is dependent on which receptors are used by a given toxin variant (118). The molecular mechanisms of action for *C. difficile* toxins have been well-reviewed in the past but we will briefly describe them here (110). After toxins bind host cell receptors, endocytosis brings toxins into the cell where both TcdA and TcdB act via Rho/Ras GTPases to cause cytopathic effects,

such as altering tight junction integrity and cytoskeletal organization.(110) Although TcdA and CDT proteins are fairly conserved when present in strains, TcdB is highly variable (113, 119). This variability could play a part in binding unique receptors to cause disparate effects in host cells leading to outcomes such as high inflammation from the release of host cellular contents (120-123).

As *C. difficile* colonization is enhanced by the altered microbiota of an inflamed, murine gut, producing toxins results in further disruption of the gut (124). Fletcher et al. demonstrated that colonization by a toxigenic *C. difficile* strain in the murine gut is higher than a toxin-negative mutant and that there was unique expression of metabolic genes in both contexts (125). *C. difficile* simultaneously uses the inflamed environment to liberate nutrients as well as suppress the growth of microbial taxa that might compete for those toxin-liberated nutrients.

C. difficile strains have also individually adapted to utilize unique toxin receptors that result in divergent cellular pathologies, and perhaps determine what nutrients are released into the gut lumen. As Pan et al. demonstrated, toxin B variants can induce multiple distinct pathological phenotypes in the mouse intestine depending on which receptors are bound on the host cell surface (123). Further work is required to understand if or how *C. difficile* strains have adapted to capitalize on these unique host outcomes and what consequences these changes have on *C. difficile* survival.

As the severity of toxin-mediated inflammation is dependent on the concentration and duration of toxin exposure, identifying ways to moderate severity is an important aspect of understanding potential treatment development. The host lessens the effects of *C. difficile* toxins by secreting bile acids, which were shown to bind and inactivate toxins

in vitro (48). Small molecules, such as ebselen, also can limit toxin activity (46, 47). Host-produced anti-toxin antibodies can also block cytotoxic activity (126). This feature led to the development of the monoclonal antibody bezlotoxumab, which targets TcdB and was FDA-approved with the indication for the reduction of *C. difficile* recurrence (45). Interestingly, a corresponding monoclonal antibody targeting TcdA did not increase efficacy in reducing recurrence, which might be due to unique roles of the two toxins in disease (127, 128). It should be noted that IgG antibodies against TcdA in patients with CDI are associated with lower rates of recurrent infections, an observation that played a role in the development of therapeutic monoclonals targeting the toxins (129). Moderating toxins' effects on the host would not only alleviate some of the severe disease outcomes but, by limiting tissue damage, would also deprive *C. difficile* of a route for nutrient acquisition (125).

1.3.3.2 Sporulation: exiting from or persisting in the gut?

The last stage of the *C. difficile* infection cycle is sporulation. This step is a process by which bacteria sequester their DNA and a minimum required amount of metabolic machinery inside a protective coat. This spore, which has substantially reduced metabolic activity, will help ensure survival amid toxic environmental conditions, in part due to the resistant shell but also due to low metabolic activity (that is, inhibitors will be less able to act on cellular activity because of overall activity reduction) (130). Although the specific mechanisms of sporulation differ, spore production occurs in several bacterial taxa. In *C. difficile*, sporulation is induced as a stress response and, as mentioned earlier, is thought to be co-regulated with toxin production (Fig. 1.3B) (131).

Most interest in *C. difficile* sporulation has been directed towards its role in survival outside of the host. As an anaerobic organism, a spore form is necessary for transmission between hosts in an oxygen-saturated environment. However, work has begun investigating the role of spores and sporulation within a host. As many recurrent infections occur with the same strain, understanding where that infection is sourced is important. Many precautions for preventing relapse involve room cleaning procedures to eliminate environmental reservoirs. However, what if sporulation enables *C. difficile* to maintain a reservoir inside the host? In 2021, Castro-Córdova et al. characterized a mechanism by which *C. difficile* spores become internalized inside the murine intestinal epithelium, which increases recurrence rates of CDI (132). Not only does internalization retains spores within the gut environment, it also protects them from exposure to germinants, which typically exist at higher relative concentrations to germination inhibitors in a perturbed gut state (79). By incorporating inhibitors of spore internalization into treatment measures, clinicians could reduce the risk of recurrent CDI by eliminating a reservoir of disease.

1.4 Mechanisms of *C. difficile* suppression in the gut

Colonization resistance arises because a diverse community fully occupies niches in an environment. In the gut, trillions of bacteria metabolize compounds and deplete resources in their surroundings (133, 134). These microbial interactions contribute to a rich and dynamic ecosystem (135, 136). The stability of this gut community excludes new microorganisms unless there is a concurrent disturbance that opens niches and increases the plasticity of the environment (90, 137). In the context of *C.* difficile, there are several key mechanisms by which colonization is suppressed (Fig. 1.4). These biotic factors

include the production of antimicrobials and predation by bacteriophage. They also include several aspects of metabolism such as that of bile acids, SCFAs as well as nutritional immunity, which involves the depletion of nutrients essential to *C. difficile* by the host and other resident microorganisms.

Although abiotic factors are often better characterized in non-animal-associated studies of the microbiota (for example, the soil), they play an integral part in gut physiology and *Clostridioides difficile* colonization (138). Here, we will briefly discuss the importance of O_2 levels and pH. As an anaerobe, *C. difficile* has a low tolerance of oxygen. In the gut environment, oxygen concentrations increase along a gradient towards the intestinal epithelium (139). Not only does this gradient have important physiological effects on the microbiota, but it also regulates *C. difficile* competitiveness (140). In addition to toxic O_2 effects, other microorganisms in these spaces might use oxygen to boost energy output, leaving *C. difficile* at a disadvantage (141). Although intricately connected to microbial metabolism, pH is an abiotic factor linked to *C. difficile* growth, with lower pH decreasing growth rates *in vitro* (142). Further characterization of these and additional abiotic factors, such as methane and hydrogen gas gradients as well as an environment's texture and/or viscosity, in the context of *C. difficile* infection is needed (143).

1.4.1 Antimicrobial peptides

Much in the manner that *C. difficile* uses toxins to remodel the intestinal environment, indigenous microorganisms produce proteins that act against other taxa in their surroundings. While the host produces antimicrobial peptides to protect the

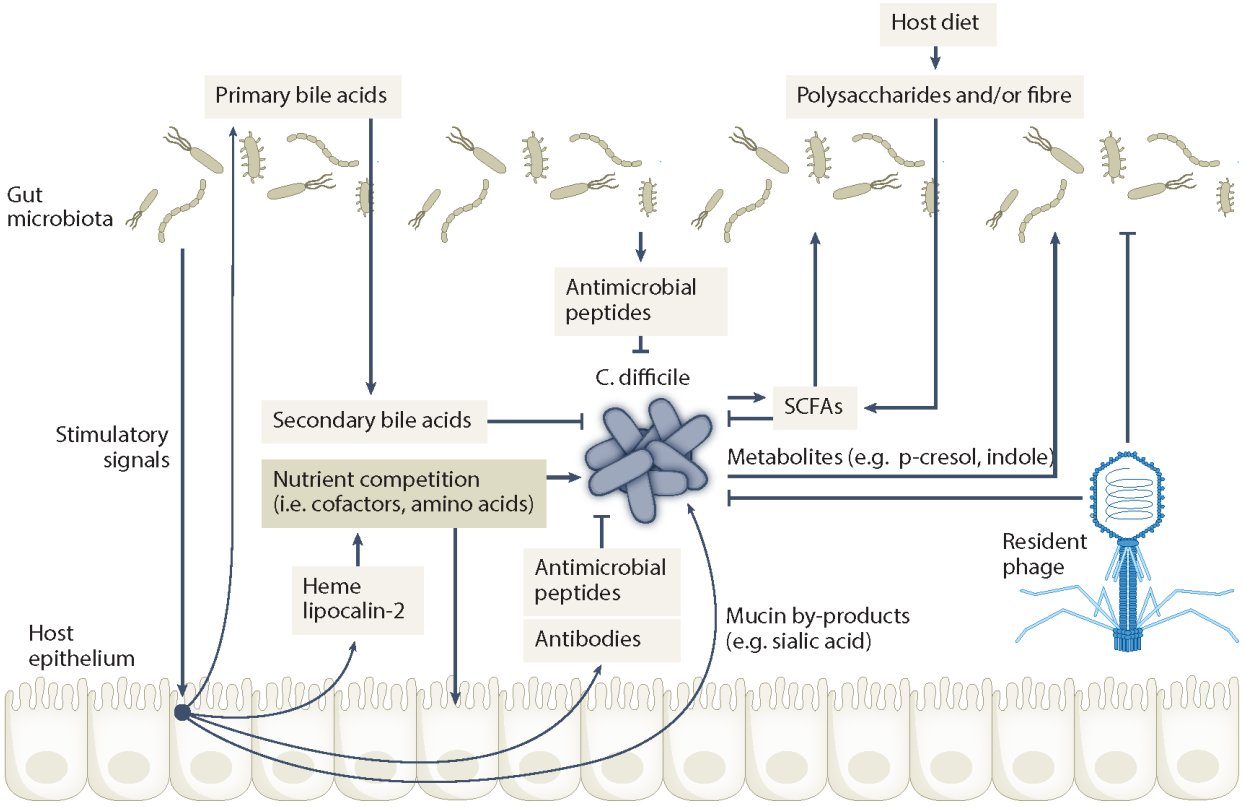

Figure 1.4 *C. difficile* interactions with its environment
In the gut, *Clostridioides difficile* must adapt to numerous inhibitory mechanisms of both host and indigenous microbiota to colonize. Microorganisms metabolize host-secreted bile acids and compete for nutrients, such as cofactors and amino acids. Microorganisms also ferment dietary polysaccharides into short-chain fatty acids (SCFAs) to toxify the environment. In addition to microbially produced antimicrobials, microbial signals stimulate the production of host-produced antimicrobials and antibodies that target *C. difficile.* Finally, bacteriophages replicating within the gut community with host ranges that cover *C. difficile* will target it upon arrival in the gut. Although net-interactions in an unperturbed gut disfavor *C. difficile*, the pathogen can feed off its environment (for example, mucin by-products) and modulate the gut by secreting molecules, such as *p*-cresol and indole.

epithelium, the microbiota secretes these products throughout the gut (144, 145).

Microorganism-produced antimicrobial peptides target Gram-positive and Gram-negative bacteria, including multiple-drug resistant organisms such as *Staphylococcus aureus* and carbapenemase-resistant enterococcaeceae (145, 146). Similar to their response to antibiotics, bacteria have adapted resistance mechanisms to remove these toxic compounds, attempting to competitively edge one another out (145). As a resident of the gut, *C. difficile* is regularly exposed to antimicrobial peptides produced by both host and resident microorganisms. To a limited extent, the variety of peptides active against *C. difficile* have been identified (147). Suárez et al. characterized a defense system in *C. difficile* that protects against antimicrobial peptides (148). Unlike many bacterial systems that respond to host-produced peptides, this system responds specifically to those produced by other microorganisms, likely by recognizing a motif present in several other bacteria-produced peptides (e.g., certain lantibiotics) (148). The presence of similar systems in the *C. difficile* genome suggests that counteracting several different microorganism-produced antimicrobials enables *C. difficile* to grow in the gut (148). Further characterization will be necessary to understand how they prevent activity, especially as tailored antimicrobial peptides are being considered as potential alternatives to antibiotic therapies (36, 37).

1.4.2 Bacteriophage

Bacteriophages are bacterial parasites that have a multifaceted role in modulating the gut microbiota (149). In the process of infecting bacteria, phage exert selective pressure by altering cellular metabolism and releasing nutrients into the environment

through cell lysis (150). Additionally, phage can facilitate lateral gene transfer by carrying genes from one species to another through transduction (151-153). Phage host range varies greatly, with some infecting only a few bacteria, whereas others targeting multiple taxa (154, 155). Microbial predation by phage has led to much research investigating phage therapy as an alternative to antibiotic use.

Phages have several roles in the dynamics of the *C. difficile* infection lifecycle. Not only are phages *C. difficile* parasites, they also mediate lateral transfer of genetic material, such as genes encoding toxins, which could enable non-toxigenic strains to acquire additional toxins or other survival factors in the gut (156). Several studies published in the past few years suggest that successful FMT in humans involves not only a successful transfer of donor bacteria but also of donor bacteriophages (33-35). The part phages play in FMT efficacy merits further study given evidence that filter-sterilized FMT, that still contains phage, successfully clears *C. difficile* (41).

Nale et al. suggested that phage cocktails might serve as a targeted alternative to antibiotics, particularly in an age with rising antibiotic resistance levels (157). The risk of transduction introducing potentially dangerous genes into *C. difficile* should be considered when introducing phage into the gut. However, using a phage cocktail not only mitigated that risk but also ensured *C. difficile* was targeted through multiple infection routes helping the treatment bypass bacterial defenses (157, 158). These studies reflect the need for a stronger understanding of an often-understudied aspect of the gut environment and even more so in the context of CDI.

1.4.3 Bile acid metabolism

Bile acids affect *C. difficile* lifecycle dynamics at both the spore and vegetive cell stages. As the effects on spore germination have been described already, here we will discuss the effects on vegetative cells. Primary bile acids, which are those synthesized directly by the host from cholesterol, are not generally toxic to *C. difficile* (Fig. 1.2). However, secondary bile acids, which are microbially modified versions of primary bile acids, are toxic, particularly the secondary bile acid deoxycholate (79, 80, 159). Current research has sought to understand how microorganisms modify these bile acids to affect *C. difficile* (160, 161).

Although the levels of bile acid toxicity on *C. difficile* have been characterized, additional work is required to understand the specific effects of bile acids on *C. difficile*. Traditionally, the effect of bile acids on *C. difficile* has been framed within the context of their primary and secondary forms, as the latter tend to have greater toxicity. However, as we learn more about the unique types of biotransformations creating the bile acids present, it becomes necessary to understand the individual effects of each compound on cellular physiology (82, 162). Sievers et al. utilized proteomics to characterize the unique effects of primary and secondary bile acids on *C. difficile* and its subsequent stress responses (163). They found that adaptations to bile acid stress are tied more to individual bile acids and their chemical precursor rather than whether the bile acid is primary or secondary. For example, stress responses due to cholate-derived bile acids tend to be more similar than those to bile acids derived from the other primary bile acid chenodeoxycholate. These bile acid-specific responses push *C. difficile* into a non-motile cellular phenotype and result in shifts in metabolism, particularly that of amino acids.

Further research is needed to understand the effect of the diversity of microbially-modified bile acids on *C. difficile* stress responses as well as the effect of simultaneous, concerted action of multiple bile acids.

Exogenously added bile acids, such as the FDA-approved drug ursodeoxycholate (UDCA), have positive effects on treating CDI. Preliminary evidence from small human studies suggests that oral UDCA is effective in treating *C. difficile*-associated ileal pouchitis (N=1) and lowering recurrence rates (N=16) (27, 28). Additionally, oral UDCA pre-treatment limited *C. difficile*-associated inflammatory responses in a mouse model of disease, suggesting that bile acids not only have direct effects on the pathogen but also can modulate innate immune responses (29).

1.4.4 Short-chain fatty acids

SCFAs are fermentation byproducts from microbial metabolism, particularly of complex dietary polysaccharides (164). Commonly known SCFAs are acetate, propionate and butyrate. These molecules have diverse effects on both host and microorganism (165). In the host, SCFAs alter colonocyte physiology through G-protein-coupled receptor signaling and epigenetic modification as well as decrease systemic inflammation by promoting regulatory T cell development (165). In microorganisms, SCFAs provide a nutrient source as well as alter physiology by acidifying the environment (166-169). In the context of human CDI, higher concentrations of butyrate are associated with recovery from *C. difficile* after a successful FMT (170). Although this metabolite could only be a marker of overall community health and metabolic functionality, butyrate has inhibitory effects on *C. difficile* cells (31). Furthermore, dietary polysaccharide-induced increases in

SCFAs levels clear *C. difficile* from the gut (31). Even though *C. difficile* can produce butyrate, which makes sense due to butyrate's role as an electron acceptor, it is unclear whether concentrations would approach inhibitory levels or that *C. difficile* preferentially uses this metabolic pathway in the gut (171, 172).

As mentioned previously, SCFAs affect gut epithelial physiology due to the closeness of microorganisms and host at the mucosal interface. Fachi et al. demonstrated that microbially produced butyrate protects the gut from *C. difficile*-induced colitis by increasing the integrity of the murine gut barrier (30). In understanding CDI dynamics, it is important to incorporate both the primary effects of compounds, such as when butyrate inhibits *C. difficile* cells, and the secondary effects microbial metabolites mediate. These findings also tie into the importance of host immunity in moderating disease severity. Although the gut microbiota is directly responsible for preventing *C. difficile* colonization and facilitating clearance, innate and adaptive host immune responses seem to be associated with the severity of infection outcomes by regulating gut inflammation and barrier integrity in both humans and mice (173, 174). Future treatment options could include some form of dietary fiber supplementation to increase microbiota SCFA production to limit gut toxicity to *C. difficile* and begin repairing some of the toxin-mediated damage.

1.4.5 Nutrient competition and nutritional immunity

The ability to acquire nutrients lies at the core of bacterial survival. If the necessary carbon sources and cofactors (that is, vitamins and minerals) are too difficult to acquire, a microorganism will be outcompeted by those that can manage to do so (2, 3, 175).

Bacteria utilize carbon sources, such as sugars and amino acids, to generate energy that drives cellular processes (176). Cofactors, such as vitamins and minerals, interact either to catalyze metabolic reactions or facilitate protein folding (177). In the mammalian gut, the availability of these two essential nutrient classes is determined by competition along two axes: the host–microorganism axis and the microorganism–microorganism axis.

Along the host-microorganism axis, hosts have a vested interest in maintaining low concentrations of essential nutrients, such as cofactors, to prevent the overgrowth of microorganisms in the gut (178). This aspect is especially true when those microorganisms have the potential of causing damage that can affect the balance of gut nutrients (178). This process, called nutritional immunity, prevents many pathogens, such as *Salmonella enterica* and *Escherichia coli*, from growing in the gut, unless those pathogens have adapted to circumvent them (179, 180). Knippel et al. demonstrated that *C. difficile* has adapted mechanisms to scavenge iron from its host's mechanisms of acquiring it by activating a system to reduce redox stress and capture host-produced heme (181, 182). A similar process occurs with zinc acquisition, in which *C. difficile* induces expression of a putative zinc transporter in the presence of calprotectin (183). Interestingly, excess zinc reduces the antibiotic concentrations needed to facilitate *C. difficile* colonization in animals, suggesting that an aspect of colonization resistance is circumvented (184, 185). These findings suggest that a dimension of colonization resistance functions to deprive *C. difficile* of necessary cofactors through their acquisition by the host.

Along the microorganism–microorganism axis, multiple different taxa compete for the same nutrients, increasing the complexity of these interactions. Jenior et al.

demonstrated this *C. difficile*–microbiota interplay in mice where *C. difficile* transcriptionally adapts to unique nutrient availability under different antibiotic treatment conditions (186). Furthermore, *C. difficile* influences the microbiota during colonization to make space for itself by excluding low abundance microorganisms, in part by utilizing nutrients but also by secreting disrupting molecules *in vivo*, such as indole and *p*-cresol (187-189).

Along both microorganism–host and microorganism–microorganism axes, host-produced mucus layers in the large intestine provide a microbial colonization niche in the gut (190). Although mucus serves to protect the host intestinal epithelium, it also serves to provide microorganisms with polysaccharide and protein sources for consumption (190). When *C. difficile* encounters the gut environment, it can sense monosaccharide by-products from microbial mucin degradation (191). Following chemotaxis, *C. difficile* can integrate into multi-species communities that colonize the outer, loose mucus layer (98, 191). Interestingly, *C. difficile* preferentially binds the types of mucins that typify the gut of *C. difficile*-infected individuals which contain lower levels of N-acetylgalactosamine and higher of N-acetylglucosamine, suggesting that microbial modifications to the mucus layer in advance of *C. difficile* exposure facilitate colonization (192). In summary, many interactions occur not only in luminal gut spaces but also in surface-associated spaces in the gut, which suggests possible treatment targets. For example, engineered microbial consortia utilize mucus degradation products to decrease *C. difficile* colonization (193).

The metabolic adaptability of *C. difficile* enables it to utilize a number of different nutrients in the gut. These nutrients include products of mucin degradation, such as sialic acid and *N*-acetyl glucosamine, as well as amino acids through Stickland fermentation

(193-198). Work suggested that the ability to utilize trehalose contributed to the spread and increased prevalence of the 027 ribotype (199). Other groups demonstrated that the capability to use trehalose does not specifically associate with increased *C. difficile* virulence (200, 201). Further work is required to understand the complex interactions that trehalose and other common dietary additives exert on the fitness of *C. difficile*. Characterizing the functional metabolic differences between susceptible and resistant communities will assist in developing defined and effective CDI treatment alternatives to FMT (23).

1.5 Outline of the Thesis

This thesis revolves around the central hypothesis that the gut environment plays an integral role in affecting *C. difficile*'s ability to successfully colonize the mammalian gastrointestinal tract. In chapter two, I describe the structure the small intestinal microbiota as being highly dynamic but tied to environmental variables such as pH and bile acid concentrations. Despite the prominent influence of the gut microbiota in altering the bile acid pool by the end of the gastrointestinal tract, microbial bile acid metabolism is at a minimum in the small intestine. This leaves an environment with high concentrations of primary, conjugated bile acids that promote *C. difficile* germination, facilitating its transition from dormant spore to actively growing vegetative cell. In chapter three, I characterize how xanthan gum, a common dietary polysaccharide additive, affects *C. difficile* colonization resistance in a murine model of CDI. While xanthan gum significantly increased butyrate concentrations, it also altered the efficacy of antibiotics used to render the gut microbiota susceptible to *C. difficile* colonization. In chapter four, I

use a continuous flow bioreactor system to model the gut microbiota independently of host interactions. I demonstrate that dilution-induced stochasticity increases the variability of how microbial communities establish. This in turn decreases the external stability (e.g., colonization resistance) to non-indigenous microbes such as *C. difficile*. Finally, in chapter five, I discuss the implications of my findings as well as areas for future research.

Chapter 2: Spatial and Temporal Analysis of the Upper Gut Microbiota Reveals Relationships Between pH, Bile Acids, and *Clostridioides difficile* Germination

Major sections of this chapter were published as (* indicates co-first authors):

Seekatz AM*, **Schnizlein MK***, Koenigsknecht MJ*, Baker JR, Hasler WL, Bleske BE, Young VB, Sun D. Spatial and Temporal Analysis of the Stomach and Small-Intestinal Microbiota in Fasted Healthy Humans. mSphere. 2019;4(2):e00126-19. doi: 10.1128/mSphere.00126-19.

2.1 Introduction

The microbiota of the proximal gastrointestinal tract in humans represent an understudied yet highly relevant microbial community (202). Physiological processes such as gastric emptying, bile acid secretion, and the transit of food can influence the proximal gastrointestinal (GI) tract and disease development (203-206). However, there is limited information on how the microbiota in this region relates to these processes, and how these impact health and disease throughout the GI tract.

Much of our knowledge about the involvement of the human GI microbiota in maintaining health and preventing disease has relied on fecal sampling, a non-invasive sampling method that is largely representative of the large intestine (207, 208). Although it is known that the microbiota across the GI tract varies in composition and density, studying the microbiota at these sites is difficult, limiting our knowledge to invasive procedures, specific patient populations, or single time points (90, 202, 209, 210). Analyses of mucosal samples from autopsies, endoscopies, and colonoscopies have revealed that *Streptococci* and *Lactobacilli,* both members of the oral and esophageal

microbiota, are abundant members of the jejunal and ileal microbiota (211-217). Studies using naso-ileal catheters and ileostoma effluent, which allow collection over time, have supported these conclusions and revealed that the small intestinal microbiota is highly dynamic over short time courses, likely reflective of physiological processes at the stomach-small intestine interface (218-221).

Understanding how the microbiota along the GI tract interacts with drugs, such as mesalamine and ibuprofen, is of physiological relevance, particularly in relation to intestinal homeostasis and disease. Recent evidence suggests that the drug mesalamine, designed to reach high concentrations in the GI tract as treatment for inflammatory bowel disease (IBD), may directly target the microbiota in addition to host effectors (222, 223). Interestingly, mesalamine is less effective in treating IBD in the upper GI tract, which manifests as Crohn's disease, than the lower GI tract, which manifests as ulcerative colitis. It is possible that some of the effectiveness of mesalamine as a treatment for IBD, or lack thereof, is mediated by the microbiota, potentiating the need to characterize these microbial communities to a fuller extent in the context of mesalamine administration. Ibuprofen is a non-steroidal anti-inflammatory drug used to treat mild pain in individuals. It is known to affect the gut microbiota of individuals consuming it as well as the microbes present in wastewater treatment systems (224, 225). However, these studies have characterized long-term affects on the order of days and months rather than hours (226-228). Much remains to be discovered regarding the short-term effects of either mesalamine or ibuprofen on the microbiota of the upper gut.

At the intersection of host and microbial physiology is the metabolism of bile acids. These compounds are synthesized by the host to help in the digestion of dietary lipids

and serve as a means to control bacterial overgrowth. Microbes modify these compounds into secondary forms to either decrease their toxicity or use them as a carbon source. While studies have broadly characterized the types of metabolism that occur in the mammalian gut, little is known about the short-term dynamics of bile acids after they enter the gut in the duodenum and travel to the jejunum. Furthermore, we know little about how bile acids intersect with the microbial populations that reside in these regions both regarding microbial bile acid metabolism as well as how bile acids control which microbes can grow.

Understanding how the microbiota fluctuates and shapes its environment in healthy individuals is important to develop our understanding what conditions pathogens encounter when they enter the gut. For example, the physiology of *Clostridioides difficile*, which is a hospital-associated pathogen, is closely tied to bile acid metabolism, particularly in its ability to germinate. Primary conjugated bile acids (e.g., taurocholic acid) promote germination whereas unconjugated primary and secondary forms can inhibit it (e.g., chenodeoxycholic acid and lithocholic acid). While individuals with a perturbed microbiota and bile acid population will become colonized, individuals with a healthy microbiota do not. Therefore, understanding how a healthy gut environment shapes *C. difficile* physiology can inform efforts to leverage this resistance as treatment options.

This study investigated the bacterial composition across the intact upper GI tract in the same healthy, fasted adults over time. We used a multi-lumen tube designed to sample multiple sites along the upper GI tract. As part of previously published studies aimed at measuring mesalamine and ibuprofen dissolution, subjects were given a dose of either mesalamine or ibuprofen and the proximal GI tract lumen was sampled over time

(229, 230). We used these samples to 1) characterize and compare microbial community dynamics over time at multiple upper GI sites within an individual, 2) identify how environmental factors, such as pH and the acute effect of mesalamine, shaped the microbiota and 3) investigate the types of bile acids present and their associations with members of the microbiota, including their effects on *C. difficile* germination. To the best of our knowledge, this is the first study to characterize the luminal microbiota across multiple upper GI sites over time within the same individual.

2.2 Materials & Methods

2.2.1 Study recruitment

Healthy individuals (age 18-55) were included who were free of medications for the past two weeks, passed routine health screening, had a BMI 18.5-35, and had no significant clinical illness within three weeks. Health screening included a review of medical history and a physical examination (checking vital signs, electrocardiography, and clinical laboratory tests) described in Yu et al. (229).

2.2.2 Catheter design and sterilization

A customized multi-channel catheter was constructed by Arndorfer Inc. (Greendale, WI), consisting of independent aspiration ports located 50 cm apart. The catheter had a channel to fit a (0.035 in x 450 cm) guidewire (Boston Scientific, Marlborough, MA), a channel connected to a balloon that could be filled with 7 ml of water to assist tube placement, and an end that was weighted with 7.75 grams of tungsten. Each single-use catheter was sterilized according to guidelines set by the American

Society for Gastrointestinal Endoscopy at the University of Michigan prior to insertion (231). For the subjects enrolled for bile acid analyses, the multi-lumen catheter had a slightly different design as described previously (230).

2.2.3 Collection of GI fluid samples

The full details of catheter placement have been previously described (229, 230). Briefly, catheter placement occurred approximately 12 hours before sample collection. The catheter was orally inserted into the GI tract with aspiration ports located in the stomach, duodenum, and the proximal, mid and distal jejunum, confirmed by fluoroscopy. Subjects were given a light liquid snack approximately 11 hours before sample collection and fasted overnight for 10 hours prior to sample collection.

For pH and microbiota analyses, a mesalamine formulation was administered to each subject at 0 hrs (Table 1). Luminal GI fluid samples (approximately 1.0 ml) were collected from up to four sites of the upper GI tract hourly up to 7 hours. Samples were collected by syringe, transferred to sterile tubes, and placed at -80°C until sample processing. A paired sample was collected to detect pH using a calibrated micro pH electrode (Thermo Scientific (Waltham, MA) Orion pH probe catalog no. 9810BN).

For bile acid and microbiota analyses, an ibuprofen formulation was administered to subjects at 0 hrs (Table 2). Subjects were randomized into a fasted group, which received 250 mL of H_2O at 0 hrs, and a fed group which received the water as well as a supplement of Pulmocare (473 mL). Since there was no effect of Pulmocare administration, all patients were analyzed as a single cohort.

Subject ID*	Mesalamine Formulation†	Age	BMI	Sex	Stomach	Duodenum	Jejunum			Stool	Total
							Proximal	*Mid*	*Distal*		
M046-A	Pentasa	38	21.2	M	1	8	-	7	-	1	17
M046-B	Apriso	38	21.3	M	-	8	-	5	6	-	19
M046-C	Lialda	38	21.7	M	8	6	-	7	-	1	22
M047	Pentasa	36	21.1	M	-	8	6	-	-	-	14
M048	Apriso	51	34.3	F	5	7	-	-	-	-	12
M053	Apriso	34	25.2	F	1	-	7	3	-	-	11
M061	Pentasa	51	21.6	M	7	8	-	-	-	-	15
M062	Pentasa	37	27.3	M	7	7	-	-	-	1	15
M063	Lialda	26	28.6	M	7	5	-	5	-	-	17
M064	Lialda	25	27.5	F	8	7	-	-	-	-	15
Summary	**40% P, 30% A, 30% L**	**37 ±8.6**	**25 ±4.4**	**70% M**	**44**	**64**	**13**	**27**	**6**	**3**	**157**

*All subjects were caucasian and none identified as hispanic/latinx.

†Pentasa = Immediate release in stomach acid; Apriso = Extended release at pH > 6; Lialda = Extended release at pH > 7

Table 2.1: Subject recruitment for pH analysis
Selected metadata and sample collections for 10 admissions (subject M046 was admitted for three visits).

Subject ID	BMI	Age	Sex	No. of Samples				
				Stomach	*Duodenum*	*Prox Jejunum*	*Mid Jejunum*	*Total*
A1	24.4	20	M	-	11	-	11	22
A2	25.1	21		4	10	-	6	20
B1	24.1	30	M	2	9	-	6	17
B2	24	30		11	8	5	-	24
C1	22.8	22	M	4	5	12	-	21
D1	27.3	54	F	-	3	-	-	3
D2	27.3	54		3	8	-	4	15
E1	27.5	20	M	1	-	7	-	8
E2	28.1	20		-	-	-	8	8
F1	35.8	30	M	6	6	-	8	20
F2	35.6	31		12	8	5	6	31
G1	24.2	26	F	4	1	1	1	7
H1	19.4	18	M	6	-	10	-	16
I1	19.6	29	F	4	12	-	-	16
I2	20.6	29		2	3	3	-	8
J1	24.4	32	M	-	6	2	9	17
K1	27.6	34	F	3	2	2	1	8
K2	27.8	34		8	3	4	4	19
L1	25.1	39	M	13	5	9	-	27
L2	25.3	40		5	3	-	6	14
M1	25.6	37	M	6	2	-	-	8
N1	31.9	28	F	6	7	-	3	16
N2	32.8	28		-	9	7	3	19
O1	31	47	M	4	-	10	-	14
O2	30.9	47		13	6	7	-	26
P1	23.3	25	M	13	9	-	4	26
Q1	21.8	28	F	9	-	-	-	9
R1	28.7	24	M	5	-	12	-	17
S1	25.8	26	F	4	6	-	7	17
T1	24.1	22	M	13	13	-	-	26
T2	24.3	22		12	7	-	10	29
U1	24.1	22	F	12	3	-	4	19
V1	35.9	49	F	6	6	7	3	22
V2	37.7	49		1	1	4	-	6
W1	21.6	30	M	9	6	-	-	15

Table 2.2: Subject recruitment for bile acid analysis
Selected metadata and sample numbers for the 23 subjects enrolled in the ibuprofen cohort used to study bile acids in the human upper gut.

2.2.4 DNA extraction and Illumina MiSeq sequencing

The detailed protocol for DNA extraction and Illumina MiSeq sequencing was followed as previously described with modifications (232). Briefly, 0.2 ml of GI fluid or 20 mg of stool was used for DNA isolation using a Qiagen (Germantown, MD) MagAttract Powermag microbiome DNA isolation kit (catalog no. 27500-4-EP). Barcoded dual-index primers specific to the V4 region of the 16S rRNA gene were used to amplify the DNA (233), using a “touchdown PCR” protocol. Multiple negative controls were run parallel to each PCR. PCRs were normalized, pooled and quantified (233), Libraries were prepared and sequenced using the 500 cycle MiSeq V2 Reagent kit (Illumina, San Diego, CA, catalog no. MS-102-2003). Raw FASTQ files, including those for negative controls, were deposited in the Sequence Read Archive database (BioProjectID: PRJNA495320; BioSampleIDs: SAMN10224451-SAMN10224634).

2.2.5 Data processing and microbiota analysis

Analysis of the V4 region of the 16S rRNA gene was done using mothur (v1.39.3) (233, 234). Full methods, including detailed processing steps, raw processed data, and code for each analysis, are described in: https://github.com/aseekatz/SI_mesalamine. Contact the corresponding author for code related to the bile acid-microbiota analyses. Briefly, following assembly, quality filtering, and trimming, reads were aligned to the SILVA 16S rRNA sequence database (v128) (235). Chimeric sequences were removed using UCHIME (236). Prior to analysis, both mock and negative control samples (water) were assessed for potential contamination; samples with < 2500 sequences were excluded. Sequences were binned into operational taxonomic units (OTUs), 97%

similarity, using the opticlust algorithm (237). The Ribosomal Database Project (v16) was used to classify OTUs or sequences directly for compositional analyses (> 80% confidence score) (238). Alpha and beta diversity measures (inverse Simpson index; the Yue & Clayton dissimilarity index, θ_{YC}) were calculated from unfiltered OTU data (239). Basic R commands were used to visualize results, calculate % OTUs shared between samples, and conduct statistics, using packages plyr, dplyr, gplots, ggplot2, tidyr, circlize, ggrepel, imputeTS, and tidyverse (240-245). The nonparametric Kruskal-Wallis test, using Dunn's test for multiple comparisons and adjusting *p*-values with the Benjamini-Hochberg method when indicated, was used for multi-group comparisons. The R packages lme4 and lmerTest were used for mixed linear models between OTU relative abundance (filtered to include OTUs present in at least half of samples collected from a subject, per site) and pH or mesalamine (246, 247).

2.2.6 Bile acid analysis

Bile acid concentrations were determined through LC-MS/MS. Briefly, 120 µL methanol and 10 µL internal standard solution were added to 30 µL gut fluid and vortexed for 10 min. Samples were centrifuged at 3500 rpm for 10 min at 4°C to precipitate protein. The supernatants were then saved for analysis by LC-MS/MS. The ultra-performance liquid chromatography (UPLC) system consisted of an ACQUITY UPLC system (Waters, Milford, MA, USA) with separation being achieved through a CORTECS T3 column (2.1x30mm, 2.7 um) maintained at 40^{o}C. The mobile phase A consisted of 0.01% formic acid and 0.2mM ammonium formate in water. Mobile phase B consisted of and 0.01% formic acid in isopropanol:acetonitrile (50:50, v:v) containing 0.2mM ammonium formate.

Gradient elution of mobile phases included four steps: 1) 10% B for 0.5 min, 2) increase to 90% B in 3.5 min, 3) decrease to 20% B in 0.01 min, and then 4) balanced for 1 min before the next injection. Flow rate was set at 1.0 mL/min and the injection volume was 2 µL. The UPLC system was coupled to a Waters TQD Tandem Quadrupole mass spectrometer equipped with an ESI source. High purity nitrogen was used as the nebulizer, heater, curtain and collision activation dissociation gas. Capillary and extractor voltage were 1.50 kV and -8 V, respectively, and flow rates of the cone and desolvation gases were 1 and 650 L/h, respectively. The source temperature and desolvation temperature were 150 and 650 ℃, respectively. Data were acquired with MassLynx 4.0 and calibrated and quantified by QuanLynx software.

2.2.7 C. difficile *germination assays*

C. difficile 630 spores were incubated for 30 minutes at 37^{o}C in gut fluid. Fluid was buffered at pH 7 by mixing in a 1:1 ratio with a phosphate-carbonate buffer containing 119 mM NaCl, 4.7 mM KCl, 2.5 mM $CaCl_2$, 1.2 mM $MgSO_4$, 1.2 mM KH_2PO_4 and 25 mM $NaHCO_3$. Following incubation, CFU of both vegetative cells and spores were enumerated by plating on TCCFA. The mixture was then heat-shocked at 65^{o}C for 30 min to kill vegetative cells and then enumerated on TCCFA a second time. CFU/mL pre- and post- heat-shock were compared to determine the relative amount of spores to vegetative cells (spores/(spores + vegetative cells)).

2.3 Results

2.3.1 Study population

Subjects recruited from the mesalamine study cohort were used in analyses pertaining to microbiota dynamics and their intersection with pH and mesalamine concentrations. Using a multi-channel catheter with multiple aspiration points, samples collected from the upper GI tract of 8 healthy subjects during 10 different study visits were processed for 16S microbial community analysis (Table 1) (229). Samples were collected hourly up to 7 hours primarily from the proximal GI tract in the following possible locations: the stomach (n=44), duodenum (n=64), proximal/mid/distal jejunum (n=46), and stool (n=3). At the beginning of the study, subjects were given one form of mesalamine (Table 1). One of the seven subjects was studied three times over the course of 10 months; for most analyses, each study visit from this subject was considered independently.

Subjects recruited from the ibuprofen study cohort were used in analyses pertaining to bile acid composition across the upper gut. We used a multi-channel catheter to collect fluid from the upper GI tract of 23 subjects, with some individuals returning for a second collection bringing the number of subject visits to 35 (Table 2). Samples were collected at intervals of 0, 0.25, 0.5, 0.75, 1, 1.5, 2, 2.5, 3, 4, 5, 6, and 7 hours from the stomach (n=201), duodenum (n=178), proximal jejunum (n=107) and mid jejunum (n=104). However, due to tube placement, not all sites or timepoints were collected from each subject (Table 2). Each study visit was considered independently for the analyses in this manuscript.

2.3.2 The proximal GI microbiota is dominated by Firmicutes and is distinct from the fecal microbiota

Analysis of the relative abundances of 16S rRNA-encoding genes from the GI tract across all timepoints and individuals demonstrated that the small intestinal microbiota was compositionally unique compared to stool (Fig. 2.1A). At all four sites in the proximal GI tract, Firmicutes composed the most abundant phyla (i.e., *Streptococcus*, *Veillonella*, and *Gemella* sp.). Higher levels of Bacteroidetes species (i.e., *Prevotella*) were detected in the stomach and duodenum. Proteobacteria and Actinobacteria predominated the remainder of the community at all sites. Diversity of the microbiota (inverse Simpson index) was decreased in sites of the upper GI tract compared to stool, which were enriched in Firmicutes (*Blautia*, Ruminococcaceae sp., and *Faecalibacterium*) and depleted in Bacteroidetes in these individuals (n=3) (Fig. 2.1B).

2.3.3 The proximal GI microbiota is individualized and variable over time

To compare the microbiota across the proximal GI tract within and across individuals, we assessed pairwise community dissimilarity using the Yue & Clayton dissimilarity index, θ_{YC}, which takes into account relative abundance of OTU compositional data. Both across (inter-individual) and within (intra-individual) subjects, stool was highly dissimilar to any proximal GI site (Fig. 2.2A-B). Across proximal GI sites, subjects were more similar to their own samples than samples across other individuals (Fig. 2.2A-D). The stomach microbiota was highly dissimilar across individuals compared to the duodenum or any part of the jejunum, which exhibited the least amount of

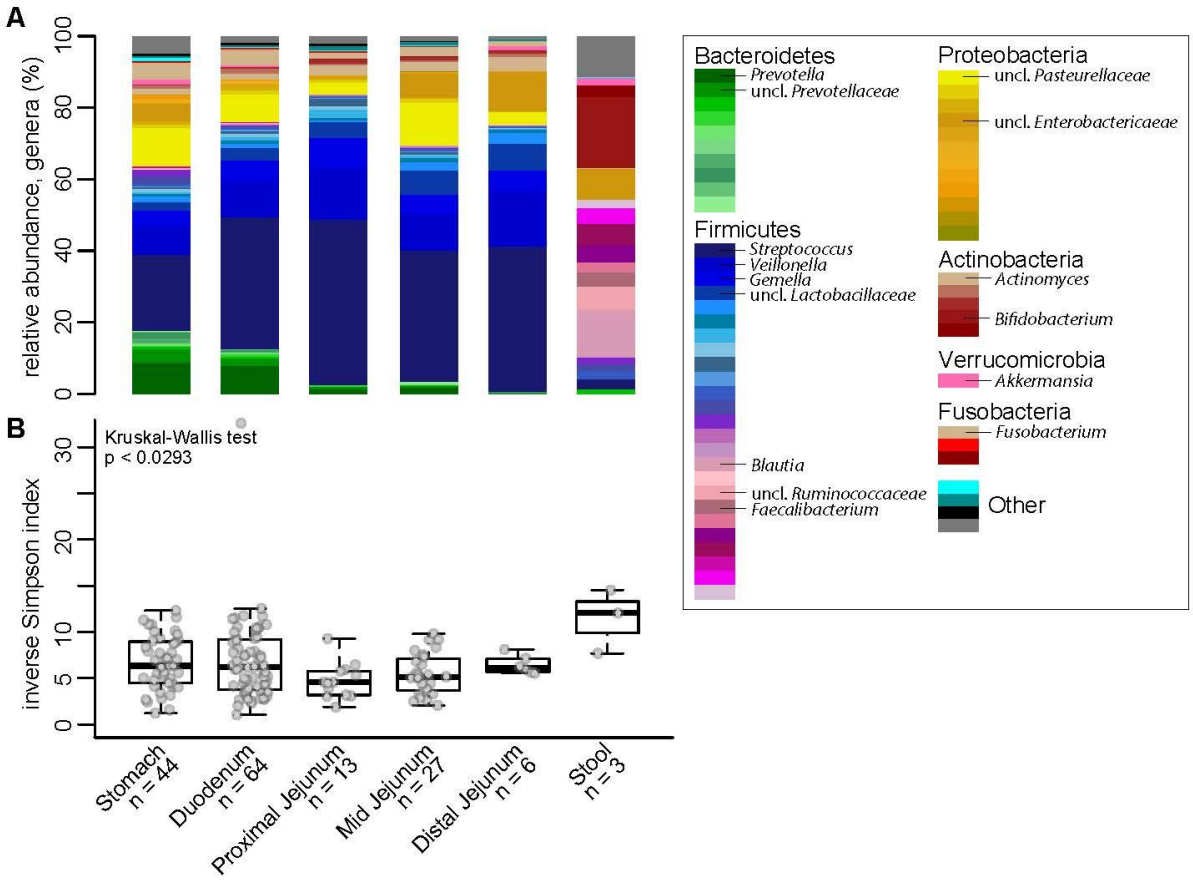

Figure 2.1: Bacterial community relative abundance and diversity in the upper GI tract
A) The mean relative abundance of genera at each GI site (sample n indicated). **B)** Boxplots of the inverse Simpson Index measuring community diversity across the GI tract (median, with first and third inter-quartile ranges). Statistical analysis: Kruskal-Wallis test (ns).

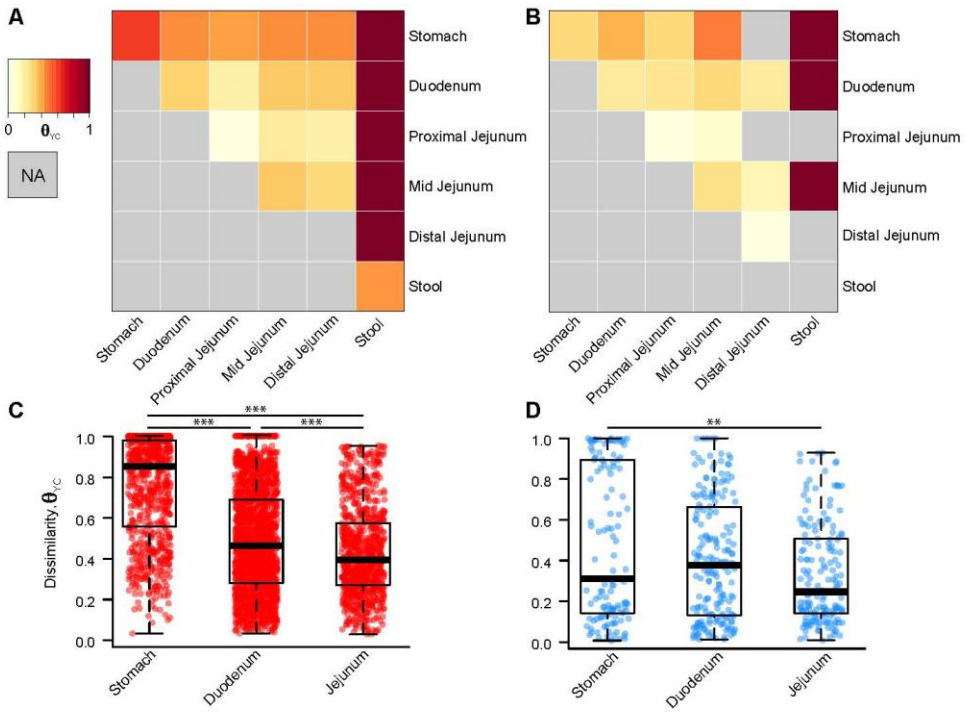

Figure 2.2: Dissimilarity of the proximal GI tract within and across individuals
Heatmap of the Yue & Clayton dissimilarity index, θ_{YC}, comparing different proximal GI sites and stool **A)** across individuals (inter-individual pairwise comparisons) and **C)** within individuals (intra-individual pairwise comparisons). **C)** Inter-individual and **D)** intra-individual dissimilarity in the stomach, duodenum, and jejunum (sites combined). Statistical analysis: Kruskal-Wallis test (will add p values to graph). We plot each sample at a given site rather than site averages since this allows us to capture potential extreme states that those communities might adopt over time. Statistical analysis: Dunn's test for multiple comparisons with a Benjamini-Hochberg p-value adjustment (*p < 0.01; **p < 0.001; ***p < 0.0001).

dissimilarity (Fig. 2.2C). A similar degree of dissimilarity was observed within an individual in the stomach, duodenum, and combined parts of the jejunum (Fig. 2.2D). Using a dissimilarity measure such as θ_{YC} allowed us to assess stability based on changes in the relative abundance of OTUs. It is possible that certain GI sites fluctuate more in total OTUs. To measure whether any site had a higher rate of flux in their community (i.e., a higher rate of OTU turnover), we calculated the % OTUs detected at a given timepoint from the total number of OTUs detected within that individual at a given site. We observed that for each proximal GI site, a mean of 36.6% of the OTUs ever detected in that subject at a given site (mean number of total OTUs ever detected per subject per site = 135; range 78-212) were detectable at a given timepoint (Fig. 2.3A). Similarly, we calculated the number of OTUs that were consistently present in all samples collected at that site within an individual (mean number of consistently detected OTUs per subject per site = 14.1; range 2-45). Overall, only 28.7% of the total OTUs ever detected at a given time point within an individual at a given site were represented by these consistently prevalent OTUs (Fig. 2.3B). However, these prevalent OTUs explained an average of 72.0% of the relative abundance observed in the samples (Fig. 2.3C). Of all sites, the relative abundance explained by the individual's most prevalent OTUs in the stomach was lowest, followed by the duodenum, suggesting more variation at these sites compared to the jejunum (Kruskal-Wallis, $p < 0.05$).

One subject (M046) returned three times over the course of 10 months, allowing us to compare long-term changes. Across the sites that were sampled during multiple visits (the duodenum and mid-jejunum), prevalent OTUs were still detected during all

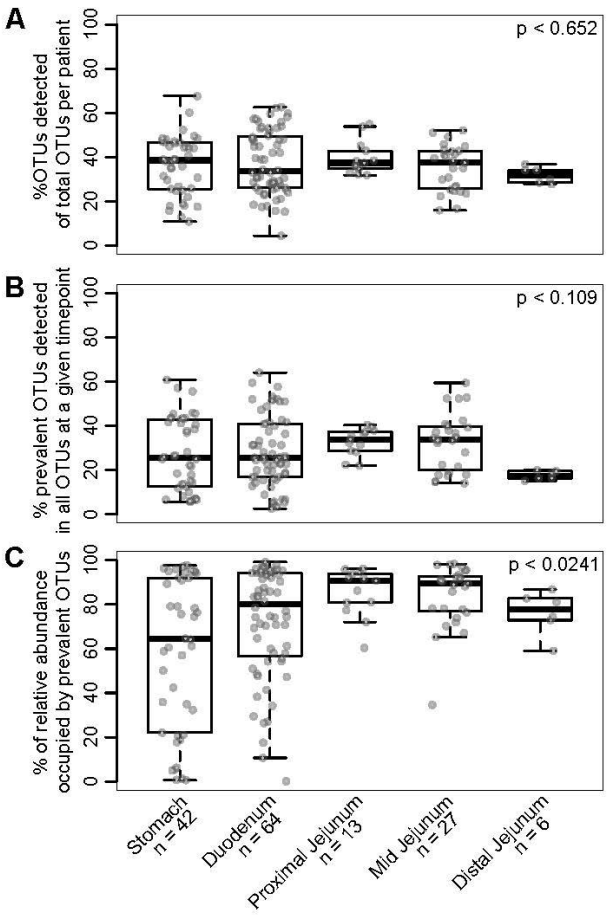

Figure 2.3: Fluctuations in prevalent OTUs observed within an individual across the proximal GI tract

A) Boxplots of the percentage of OTUs detected in a given sample out of all OTUs detected (all OTUs possible for that individual) at a subject-site. **B)** Boxplots of the percentage of OTUs that were consistently detected at a subject-site out of the total OTUs detected in a given sample. **C)** The percent of relative abundance explained by prevalent OTUs at a subject-site in a given sample. Statistical analysis: Kruskal-Wallis test.

three visits, explaining 74.4% and 66.1% OTUs in the duodenum and mid-jejunum, respectively (Fig. S2.1).

2.3.4 Large fluctuations in the duodenal microbiota are associated with pH but not mesalamine

We next investigated how these compositional trends changed over time across the subjects. We focused on the duodenum and stomach since these sites were highly sampled across and within individuals and demonstrated variable pH. In the duodenum, we observed large fluctuations in genus-level composition across hourly timepoints within individuals (Fig. 2.4, Fig. S2.2 & Fig. S2.3). Specifically, the relative abundance of *Streptococcus*, *Prevotella*, and an unclassified Pasteurellaceae species fluctuated in all individuals. We hypothesized that these fluctuations could be driven by mesalamine, administered in different forms to each subject at study onset. However, no visible pattern was observed with mesalamine levels. Interestingly, we observed that these compositional changes tracked with pH fluctuations (Fig. 2.4). These patterns were less apparent in the stomach, where individuals displayed variable dynamics and highly individualized compositional patterns independent of mesalamine levels or pH. A similar trend was observed in the jejunum of the subject with three different admissions, where pH fluctuated less (Fig. S2.1 & Fig. S2.2).

To identify whether any singular OTUs correlated with changes in pH, we applied a generalized linear mixed model approach that takes into account subject specificity (248-250). Within duodenal samples (n=56), we observed 15 OTUs that significantly

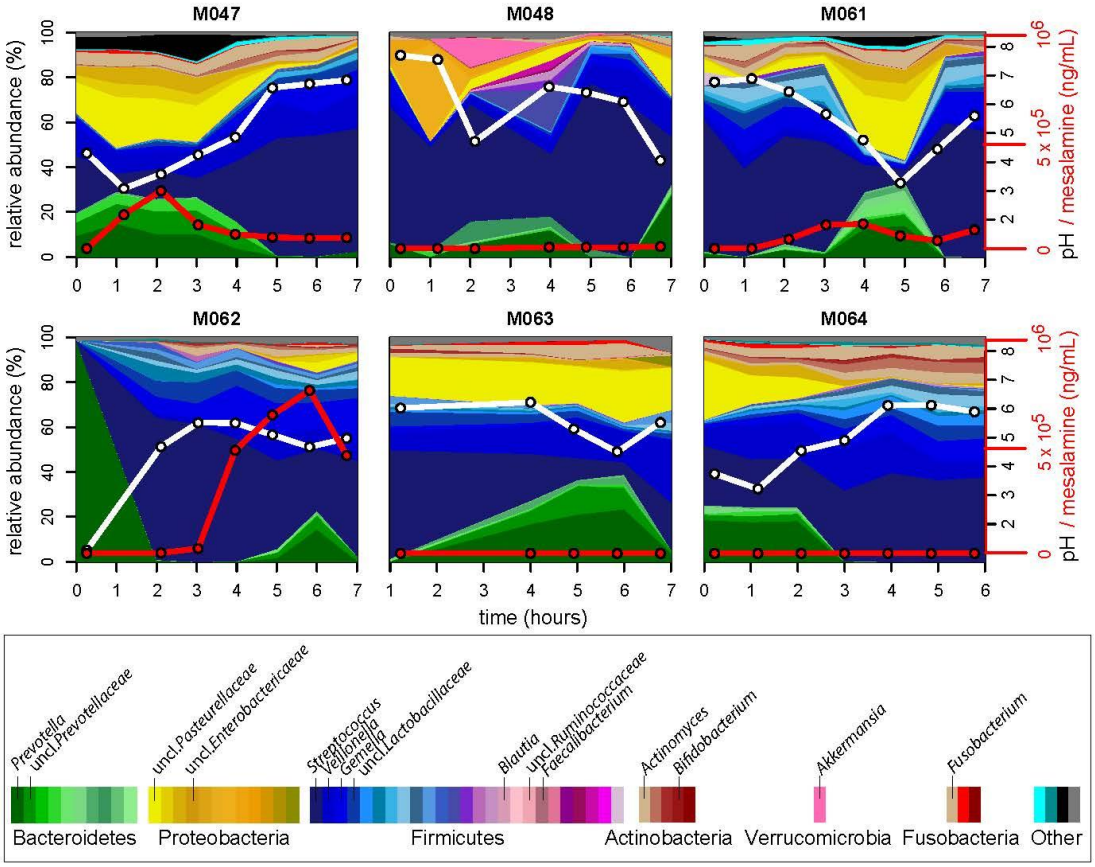

Figure 2.4: Longitudinal compositional dynamics, mesalamine levels, and pH in the duodenum
Streamplots of genus-level composition over time in the duodenum of six individuals (%, left y-axis; genera coded in legend). White lines indicate pH measurements (black y-axis labels on right) and red lines indicate mesalamine concentration (red y-axis labels on right).

correlated with pH changes. Linear regression of pH and relative abundance of these OTUs was significant across all samples (Fig. 2.5). Of the negatively correlated OTUs, six OTUs were classified as Bacteroidetes, mainly *Prevotella*, and two OTUs were classified as Pasteurellaceae sp. (Proteobacteria). The majority of the OTUs that were positively correlated with pH were Firmicutes, mainly *Streptococcus*, alongside an *Actinomyces* OTU (Actinobacteria). Only one OTU in the duodenum was significantly correlated to mesalamine. We identified 17 OTUs that correlated with pH or mesalamine in the stomach; however, these were not representative at all sites.

2.3.5 Conjugated bile acids predominate in the upper gut

Using LC-MS/MS, we measured the concentrations of 15 bile acids present in the human upper gut. Bile acids were almost entirely of conjugated primary and secondary forms (Fig. 2.6A). Cholate derivatives predominated (e.g., taurocholate and glycocholate), making up about 60% of bile acids with chenodeoxycholate derivatives in the minority (Fig. 2.6B and Fig. S2.4). Bile acid concentrations and ratios were consistent across the duodenum, proximal jejunum and mid jejunum. The stomach contained a much lower concentration of bile acids (Fig. 2.6B). While we expected lower concentrations in that site, the presence of any bile acids may be an artifact of our sampling tube, which prevents full closure of the pyloric sphincter. Averages of all samples in a given subject suggest that while there is variation across subjects, relative ratios of bile acids remain fairly consistent (Fig. 2.6C-E).

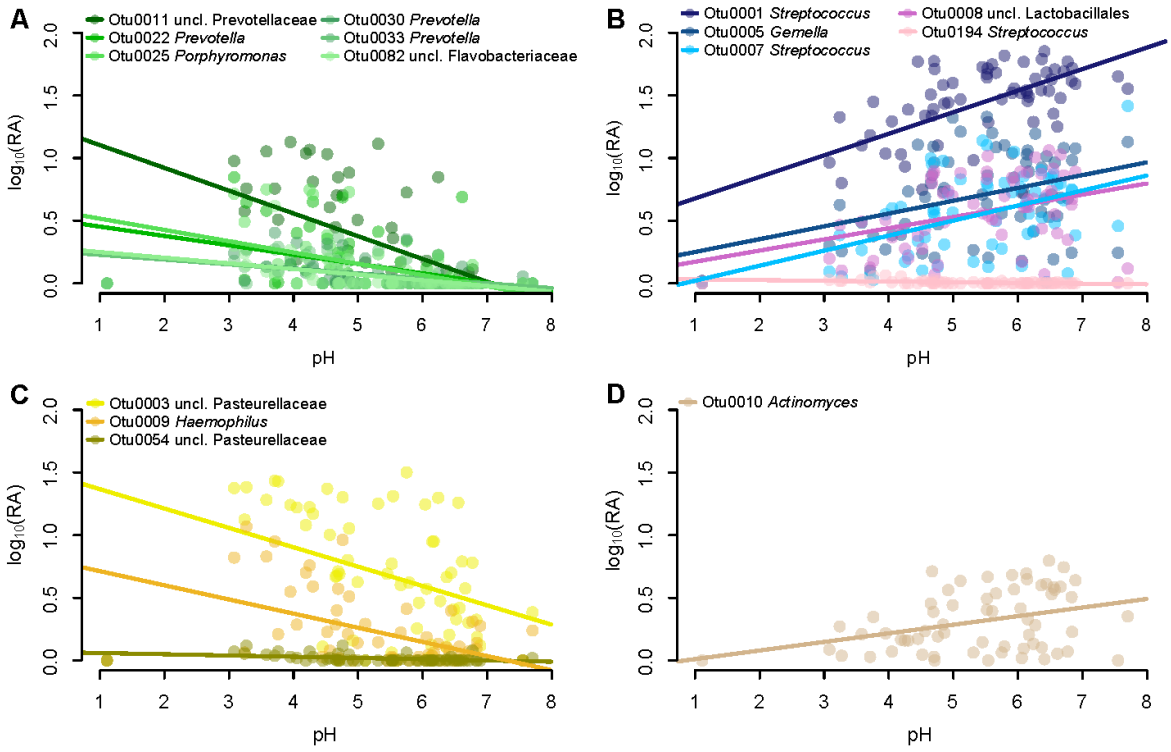

Figure 2.5: Relative abundance of significant OTUs vs. pH
Log relative abundance (log(RA)) as a function of pH of OTUs found to be significantly correlated with pH using linear mixed models (all samples with measurable pH). Lines represent linear fit per OTU. OTUs classified as **A)** Firmicutes, **B)** Bacteroidetes, **C)** Proteobacteria, and **D)** Actinobacteria are depicted (genus-level OTU classification coded by legends).

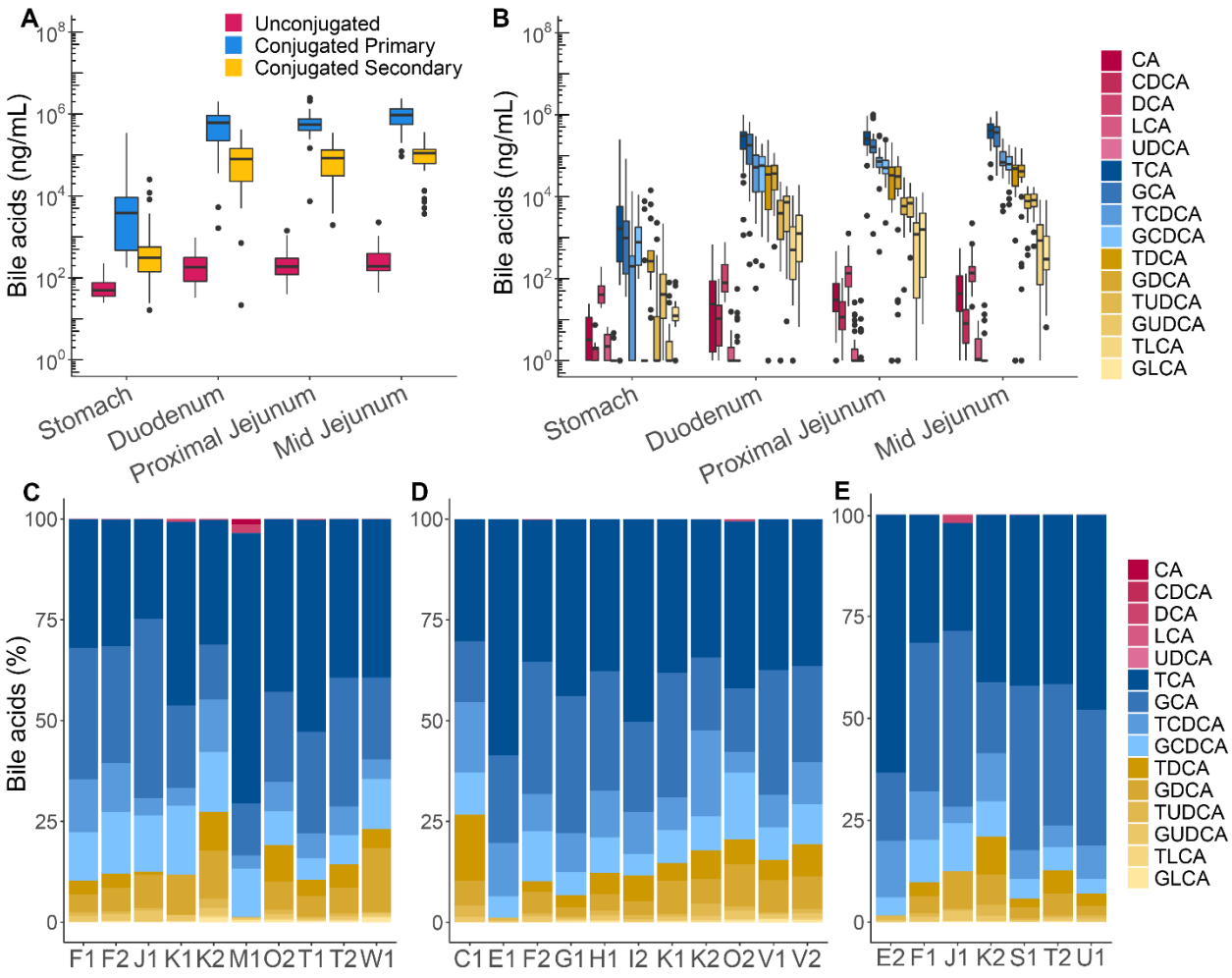

Figure 2.6: Abundance of bile acids in the human upper gut
Bile acid abundance as measured by LC-MS/MS in four regions of the upper gut either clustered by **A)** bile acid class or **B)** individually. Average relative abundance of bile acids in each of subject in the **C)** duodenum, **D)** proximal jejunum and **E)** mid jejunum. Each letter indicates a different subject, while the number indicates whether it was the first or second visit. Individual bile acids are colored in shades of their corresponding class (red = unconjugated, blue = conjugated primary, yellow = conjugated secondary).

2.3.6 Bile acid density associates with microbial phyla

Since microbial bile acid modification plays important physiological roles for both the host as well as microbes, we investigated the ratios of specific “metabolic-pairs” (i.e., precursor and product) to try and identify whether microbes were metabolizing bile acids in the upper gut. For example, microbial bile salt hydrolases can deconjugate the amino acid group (i.e., (T/G)CA to CA and (T/G)CDCA to CDCA) and 7α-dehydroxylases will modify -OH groups attached to the steroid ring (i.e., CA to DCA or CDCA to LCA). We limited these comparisons to samples from the initial timepoint (i.e., T_O) to measure baseline levels which would be unimpacted by any flux associated with the study drug. The consistency of the ratios of these pairs across the duodenum, proximal jejunum and mid jejunum suggests little, if any, of these microbial metabolic processes are occurring this early in the gut (Fig. S2.5A-F). While microbes may not be modifying the bile acid population, we might expect to see effects of bile acids on the microbiota, since bile acids are known to control bacterial abundance in the upper gut. Using mixed-effect models, we observed correlations between bile acids and major taxa in the upper gut independent of location. Higher concentrations of bile acids were associated with Firmicutes and Actinobacteria, and lower concentrations were associated with Bacteroidetes independent of upper gut location (Fig. S2.6A). Bile acid concentrations were negatively associated with microbiota diversity, indicating that under lower bile acid density a more diverse microbial community might be allowed to flourish (Fig. S2.6B). If these correlations were due strictly to the introduction of fluid into the upper gut, we might expect to see concurrent correlations between microbial taxa and ibuprofen as well. However, bacterial phyla do not associate with ibuprofen concentrations (Fig. S2.6C).

2.3.7 Short-term exposure to gut fluid triggers the germination of C. difficile

In addition to the effect of bile acids on the microbiota as a whole, we wanted to investigate aspects of bacterial physiology that can occur over short periods of time, such as spore germination. Therefore, we assessed whether the fluid from the upper gut would support the germination of the model organism *Clostridioides difficile*. Since primary conjugated bile acids (e.g., taurocholate) are known to promote *C. difficile* germination, we hypothesized that fluid from the upper gut would be conducive for germination. Using a heat resistance loss assay, we observed significantly more germination in the proximal and mid jejunum relative to the duodenum (Fig. 2.7A). While we also observed a correlation between *C. difficile* germination and taurocholate concentrations (e.g., the most potent bile acid germinant), germination was tied more to overall bile acid concentrations rather than the flux of the one particular bile acid (Fig. 2.7B). As discussed previously, relative ratios of bile acids in the upper gut do not change much over the short period of time we measured. Therefore, it is not surprising that the effects of taurocholate are mirrored by total bile acid concentrations.

2.4 Discussion

Our results demonstrate that the microbial communities inhabiting the GI tract are distinct and dynamic across different sites within the proximal GI tract. Our sampling procedure provided us with an opportunity to longitudinally characterize such microbial populations in conjunction with the administration of the commonly used drugs

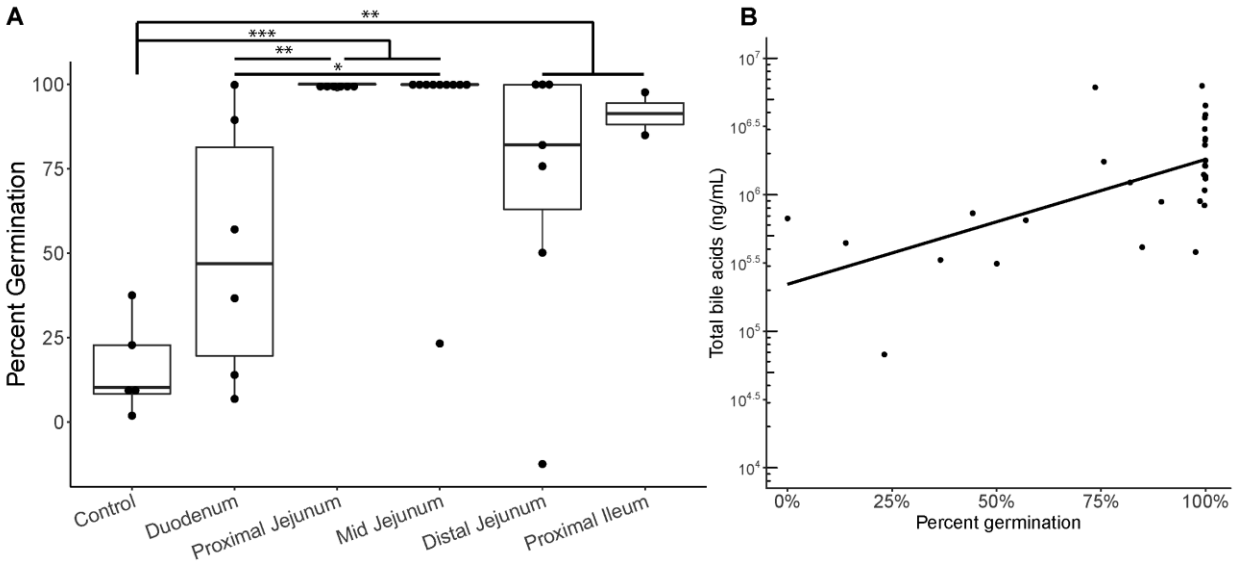

Figure 2.7: *C. difficile* germination in upper gut fluid correlates with total bile acids
A) *C. difficile* percent germination in upper gut fluid from the mesalamine study buffered at a pH of 7 (linear regression; * indicates $p < 0.05$; **, $p < 0.01$; ***, $p < 0.001$). **B)** Total bile acids (ng/mL) are plotted against *C. difficile* percent germination (linear regression, $p < 0.001$).

mesalamine and ibuprofen. We observed high stability of the microbiota in the jejunum compared to the stomach or duodenum, indicating that the indigenous microbiota residing in more proximal regions of the GI tract may experience greater changes. While we did not observe strong correlations between mesalamine or ibuprofen concentrations and particular microbiota members at any site, we did observe a strong correlation between the microbiota composition and pH, particularly in the duodenum. We also observed strong correlations between microbial phyla and total bile acid concentrations.

In this report, we describe the use of a multi-lumen catheter design with unique aspiration ports that enabled sampling of small intestinal content over the course of seven hours (229). Many studies aimed at investigating the microbiota of the proximal GI have overcome sampling difficulty in this region by using ileostoma effluent, samples from newly deceased individuals, or naso-ileal tubes. Although easy to access, ileostoma effluent does not fully recapitulate the distal small intestine, as it more closely resembles the colon than the small intestine due to increased oxygen concentrations near the stoma (251-254). Single lumen naso-ileal tubes are unable to sample multiple sites simultaneously (218, 220, 221, 255). GI fluid collected with our methodology was sufficient for determining mesalamine concentration, assaying fluid pH, and isolating microbial DNA across time and GI sites, which has not been previously described (229).

Our results support previous observations that the small intestine is dynamic with higher inter-individual than intra-individual variability (218, 221, 256). However, the mid to distal small intestine also contains a resilient microbial community composed of several highly abundant OTUs. This resilience is demonstrated by the shift from an altered to a normal ileal microbiota following the resolution of an ileostoma (257). This mirrors the

colonic microbiota, which also has a small community which is stable over long periods of time (253, 258, 259).

This and other studies have shown that the jejunal and proximal ileal microbiota are distinct from the colonic microbiota (90, 260). Despite changes in overall community structure and an overall decrease in microbial diversity across the stomach and small intestine compared stool, many of the same organisms commonly observed in stool were also present in the upper GI tract, albeit at very different abundances (90). Interestingly, colonic resection and ileal pouch-anal anastomosis has been shown to shift the terminal ileum microbiota to a state similar to the colon, suggesting that a colonic community structure can develop at these sites given the right conditions (221, 254, 260-262).

Many of the abundant microbes observed in our study, *Streptococcus*, *Veillonella*, *Gemella*, and Pasteurellaceae species, are also common residents of the oral cavity, which reflects the proximity of these locations in the GI tract. Populations of Proteobacteria, such as Pasteurellaceae, have also been observed consistently in the small intestinal microbiota in other studies, particularly in patients with IBD (214, 263-265). In our study, *Streptococcus* and *Veillonella* were correlated with pH in duodenal samples. It is possible that growth of these organisms drives a decrease in pH via metabolism of short-chain fatty acids, an observed functional capacity of these genera (221, 266). Conversely, large fluctuations in environmental pH may select for genera like *Streptococcus*, which have evolved a variety of mechanisms to control pH intracellularly (267-270). In any case, our data suggests a relationship between microbial dynamics and environmental physiology of the duodenum, which is an important observation to consider when comparing this site across individuals.

We observed little association between mesalamine and ibuprofen concentrations and changes in microbial relative abundance in our cohort. Several studies have reported differences in the fecal microbiota of patients with or without IBD, in particular Crohn's disease, which can affect the small intestine (263). Compositional shifts in the small intestine have been reported during IBD, specifically increased levels of Enterobacteriaceae species, such as *Enterococcus*, as well as others, such as *Fusobacterium* and *Haemophilus* (214, 264, 265). It has been hypothesized that mesalamine's ability to reduce inflammation in patients with ulcerative colitis could be by altering the microbiota (222, 223). While acute effects of mesalamine on the microbiota have not previously been reported, earlier work has demonstrated that mesalamine decreases bacterial polyphosphate accumulation and pathogen fitness, suggesting an influence on the microbiota (223). We did not observe strong correlations between mesalamine concentration and the microbiota here. However, our study was small, used different doses of mesalamine that may be metabolized differently across GI sites, and was conducted in healthy individuals (229). It is possible that mesalamine is less likely to impact the small intestinal microbiota compared to the large intestine; indeed, mesalamine is historically known to have a lower efficacy in treating Crohn's Disease, which manifests in the small intestine, compared to ulcerative colitis, which manifests in the large intestine (222, 271, 272). As indicated by the variability of mesalamine in the subjects in this study, the effects of mesalamine on the small intestinal microbiota may be highly individualized (229, 273-275). Furthermore, individuals with disease may harbor a distinct microbiota that responds to mesalamine differently. In regard to ibuprofen, while it can affect metabolism of certain bacteria in the short term, most of ibuprofen's effects

are observed to occur after days of continuous exposure (224-228). Therefore, our data confirm that short-term of exposure to ibuprofen has limited effects on the microbiota.

In addition to monitoring the effect of these drugs on the microbiota, we also measured correlations between bile acids and the microbiota. While we see associations between Firmicutes and Bacteroidetes and total bile acid concentrations, the interactions are obscured by what we know of bile acid effects on microbes *in vitro*. Traditionally, bile acids are more toxic to Gram-positive organisms (e.g., Firmicutes) and less to toxic to Gram-negative ones (e.g., Bacteroidetes) (276, 277). However, our results suggest as relationship that runs counter to these observations from *in vitro* experiments (276). Interestingly, rats given cholic acid in their diet experienced a marked decrease in the cecal Bacteroidetes/Firmicutes ratio as well as a loss in cecal community diversity (278). As Islam et al. observed, these changes are similar that which occur under a high fat diet (278, 279). Perhaps environments with high bile acid concentrations tend to also be associated with more accessible lipids for bacterial consumption due to the detergent like nature of bile acids. The opposite shift (i.e., a high Bacteroidetes/Firmicutes ratio) is observed in fecal communities of cirrhotic individuals, who tend to have much lower total bile acid concentrations (280). Another explanation is that these two community populations are spatially segregated, and our sampling method is unable to distinguish between mucosal- and luminal-associated communities. However, while sampling different spaces in the gut may explain some of the short-term variation we observe, previous work characterizing the microbiota of the upper gut has shown mixed results regarding the spatial organization of the small intestine, with some suggesting higher

Bacteroidetes abundance near the mucosa and some showing little difference (90, 211-213).

Based on our results, we see little bile acid metabolism in the upper gut. As bile acids travel the course of the gut, they are transformed from almost entirely conjugated bile acids with a relatively even mixture of primary and secondary bile, the latter having been recycled through enterohepatic circulation, to entirely unconjugated secondary forms. The geography of these transitions has not been well characterized until recently. In mice, bile acid modification occurs largely in the cecum and colon (281, 282). However, coprophagy can lead to higher bacterial abundance and bile acid metabolism in the small intestine (283, 284). This mirrors small intestinal bacterial overgrowth in the human gut and the resulting increased rate of deconjugation by microbes growing there (285, 286). Previous work in healthy humans has suggested that deconjugation occurs in the distal small intestine (e.g., ileum) and that 7α-dehydroxylation may not occur until the distal colon (287, 288). Our results build off this data to show that deconjugation does not occur until after the distal jejunum leaving conjugated bile acids intact for most of the small intestine. Together, these data suggest that metabolism requires a critical density of microbes that does not occur until later in the gut.

Bacteria entering the small intestine will encounter these high concentrations of conjugated bile acids. In the context of *C. difficile* colonization, conjugated bile acids (e.g., taurocholate) are key signals for its transition from dormant spore to actively growing cell. As has previously been suggested in murine models, our data provide the first evidence in humans that the bile acids present in the small intestine facilitate *C. difficile* spore germination (86, 289). Further research is required to understand the role germinating in

the small intestine plays in *C. difficile* infection and why *C. difficile*-associated disease is not observed in the small intestine, despite the possibility that it may be actively growing.

Despite the opportunity provided by our method to characterize the microbiota across the GI tract, our study has some lingering questions. Movement by the subject during the study can result in movement of each sampling port, particularly between the distal stomach and antrum. This may explain the inconsistent pH values and severe fluctuations of the microbiota observed in the stomach. Similarly, the shorter length of the sampling device, as compared to a naso-ileal catheter, prevented reliable collection of fluid from the distal small intestine, limiting our sampling to the proximal region. While we detected bile acids in the stomach, it is unclear what their physiological role is in this organ. It is also unclear whether the observed concentrations in the stomach are due to normal biological processes or due to the catheter holding the pyloric sphincter open during the sampling process. We also were limited to three concurrent fecal samples, each of which was low in Bacteroidetes, a profile generally observed in individuals on low fat-high fiber, non-Western diets (290). Due to an insufficient N, we were unable to ascertain whether this fecal microbiota composition was typical of our study population.

The use of a novel catheter allowed us to assess the microbiota across several proximal GI sites overtime, representing a powerful clinical and/or investigative tool for studying the small intestinal microbiota. Future studies on the upper GI microbiota should collect concurrent oral swab/sputum and fecal samples to strengthen the ability to “track” microbial populations across the GI tract, potentiating our ability to correlate the microbiota from fecal sampling, a more convenient method to study the microbiota, to other sites of the GI tract.

2.5 Supplemental Figures

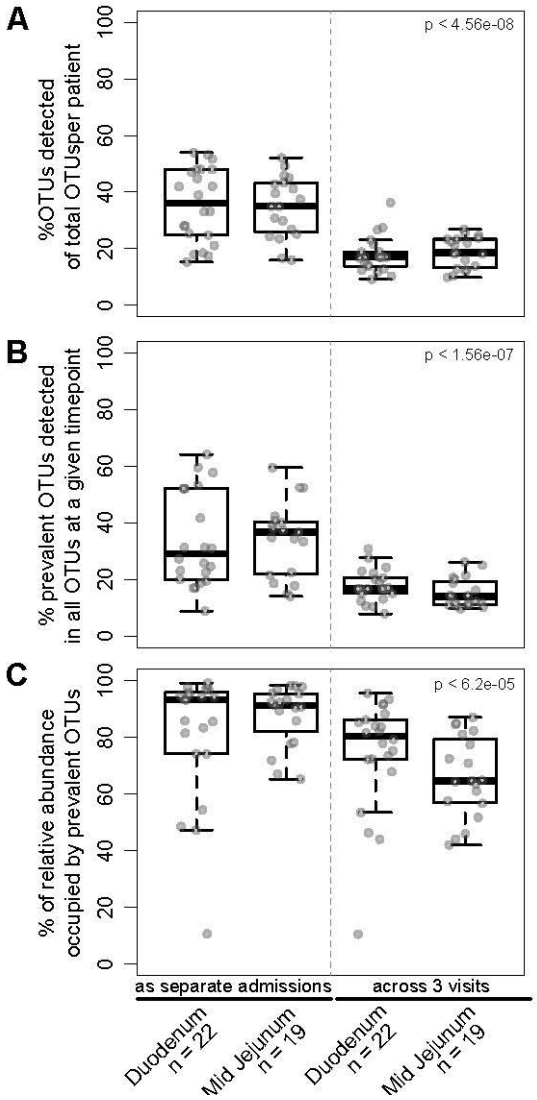

Supplemental Figure 2.1: Fluctuations in prevalent OTUs observed within subject M046 across the proximal GI tract over the course of three visits

Boxplots of **A)** the percentage of OTUs detected in a given sample out of all OTUs detected (all OTUs possible for that individual), **B)** the percentage of OTUs that were consistently detected at a subject-site out of the total OTUs detected in a given sample at a subject-site, and **C)** percent relative abundance explained by prevalent OTUs at a subject-site in the duodenum or stomach. The left-hand panel shows the data when the subject is treated as three separate admissions; the righthand panel shows the data when the subject is treated as the same individual across the board (example: a prevalent OTU would have to be present in all duodenal samples across all three visits to be considered a prevalent OTU in B). Statistical analysis: Kruskal-Wallis test.

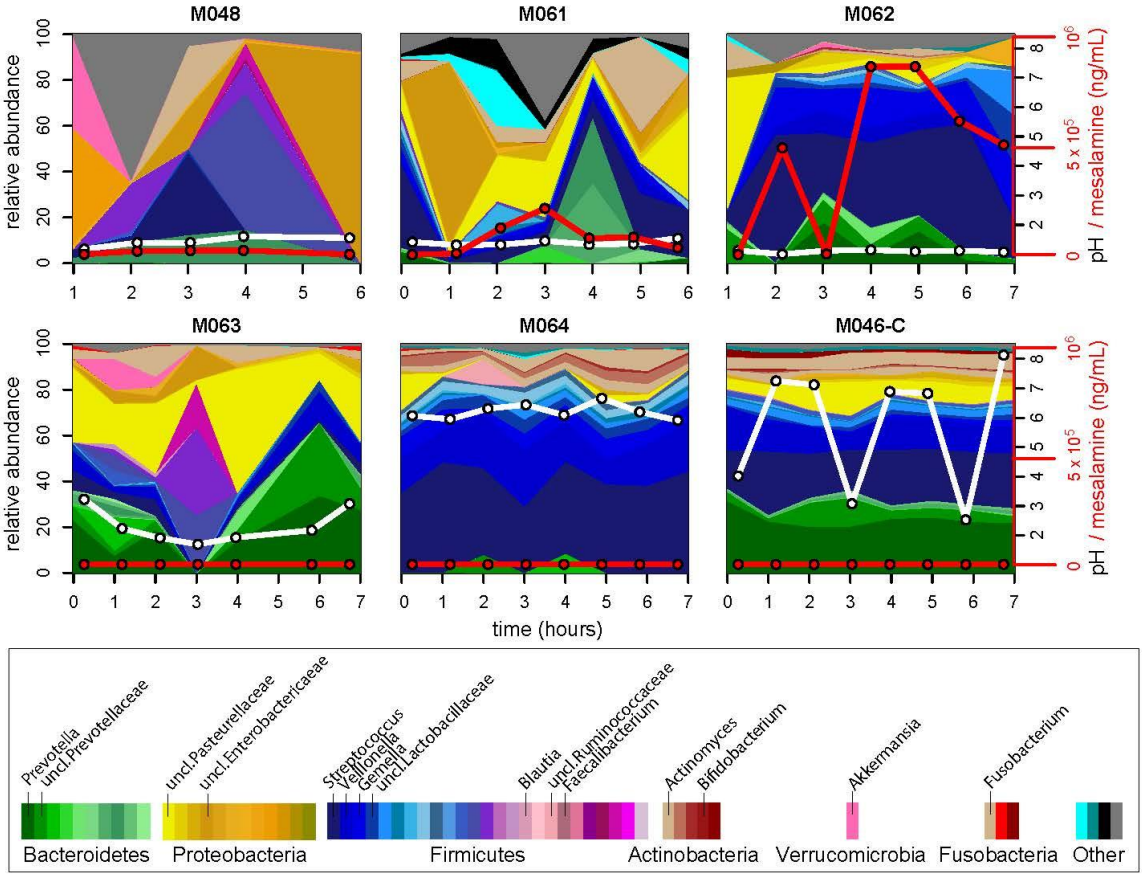

Supplemental Figure 2.2: Longitudinal compositional dynamics, mesalamine levels, and pH in the stomach

Streamplots of genus-level composition over time in the stomach of six individuals (%, left y-axis; genera coded in legend). White lines indicate pH measurements (black y-axis labels on right) and red lines indicate mesalamine concentration (red y-axis labels on right).

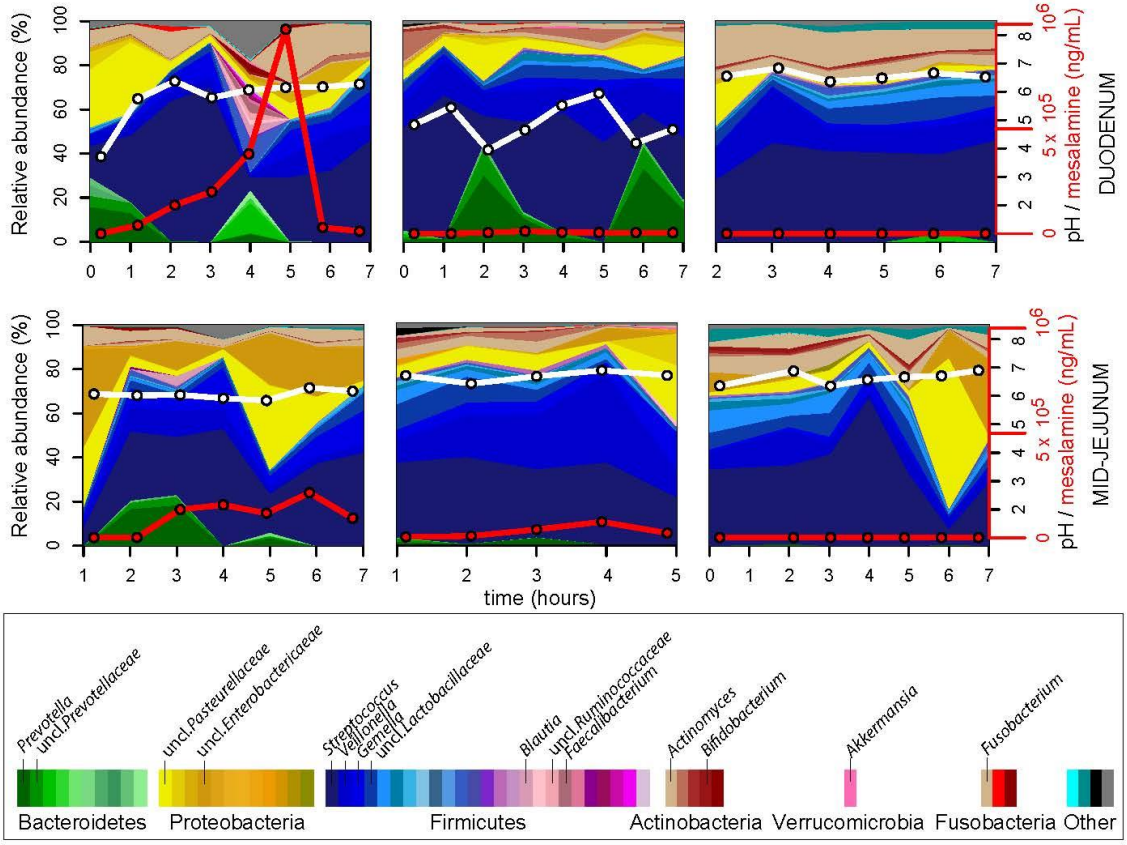

Supplemental Figure 2.3: Longitudinal compositional dynamics, mesalamine levels, and pH in the duodenum and jejunum of subject M046

Streamplots of genus-level composition over time in the duodenum (upper panels) and jejunum (lower panels) of one individual across three different visits (%, left y-axis; genera coded in legend). White lines indicate pH measurements (black y-axis labels on right) and red lines indicate mesalamine concentration (red y-axis labels on right).

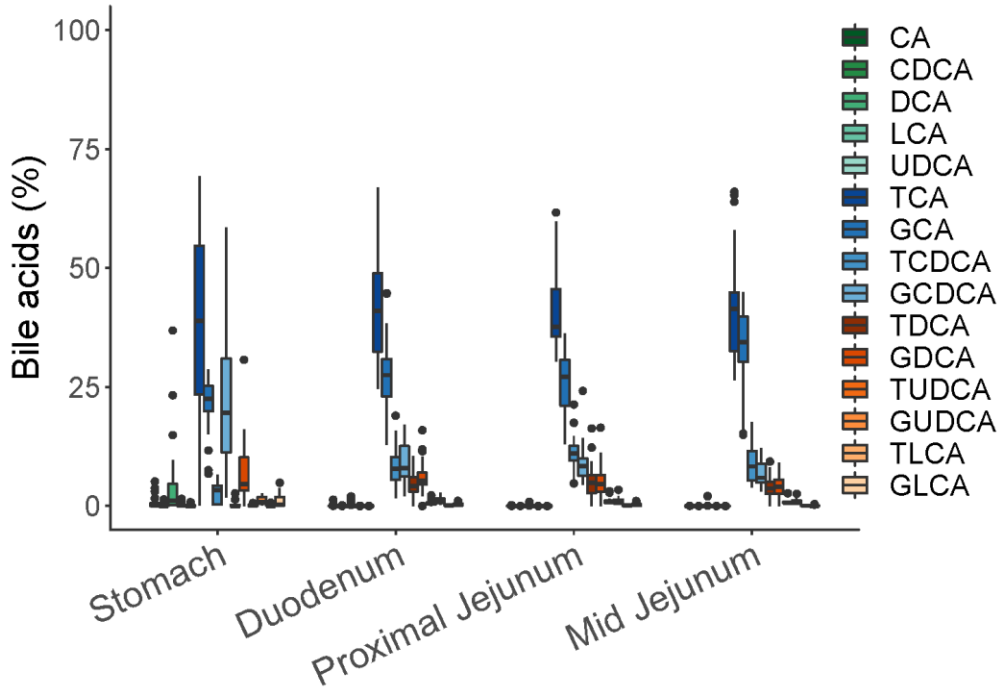

Supplemental Figure 2.4: Relative abundance of bile acids across the upper gut
Relative bile acid concentrations from all ibuprofen subjects plotted by upper gut site. Individual bile acids are colored in shades of their corresponding class (green = unconjugated, blue/purple = conjugated primary, orange = conjugated secondary).

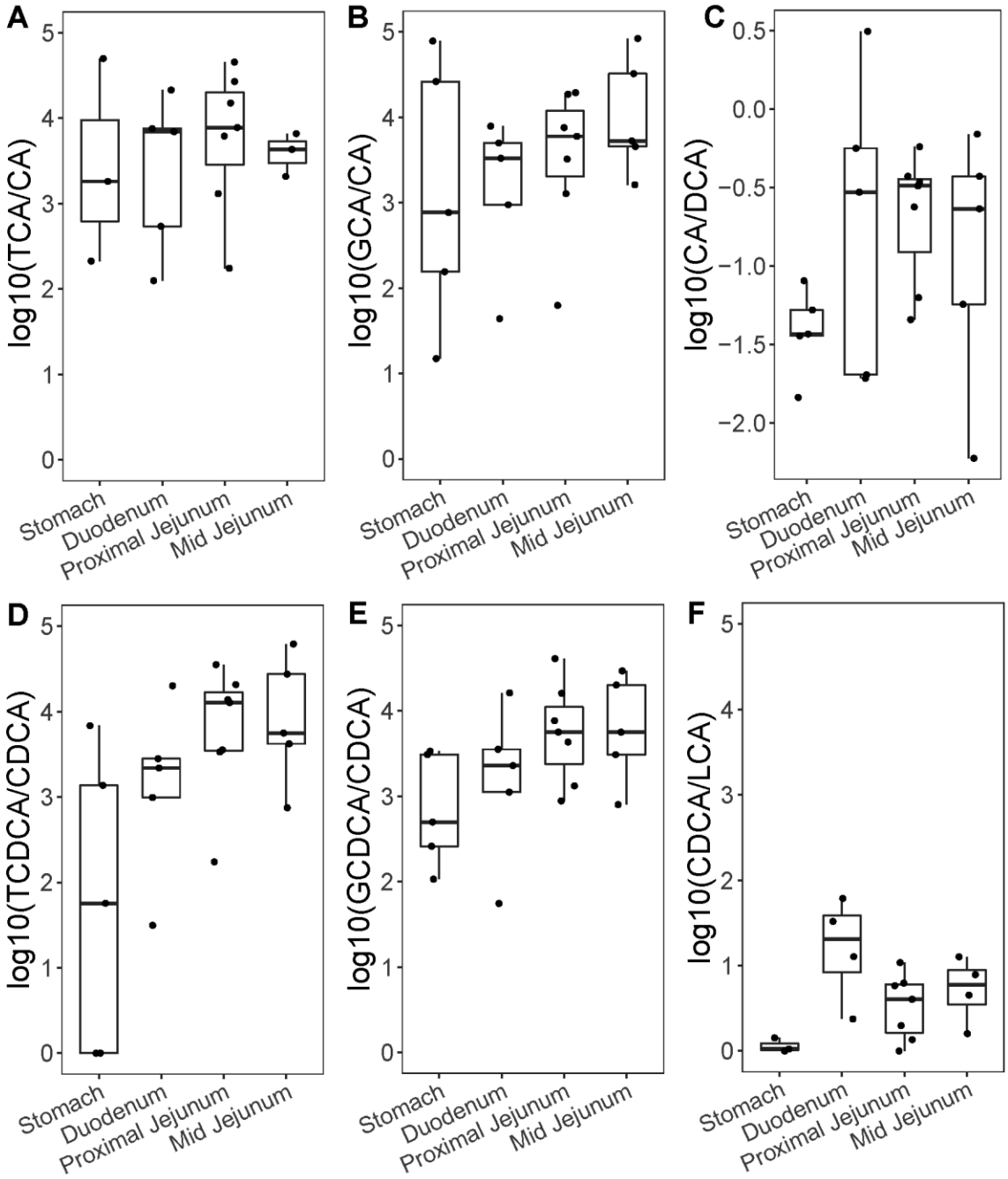

Supplemental Figure 2.5: Bile acid ratios at initial time points across the upper gut
The log10-transformed ratios of bile acids that are “metabolic pairs” in each section of the upper gut. Bile salt hydrolases deconjugate the **A & D)** taurine or **B & E)** glycine from primary bile acids. 7α-dehydroxylases can modify unconjugated primary bile acids into secondary forms, such as **C)** cholic acid into deoxycholic acid and **F)** chenodeoxycholic acid into lithocholic acid. Statistical test: Kruskal-Wallis (all comparisons are not significant).

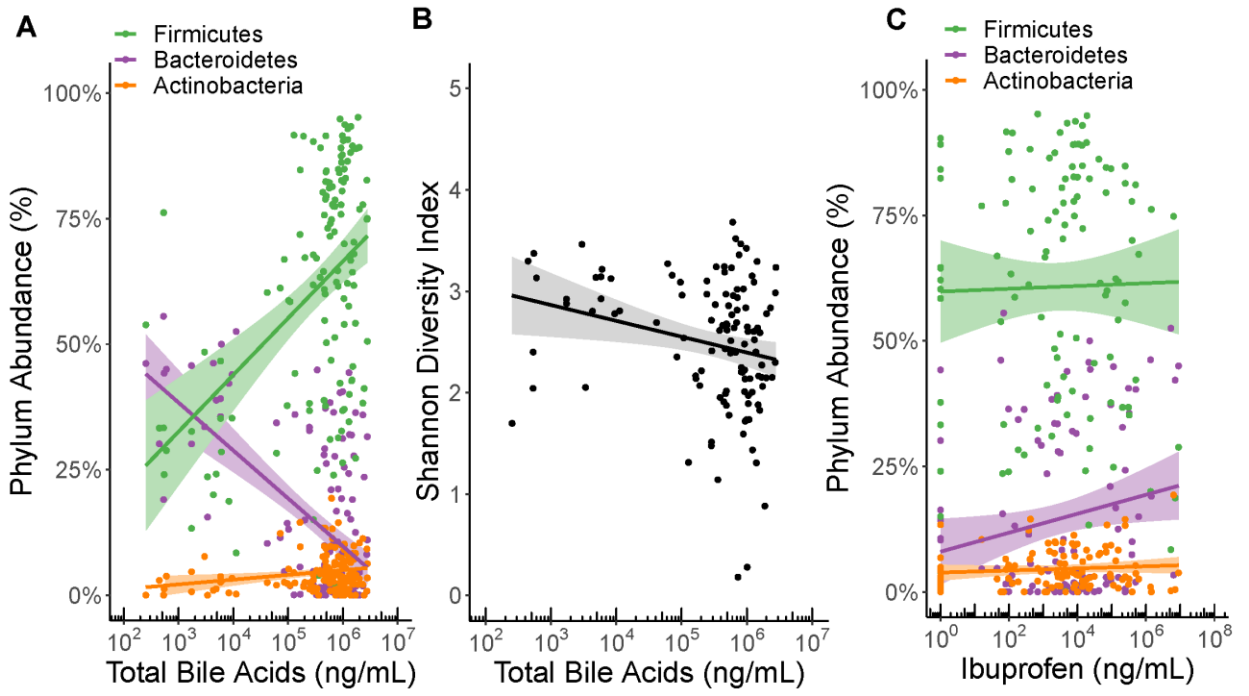

Supplemental Figure 2.6: Associations between microbial phyla and both bile acids and ibuprofen The three most abundant bacterial phyla (Firmicutes, Bacteroidetes, and Actinobacteria) were compared to **A)** total bile acid and **C)** ibuprofen concentrations. Associations from fed and fasted individuals are plotted side by side. Firmicutes ($p < 0.05$) and Bacteroidetes ($p < 0.05$) associated with the total bile acid concentrations but not Actinobacteria ($p = 0.92$). None were associated with ibuprofen concentrations. **B)** Shannon diversity index is compared to total bile acid concentrations (statistical analysis: mixed effect model, $p < 0.05$).

Chapter 3: Dietary Xanthan Gum Alters Antibiotic Efficacy Against the Murine Gut Microbiota and Attenuates *Clostridioides difficile* Colonization

A version of this chapter was published as:

Schnizlein MK, Vendrov KC, Edwards SJ, Martens EC, Young VB. Dietary Xanthan Gum Alters Antibiotic Efficacy against the Murine Gut Microbiota and Attenuates *Clostridioides difficile* Colonization. mSphere. 2020;5(1). doi: 10.1128/mSphere.00708-19.

3.1 Introduction

The microbiota plays an integral role in gut health by aiding in digestion and regulating colonic physiology (291, 292). Manipulating the microbiota to improve human health by either administering live bacteria (i.e., probiotics) or adding nondigestible, microbiota-accessible ingredients to the host's diet (i.e., prebiotics) has become a prominent area of biomedical research. While probiotics rely on exogenously added microbes for their effect, diet modification uses indigenous microbes already present in the gut to generate the beneficial effects described above. While the community as a whole may remain intact, diet modification can affect subsets of the community that are better suited to utilize the altered nutrient composition (293). This effect is most prominent in hunter-forager societies where seasonal dietary changes modulate the microbiota (290). In Western diets, a great emphasis has been placed on the types and abundance of host indigestible fiber polysaccharides that are only accessible by the microbiota, such as resistant starch, inulin or the fibers naturally present in fruits, vegetables and whole grains.

Dietary fiber promotes microbial short-chain fatty acid (SCFA) production. While SCFA profiles are unique from individual to individual, they provide a variety of benefits including increased colonic barrier integrity and decreased inflammation (294-299). Depending on the structure of the fiber backbone and side chains, polysaccharides select for unique taxa and as a result, unique fermentation profiles (300). Several key species may be responsible for degrading the fiber's carbohydrate structure, the byproducts of which go on to be metabolized by a number of additional taxa (134). Butyrate, a short chain fatty acid and product of fiber degradation, has been linked to increased gut barrier integrity and decreased inflammation (301-303). Fiber degradation and SCFA production are also associated with clearance of *Clostridioides difficile*, formerly known as *Clostridium difficile*, following fecal microbiota transfer (FMT) (170). Switching mice to a high fiber diet while colonized with *C. difficile* increased SCFA concentrations and also cleared the infection (31). Since *C. difficile* infection represents a significant healthcare burden, characterizing how these polysaccharides shape the gut environment and impact *C. difficile*'s ability to colonize will provide insight into how they might be used to improve patient outcomes.

Some polysaccharides included in food are added to alter texture rather than for nutritional benefit. Xanthan gum, synthesized by the bacteria *Xanthamonas campestris*, is a common food additive used as a thickener, particularly in gluten free foods, where industrial production is worth approximately $0.4 billion each year. Xanthan gum structure consists of (1→4)-linked *β*-D-glucose with trisaccharide chains containing two mannose and one glucuronic acid residues linked to every other glucose molecule in the backbone, with possible acetylation on the first branching mannose and 3,6-pyruvylation on the

terminal mannose (304). These negatively charged side chains give xanthan gum its viscous, gel-like properties. Although not specifically included in foods for its potential prebiotic activity, bacteria can degrade xanthan gum to increase fecal SCFA concentrations (305, 306). However, little is known about what bacterial taxa are involved in these transformations.

This study investigated the effect of xanthan gum on the bacterial composition of specific pathogen-free C57Bl/6 mice and its effect during an antibiotic model of *C. difficile* infection. Our goal for this paper was to (i) characterize the effects of xanthan gum on the mouse microbiota and (ii) characterize the effects of xanthan gum on *C. difficile* colonization. Surprisingly, we found that xanthan gum administration alters mouse susceptibility to *C. difficile* colonization by maintaining the microbiota during antibiotic treatment.

3.2 Methods

3.2.1 Ethics statement

The University Committee on Use and Care of Animals of the University of Michigan, Ann Arbor, approved all animal protocols used in the present study (PRO00008114). These guidelines comply with those set by the Public Health Service policy on Humane Care and Use of Laboratory Animals.

3.2.2 Animals and housing

We obtained five- to eight-week old, male and female mice from an established breeding colony at the University of Michigan. These mice were originally sourced from

Jackson Labs. We housed mice in specific pathogen-free and biohazard AALAC-accredited facilities maintained with 12 h light/dark cycles at an ambient temperature of 22 ±2^{o}C. All bedding and water were autoclaved. Mice received gamma-irradiated food (LabSupply 5L0D PicoLab Rodent Diet, a gamma-irradiated version of LabSupply 5001 Rodent LabDiet) or an equivalent diet with 5% xanthan gum added (95% LabSupply 5001 Rodent LabDiet, 5% xanthan gum [Sigma]; gamma-irradiated by manufacturer). We housed mice in groups of two to five animals per cage, with multiple cages per treatment group.

All cage changes, infection procedures, and sample collections were conducted in a biological safety cabinet (BSC) using appropriate sterile personal protective equipment between cage contacts. The BSC was sterilized with Perisept (Triple S, Billerica, MA) between treatment groups. Gloves were thoroughly sprayed with Perisept between each cage and completely changed between groups. A description of the metadata for the mouse experiments including cage number and treatment group can be found in Table S1.

3.2.3 Xanthan gum-cefoperazone mouse model

To investigate the effect of xanthan gum on cefoperazone treated mice, we switched mice to a diet containing 5% xanthan gum on day zero. Two days later, we gave mice 0.5 mg/mL cefoperazone (MP Biomedicals, Solon, OH) in the drinking water for 10 days as previously described to render the mice susceptible to *C. difficile* colonization (173, 307). We changed the antibiotic-water preparation every 2 days. Following 10 days of cefoperazone, we switched mice to Gibco distilled water. We orally gavaged mice with

between 10^2 and 10^4 *C. difficile* 630g spores or vehicle control (sterile water) 2 days after removing the mice from antibiotics. Spores were prepared as previously described and then suspended in 200 uL of Gibco distilled water and heat-shocked (173). Viable spores were quantified immediately after gavage using taurocholate cycloserine cefoxitin fructose agar (TCCFA) as previously described (173). To monitor infection severity, mice were weighed over the course of the model.

3.2.4 Xanthan gum-antibiotic cocktail mouse model

To investigate the effect of xanthan gum on an alternative antibiotic model (antibiotic cocktail with clindamycin), we switched mice to a 5% xanthan gum diet on day zero and then put on an antibiotic cocktail (0.4 mg/mL kanamycin, 0.035 mg/mL gentamicin, 850 U/mL colistin, 0.215 mg/mL metronidazole, and 0.045 mg/mL vancomycin; Sigma-Aldritch) for 3 days in their drinking water as previously described (308, 309). On day 5, we removed mice from oral antibiotic administration and returned them to regular drinking water. On day 7, mice were given an intraperitoneal (IP) injection of clindamycin hydrochloride (10 mg/kg). 1 day following the ip injection, we orally gavaged mice with between 10^2 and 10^4 *C. difficile* 630g spores and weighed mice as described above.

3.2.5 Quantitative culture

We suspended fresh fecal pellets in sterile, pre-reduced Gibco PBS (ThermoFisher) using a ratio of 1 part feces to 9 parts Gibco PBS, wt/vol (ThermoFisher,

Waltham, MA). We serially diluted these suspensions, plated them on TCCFA, and incubated the plates anaerobically at 37ºC for 18-24 hrs before counting colonies.

3.2.6 Fecal cefoperazone activity assay

We used fecal supernatant obtained from mice six days following the beginning of cefoperazone treatment (Day 8). The fecal content was diluted by a factor of 10 in PBS to test its activity on a lawn of *Escherichia coli* str. ECOR2, which is susceptible to cefoperazone. 10 uL of supernatant was added to a 0.7-cm diameter autoclaved Whatman filter paper (Sigma-Aldrich) disk and laid in duplicate onto an LB agar plate (BD Difco, Miller) streaked for lawn growth of *E. coli*. After incubating plates anaerobically at 37ºC for 24 hrs, we measured zones of inhibition (ZOI) and then confirmed after another 24 hrs of anaerobic growth. ZOI from samples were compared to those of fecal supernatant from mice not on antibiotics and PBS controls.

3.2.7 Lipocalin-2 ELISA

Fecal supernatants were diluted by 100-fold in PBS + 0.1% Tween 20 (USB Corp., Cleveland, OH) and then tested using the standard protocol for DuoSet ELISA kit for Mouse Lipocalin-2/NGAL (R&D Systems, Minneapolis, MN). Sample concentrations were normalized to g of feces and analyzed in duplicate.

3.2.8 **E. coli** *growth curve with cefoperazone*

We grew *Escherichia coli* str. ECOR2 overnight in LB broth (Difco LB Broth, Lennox; BD), pelleted the culture and then resuspended it in fresh LB. We back-diluted

this bacterial suspension into LB or LB containing 0.25% xanthan gum. Finally, we added cefoperazone to the growth medium before placing the cultures in a Sunrise microplate reader (Tecan, Switzerland) and monitoring growth for 48 hrs. OD600 measurements were automatically taken every 15 minutes with 60 seconds of shaking immediately prior to measurement.

3.2.9 16S rRNA-gene qPCR

We suspended fecal pellets in PBS as described above and centrifuged them at 6,000 rpm for 1 minute. 100-400 uL of supernatant was removed for metabolite analysis. Using the sedimented fecal content, we performed DNA extractions using the DNeasy PowerSoil Kit (Qiagen, Germantown, MD), according to the manufacturer's protocol. We immediately stored extracted DNA at -20°C until further use. We then performed qPCR on a LightCycler® 96 thermocylcer (Roche, Basel, Switzerland) using the PrimeTime® Gene Expression Master Mix (IDT, Coralville, IA) and a set of broad range 16S rRNA gene primers (310). All fecal DNA was amplified in triplicate with *Escherichia coli* genomic DNA standards in duplicate and negative controls in triplicate. The LightCycler reaction conditions were as follows: 95°C for 3 minutes, followed by 45 cycles of 2-step amplification at 60°C for 60 s and 95°C for 15 s. C_q values for each reaction were determined using the LightCycler® 96 software, and fecal DNA concentrations were determined by comparing C_q values to the standards in each plate and normalizing to each individual sample's fecal mass. We used Welch's 2-Sample T-Test to test for significance.

3.2.10 Short-chain fatty acid analysis

100 uL of fecal supernatants were filtered at 4^{o}C using 0.22 micron 96-well filter plates and stored at -80^{o}C until analysis. We transferred the filtrate to 1.5 mL screw cap vials with 100 uL inserts for high performance liquid chromatography analysis (HPLC) and then randomized them. We quantified acetate, propionate, and butyrate concentrations using a refractive index detector as part of a Shimadzu HPLC system (Shimadzu Scientific Instruments, Columbia, MD) as previously described (297). Briefly, we used a 0.01 N H_2SO_4 mobile phase through an Aminex HPX87H column (Bio-Rad Laboratories, Hercules, CA). Sample areas under the curve were compared to volatile fatty acid standards with concentrations of 40, 20, 10, 5, 2.5, 1, 0.5, 0.25, and 0.1 mM. Through blinded curation, we assessed baseline and peak quality and excluded poor quality data if necessary.

3.2.11 DNA Extraction and Illumina MiSeq sequencing

The detailed protocol for DNA extraction and Illumina MiSeq sequencing was followed as described in previous publications with modifications (173). Briefly, 200-300 uL of 10x diluted fecal pellet was submitted for DNA isolation using the MagAttract PowerMicrobiome DNA isolation kit (Qiagen, Germantown, MD). Samples were randomized into each extraction plate. To amplify the DNA, we used barcoded dual-index primers specific to the V4 region of the 16S rRNA-gene (233). Negative and positive controls were run in each sequencing plate. Libraries were prepared and sequenced using the 500-cycle MiSeq V2 reagent kit (Illumina, San Diego, CA). Raw FASTQ files,

including the appropriate controls, were deposited in the Sequence Read Archive (SRA) database (accession numbers SRX6897486 to SRX6897789).

3.2.12 Data processing and microbiota analysis

16S rRNA-gene sequencing was performed as previously described using the V4 variable region and analyzed using mothur. Detailed methods, processed read data, and data analysis code are described on GitHub (https://github.com/mschnizlein/xg_microbiota). Briefly, after assembly and quality control, such as filtering and trimming, we aligned contigs to the Silva v.128 16S rRNA database. We removed chimeras using UCHIME and excluded samples with less than 5000 sequences. We binned contigs by 97% percent similarity (OTU) using Opticlust and then used the Silva rRNA sequence database to classify those sequences. Alpha and beta diversity metrics were calculated from unfiltered OTU samples. We used LEfSe to identify OTUs that significantly associated with changes across diets and antibiotic treatments (311). We performed all statistical analyses in R (v.3.5.2).

3.2.13 Availability of data

Raw FASTQ files are available on the SRA. Code and detailed processing information, as well as raw data are available on GitHub (https://github.com/mschnizlein/xg_microbiota).

3.3 Results

3.3.1 Xanthan gum maintains the abundance of microbial taxa during cefoperazone treatment

Using C57Bl/6 mice, we tested the effects of xanthan gum on the microbiota using mouse models designed to study the effects of antibiotic perturbation. Since our initial goal was to study the effects of xanthan gum on *C. difficile* infection in mice, these models entailed multiple days of antibiotic treatment necessary to make the microbiota susceptible to *C. difficile* (Fig. 3.1A & Fig. S3.1A). Some mice were kept on a standard mouse chow diet; the rest were put on an equivalent diet supplemented with 5% xanthan gum.

In the cefoperazone mouse model, 16S rRNA-gene analysis of mouse fecal samples revealed a baseline microbiota dominated by Bacteroidetes (~45%) and Firmicutes (~35%), with the remainder of the community composed of Actinobacteria, Proteobacteria and Verrucomicrobia (Fig. 3.1B-C). Following cefoperazone treatment of mice on standard chow, Lactobacillaceae predominated a fluctuating community, as evidenced by increased mean Bray-Curtis distances between timepoints. While we also observed higher dissimilarity in the xanthan gum chow group following antibiotics, microbial communities were significantly more similar in the xanthan gum chow group compared to the standard chow group, as measured by Bray-Curtis distances. These data also indicated that by day 23 the microbial community in the standard chow group had not returned to the pre-antibiotic baseline (Mean Bray-Curtis day 2-day 23: 0.86) compared to the xanthan gum chow group (Mean Bray-Curtis day 2-day 23: 0.52).

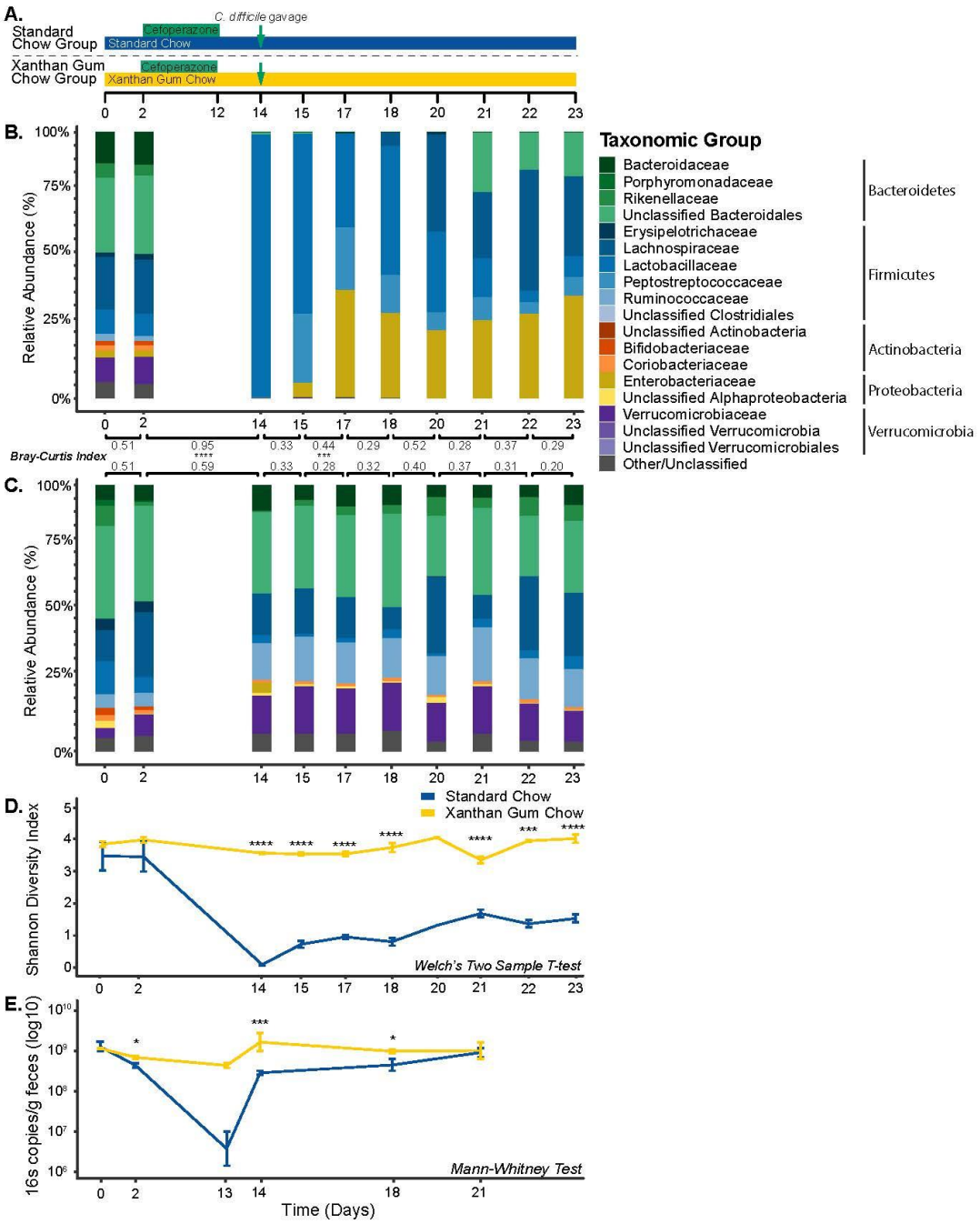

Figure 3.1: Fecal bacterial diversity and abundance during xanthan gum and cefoperazone administration

A) Timecourse of the experimental model for the mice on standard and xanthan gum chows. Mice were challenged with *C. difficile* on day 14. **B)** Microbiota mean relative abundance in mice on standard chow (N = 5). **C)** Microbiota mean relative abundance in mice on xanthan gum chow (N=6). Bray-Curtis dissimilarity index is shown comparing each timepoint. **D)** Mean Shannon diversity index of the bacterial communities shown in B. and C. (error bars indicate 1 std dev.). Statistical testing with Welch's Two-Sample T-test. **E)** Bacterial absolute abundance indicated by qPCR using "universal" primers for the 16S rRNA-gene (normalized to g of feces; error bars indicate 1 std. dev.). Statistical analysis: Mann-Whitney for β-diversity and 16S qPCR as well as Welch's Two-Sample T-test for Shannon Diversity (* indicates $p < 0.05$; ** $p < 0.01$, *** $p < 0.001$, **** $p < 0.0001$).

However, the relative abundance of bacterial taxa remained similar after cefoperazone treatment in mice fed 5% xanthan gum (Fig. 3.1C). These protective effects are reflected in a significantly higher Shannon Diversity and absolute abundance of fecal bacteria in xanthan gum-fed mice following cefoperazone treatment compared to those on standard chow (Fig. 3.1D-E). We also observed similar antimicrobial activity against an *Escherichia coli* strain ECOR2 lawn from fecal extracts obtained during antibiotic administration between diet groups and no inhibitory activity in fecal extracts from non-antibiotic treated control mice (Fig. S3.5B). These data suggest that high concentrations of xanthan gum prevent cefoperazone-mediated alterations to the mouse microbiota. To see if xanthan gum had a similar protective effect for other antibiotics, we also used an oral antibiotic cocktail model coupled with intraperitoneal clindamycin, which has also been shown to render mice susceptible to *C. difficile* colonization (308, 309). However, the microbiota differences between chow groups were less pronounced (Fig. S3.1B-C). Taken together, our results show that xanthan gum administration maintains both diversity and overall abundance of microbes in the gut during cefoperazone treatment.

Using the linear discriminant analysis algorithm LEfSe, we identified 35 OTUs that were significantly increased two days following the switch from standard to xanthan gum chow (Fig. S3.3). We also observed a shift in bacterial metabolism marked by significantly higher butyrate and propionate concentrations in mice on xanthan gum chow compared to those on standard chow (Fig. S3.4). No OTU abundances were identified as being significantly different when comparing the same timepoints in the standard chow group. Following cefoperazone treatment, 4 OTUs were increased and 80 OTUs were decreased in the xanthan gum group (Fig. S3.4). In the standard chow group, only 1 OTU

(Lactobacillus) significantly increased following cefoperazone treatment (Fig. S3.6). Unsurprisingly, 48 of the 112 OTUs that were negatively correlated with cefoperazone treatment in the standard chow group were also negatively correlated in the xanthan gum group.

3.3.2 Xanthan gum-mediated microbiota protection limits C. difficile *colonization*

Two days after the mice were removed from cefoperazone, they were challenged with *C. difficile* strain 630g spores administered by oral gavage. By monitoring feces for colony-forming units (both vegetative cells and spores), we observed approximately $1x10^6$ CFU/g feces *C. difficile* in mice on standard chow 1 day post-gavage (Day 15), which rose to $1x10^7$ for the duration of the experiment (Fig. 3.2). However, when on xanthan gum, only a small number of CFU was observed 1 day post-gavage but by day 4 (Day 19) all mice had cleared *C. difficile* (Fig. 3.2). In the antibiotic cocktail model, *C. difficile* colonized mice on both standard and xanthan gum chow similarly until 7 days post-gavage (Day 15) when *C. difficile* colonization levels were significantly lower in the mice on xanthan gum chow (Fig. S3.7).

3.4 Discussion

The use of dietary polysaccharides for their beneficial health effects, either directly on the host or indirectly through the microbiota, has been widely demonstrated (303, 305). In the context of *C. difficile,* diet may play a role in pathogen evolution, such as with trehalose, or influence colonization resistance, such as with dietary fiber and zinc

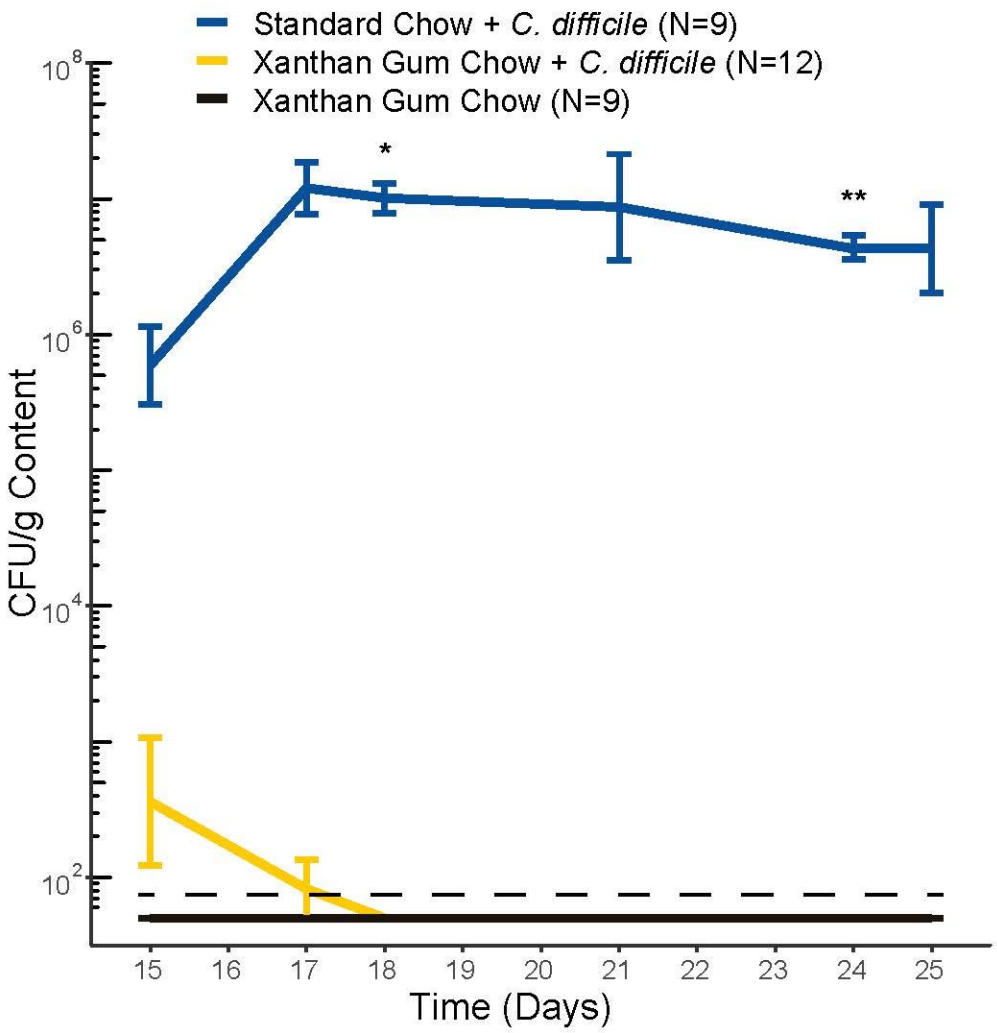

Figure 3.2: *C. difficile* colonization in mice on standard and xanthan gum chows
C. difficile colony-forming units (CFUs) in cefoperazone treated mice were normalized to fecal mass. Lines indicate mean CFU levels (error bars indicate 1 std dev). Data shown are from both experiments 1 and 2. Statistical testing was performed using Welch's 2 Sample T-Test (* indicates $p < 0.05$; ** $p < 0.01$).

(31, 199, 200, 312). Dietary alteration may shape the intestinal environment by altering the nutrients available or by modulating the concentrations of compounds toxic to *C. difficile*, such as secondary bile salts. As a common food additive, xanthan gum's physicochemical properties are well known (304). However, its impacts on the gut microbiota are poorly understood. Although we were not able to test whether xanthan gum enriches for fiber-degrading bacteria to increase colonization resistance, we did observe that xanthan gum interferes with the activity of orally administered antibiotics to protect mice from *C. difficile* colonization. These protective effects vary by type of antibiotic. While xanthan gum may have enriched for taxa capable of degrading it, these changes were minor compared to the much larger differences observed between diet groups during antibiotic treatment.

As a third-generation cephalosporin, cefoperazone has broad-spectrum efficacy (313, 314). As a result, it is not surprising that, in the standard chow group, it had a significant impact on microbiota community structure. These results agree with previously published work on cefoperazone's ability to disrupt the murine gut microbiota and cause lasting alterations even 6 weeks following cessation of treatment (232, 315). As demonstrated in this study, diet can affect antibiotic efficacy in unexpected ways. While both bacterial diversity and abundance were maintained in mice on xanthan gum, the similarities in OTUs identified by LEfSe between the two groups indicates that cefoperazone affected the microbiota in both groups but was attenuated in the xanthan gum chow group. Since we observed similar antimicrobial activity in feces from each diet group, our data suggests that cefoperazone is still active in the feces from these mice. We also demonstrated that xanthan gum chow itself did not have any inhibitory effect

directly on *C. difficile* (data not shown). These data indicate that cefoperazone retained antibiotic activity in the presence of xanthan gum, but its effect on the microbiota *in vivo* was somehow interfered with. This decreased antibiotic activity in the gut of xanthan gum-fed mice allowed the bacterial community to recover faster than in animals on standard chow.

By at least partially protecting the microbiota from the effects of cefoperazone, xanthan gum administration preserved colonization resistance to *C. difficile*. Colonization resistance comprises a variety of mechanisms including the metabolism of bile salts and competition for nutrients (316). Microbially-modified secondary bile salts inhibit *C. difficile* outgrowth much more than their primary precursors (79). Microbial metabolism mediates a variety of modifications to primary bile salts, including deconjugation by *Lactobacillus* and *Bifidobacterium* sp. as well as 7α-dehydroxylation by *Clostridium* sp. (317-320). The lack of secondary metabolites produced by these taxa has been correlated with a lack of colonization resistance (79, 80, 160, 321). The indigenous microbiota also prevents *C. difficile* from establishing itself within the colonic environment by limiting the nutrients available for growth (186, 322). A number of taxa, including the Lachnospiraceae, have been shown to provide resistance to *C. difficile* colonization, which may occur through niche competition (323, 324). Despite increased SCFA concentrations immediately following xanthan gum administration, direct alterations of the microbiota by xanthan gum did not appear to affect colonization resistance on the day of *C. difficile* gavage since SCFA concentrations had returned to baseline levels. By protecting the microbiota during antibiotic treatment, xanthan gum likely maintained these metabolic mechanisms to

exclude *C. difficile* from the gut. This suggested that while the community was altered, enough bacterial taxa remained to exclude *C. difficile*.

While we did not demonstrate a mechanism for xanthan gum's effect, its gel-like nature may interrupt the activity of antibiotics by altering their pharmacokinetics. Several large polysaccharides with negatively charged or polar sidechains, such as hydroxypropylmethyl cellulose, mannan oligosaccharides and guar gum, increase the excretion of cholesterol and bile salts in feces by limiting their absorption (325-331). While not previously reported, xanthan gum may also interact with these compounds. Similarities between the chemical structures of these sterol ring-containing compounds and of cefoperazone may result in interactions between xanthan gum and the antibiotic. The greater efficacy of the antibiotic cocktail plus clindamycin model against the microbiota is likely due to varied interactions with the five antibiotics in addition to the effect of the intraperitoneal injection of clindamycin. While potential alterations to the bile salt pool by xanthan gum may have limited *C. difficile* germination, we observed more fecal CFUs 1 day post-gavage (day 15) than what we used to inoculate the mice on day 14, suggesting that any disruptions to enterohepatic circulation did not prevent germination as there was some vegetative cell outgrowth. Furthermore, we have previously observed that few spores (i.e., <100) are sufficient to infect antibiotic-treated mice, suggesting that even if only a few spores germinated the mice would still become infected given that the vegetative cells can outgrow (unpublished data).

Polysaccharide-drug interactions are frequently explored as means to delay drug release *in vivo*. When mice consume xanthan gum in their chow, orally administered antibiotics may become trapped inside the gel formed by hydrated xanthan gum. Previous

research has shown that xanthan gum would provide time-dependent release that occurs at a slower rate than other large, polar polysaccharides. For example, hydroxypropylmethyl cellulose requires three times the concentration to achieve similar drug binding levels as xanthan gum (332, 333). The binding affinity of xanthan gum is pH-dependent, where higher pH limits drug release due to increased integrity of the polymer structure (333). Furthermore, environments with higher ionic strength as well as the presence of other polysaccharides increases xanthan gum's drug retaining efficiency (334, 335). Thus, the colonic environment would be conducive for high xanthan gum affinity for binding compounds such as cefoperazone due to its relatively higher pH.

In our study, dietary xanthan gum administration protected the microbiota during antibiotic treatment leading to the exclusion of *C. difficile* from the gut. While our study suggests that a common dietary polysaccharide interacts with the effects of antibiotics, there are several limitations that merit future research. Since few individuals will consume xanthan gum at the concentrations we used, titering in lower doses of xanthan gum to get closer to physiological levels would elucidate the effects of xanthan gum in a normal human diet. Future research should also characterize how polar polysaccharides such as xanthan gum interact with compounds in the gut. This would be important for understanding drug pharmacokinetics as well as the impact of xanthan gum on bile salts and enterohepatic circulation. Further work characterizing this common food additive would provide a greater understanding not only of how it is degraded in the gut it but also the potential positive effects of its fermentative byproducts.

3.5 Supplemental Figures

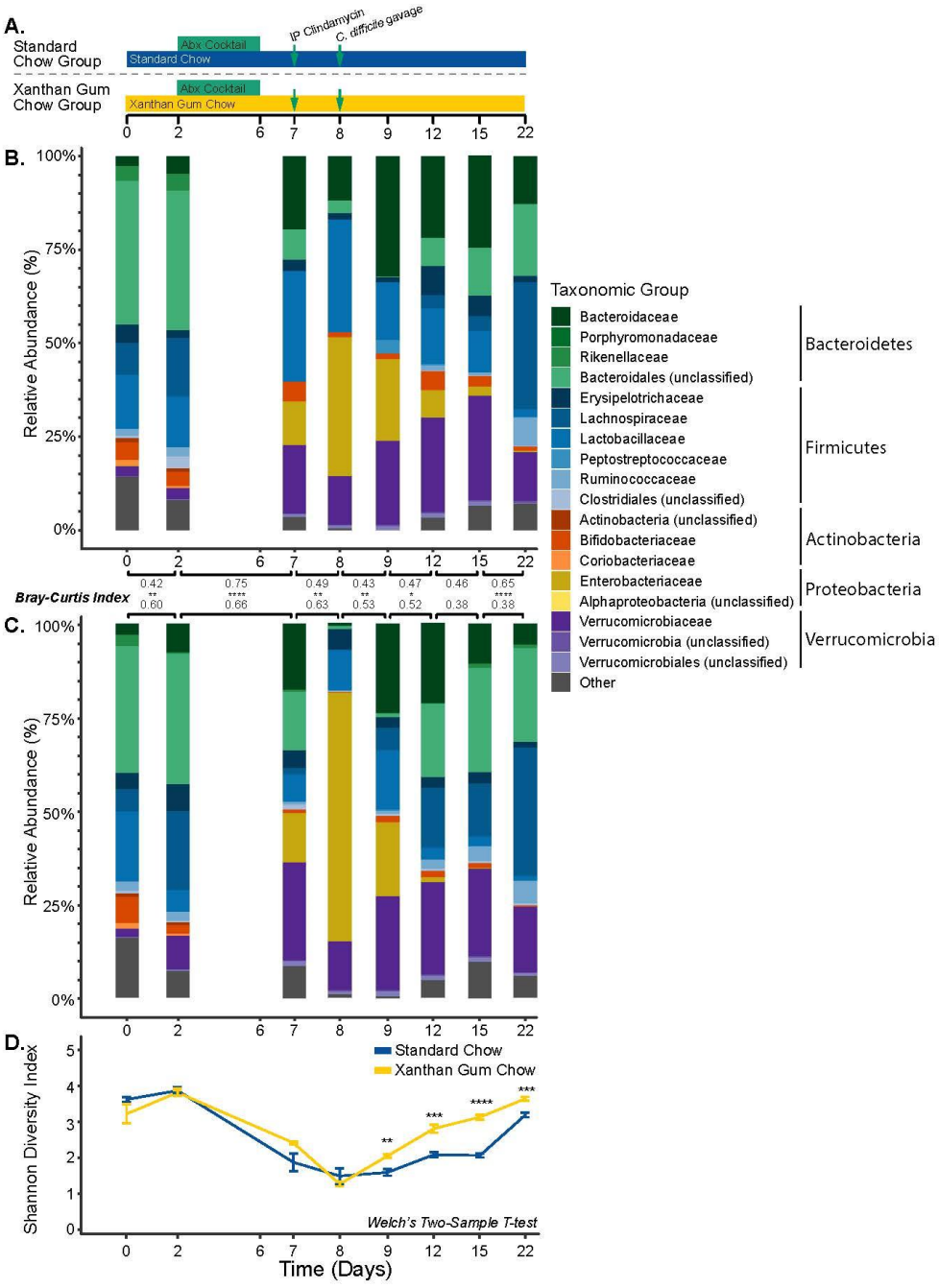

Supplemental Figure 3.1: Fecal (Days 0-15) and cecal (Day 22) bacterial diversity and relative abundance during xanthan gum and antibiotic cocktail administration
A) Time course of the experimental model for the mice on standard and xanthan gum chows. Mice were challenged with *C. difficile* on day 14. **B)** Microbiota mean relative abundance in mice on standard chow (N = 5). **C)** Microbiota mean relative abundance in mice on xanthan gum chow (N=7). Bray-Curtis dissimilarity index is shown comparing each timepoint. **D)** Mean Shannon diversity index of the bacterial communities shown in B. and C. (error bars indicate 1 std dev.). Statistical analyses: Mann-Whitney for β-diversity as well as Welch's Two-Sample T-test for Shannon Diversity (* indicates $p < 0.05$; ** $p < 0.01$, *** $p < 0.001$, **** $p < 0.0001$).

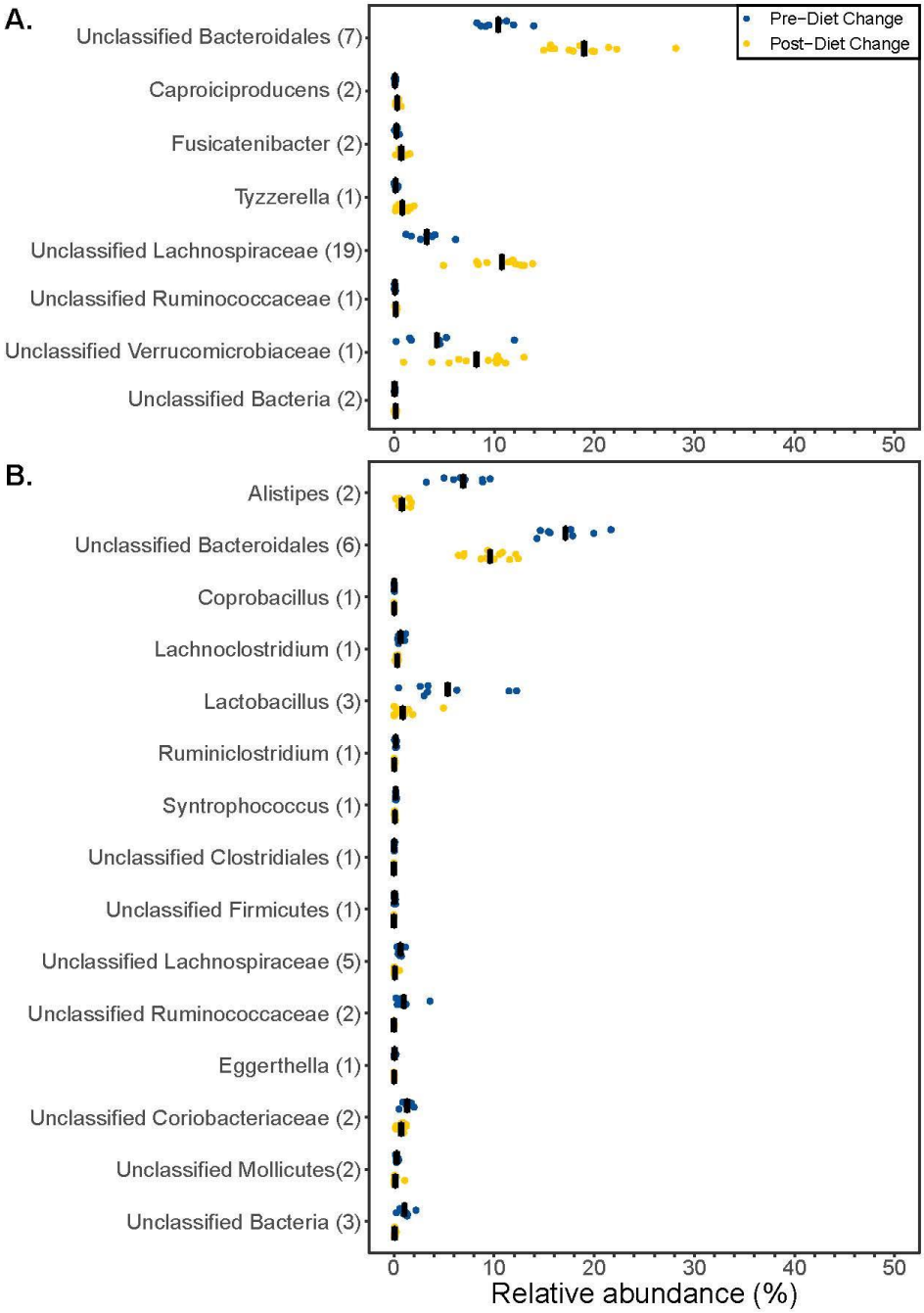

Supplemental Figure 3.2: LEfSe analysis of the microbiota of mice before and after the start of xanthan gum administration
Bacterial taxa that were **A)** increased or **B)** decreased following the switch to xanthan gum. The numbers in parentheses indicate the number of OTUs that fall under that particular taxonomic classification.

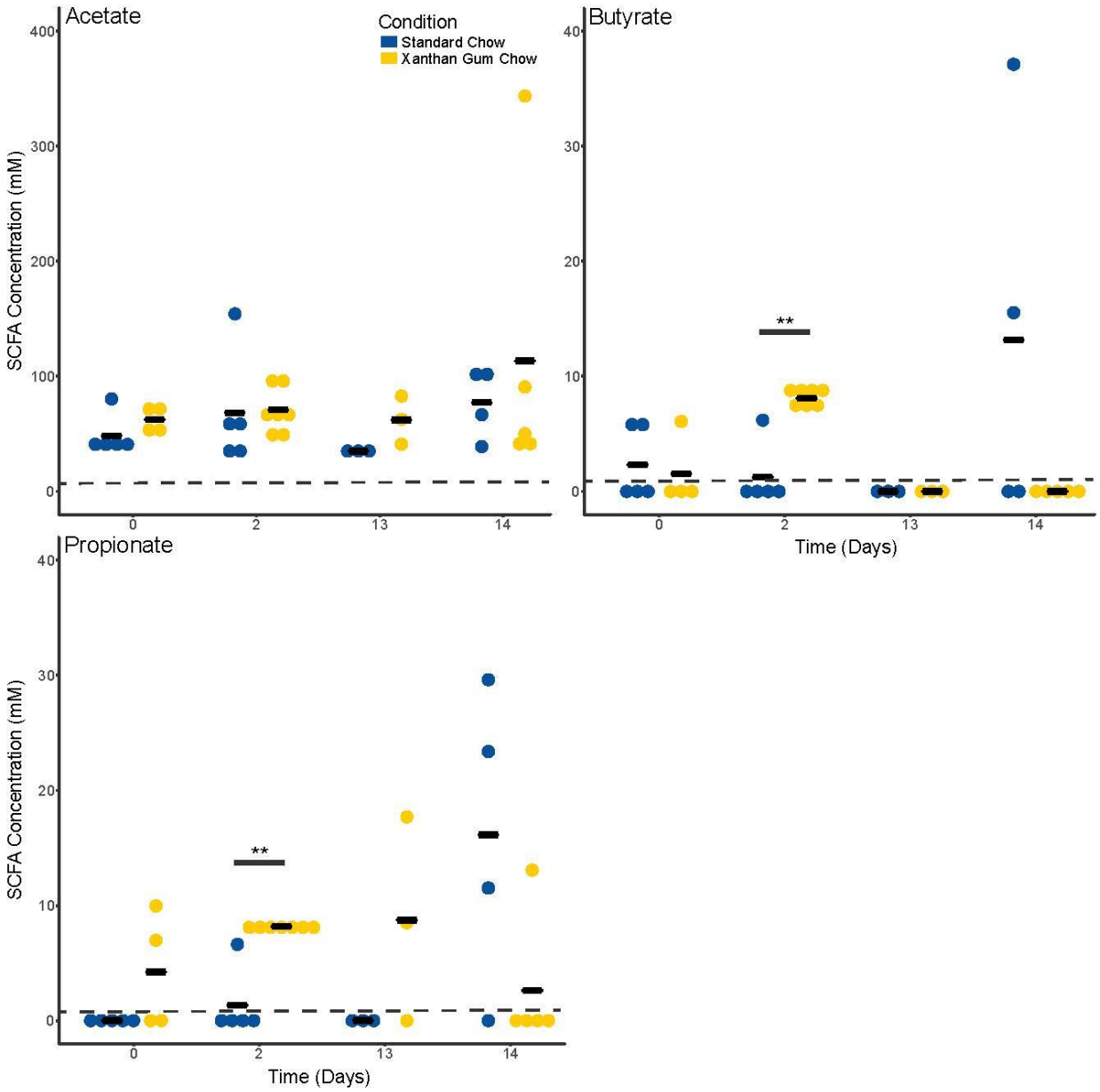

Supplemental Figure 3.3: Short chain fatty acid analysis
SCFA analysis (acetate, propionate, and butyrate) of mouse fecal content from the cefoperazone model. Time points show before (Day 0) and after diet change (Day 2) as well as after antibiotic treatment (Days 13 and 14). Statistics were performed using Welch's Two-Sample T-test. (** indicates $p < 0.01$).

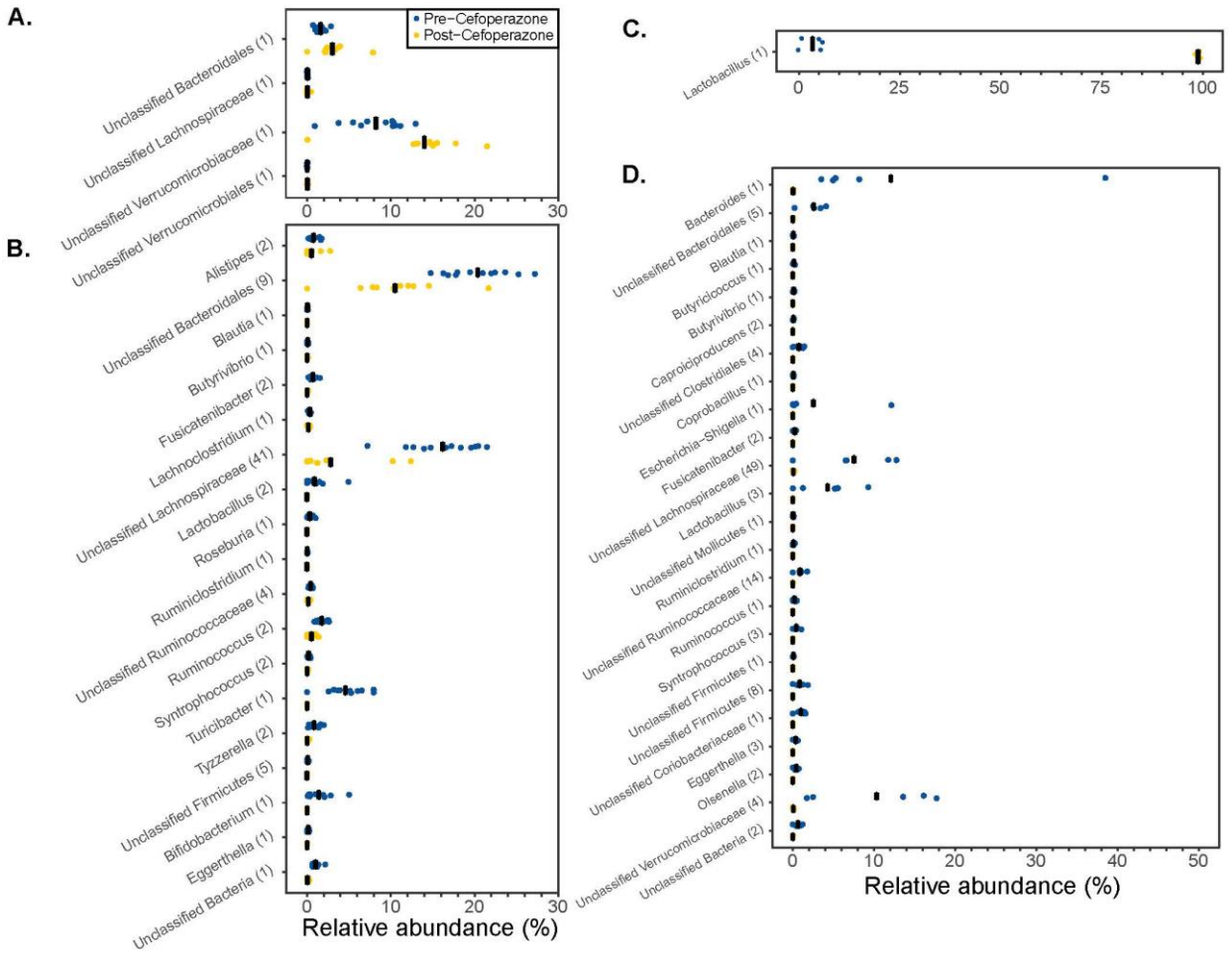

Supplemental Figure 3.4: LEfSe analysis of the microbiota in mice on xanthan gum (A. & B.) and standard chows (C. & D.) during cefoperazone treatment
Bacterial taxa that were **A** & **C)** increased or **B & D)** decreased following cefoperazone treatment. The numbers in parentheses indicate the number of OTUs that fall under that particular taxonomic classification.

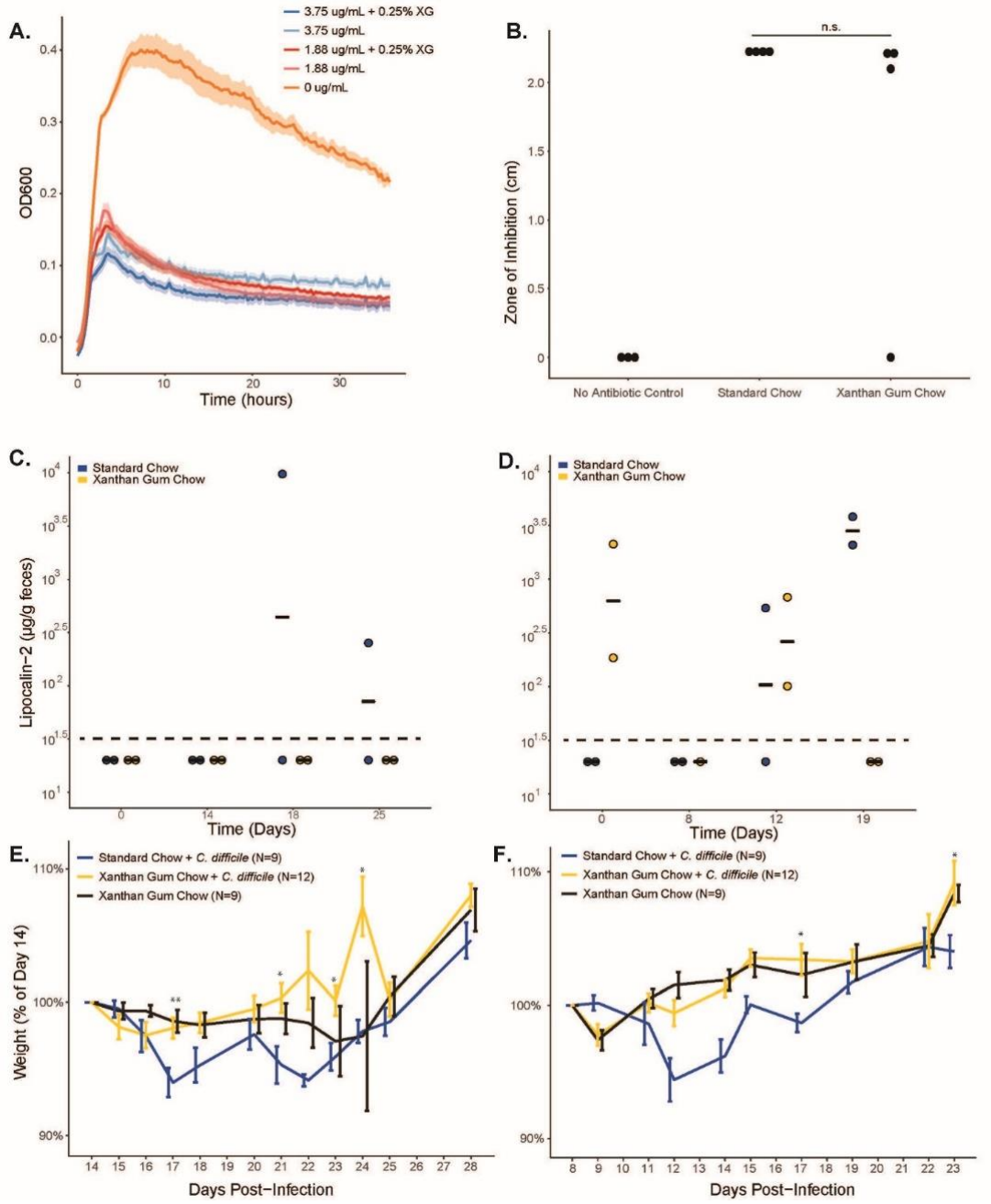

Supplemental Figure 3.5: Investigating the effect of xanthan gum in the *C. difficile* mouse model
A) *Escherichia coli* str. ECOR2 was grown in LB medium with concentrations of cefoperazone and low levels of xanthan gum. Line represents the average of three technical replicates and two biological replicates. **B)** Fecal cefoperazone activity was measured from fecal supernatants at day 8. The diameters of the zones of inhibition are plotted versus the dietary group. Supernatants from cefoperazone-treated mice on standard chow and xanthan gum chow were compared with healthy mouse fecal supernatant not on cefoperazone. Statistical analysis: Welsh's Two-Sample T-test (n.s. = not significant). Each dot represents the average of two technical replicates. **C-D)** Fecal lipocalin-2 was measured from fecal supernatants from mice in both the **C)** cefoperazone and **D)** antibiotic cocktail models. Each dot represents the average of two technical replicates. **E-F)** Mouse body weight was measured and is presented as a percentage of body weight on the day of *C. difficile* gavage in the **E)** cefoperazone and **F)** antibiotic cocktail models.

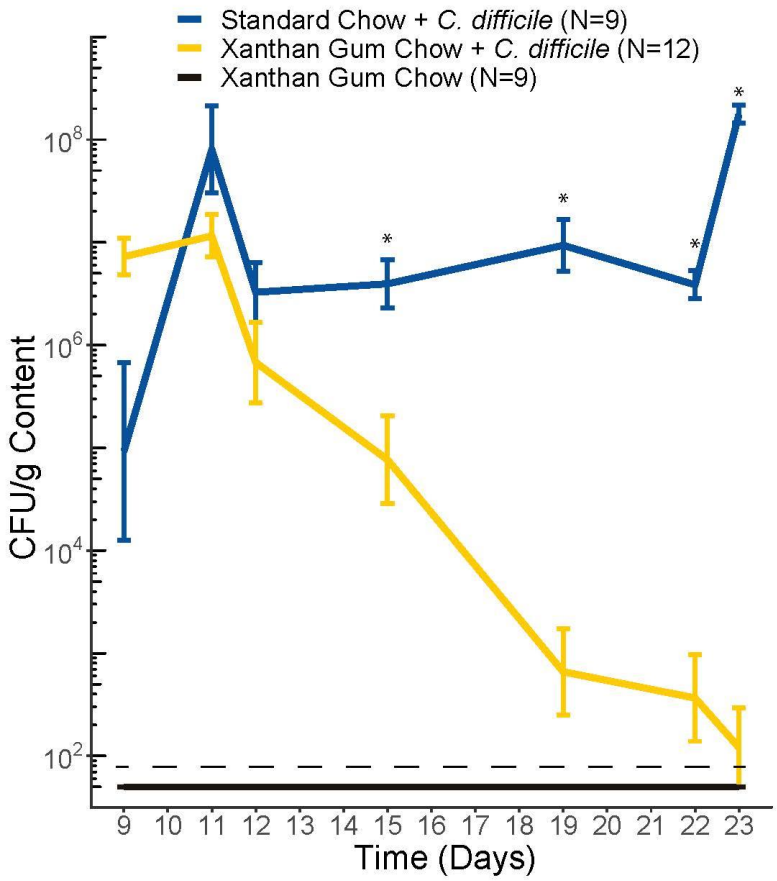

Supplemental Figure 3.6: *C. difficile* CFU in mice in the antibiotic cocktail model
C. difficile colony-forming units (CFUs) in antibiotic cocktail treated mice were normalized to fecal mass. Lines indicate mean CFU levels (error bars indicate 1 std dev). Data shown are from both experiments 3 and 4. Statistical testing was performed using Welch's 2 Sample T-Test (* indicates $p < 0.05$).

Chapter 4: Differences in Gut Microbiota Assembly Alter Its Ability to Metabolize Dietary Polysaccharides and Resist *Clostridioides difficile* Colonization

4.1 Introduction

The mammalian gut contains a complex ecosystem with a variety of fungal, bacterial, archaeal and viral organisms that exist in a network of metabolic interactions. These vast arrays of interactions regulate microbial competition and impact the host. External stability otherwise known as colonization resistance, is a complex phenomenon in which resident taxa prevent the invasion of foreign ones by occupying niches in an environment. For example, probiotic organisms fail to exist long-term in the gut because resident microbes are better able to compete for niche space (90). These interactions have also been observed to prevent colonization of pathogenic organisms such as *Escherichia coli*, *Salmonella* Typhimurium, and *Clostridioides difficile* (60-62).

In studying colonization resistance, several models have been used to ascertain characteristics of a resistant environment, including humans, mice, enteroids and bioreactors (336-343). Each of these models supports a unique level of complexity that may consider host-microbe interactions, microbe-microbe, and microbe-environment. Bioreactors have been used extensively to study the microbiota of the gut environment, particularly the dynamics of microbe-mediated colonization resistance. This is due in part to the controlled way nutrients flow in and out of the system. In the context of resistance to *C. difficile*, healthy human stool established in these reactors prevents or limits

colonization (344, 345). However, alterations to the resident microbiota can reduce the ecosystem's ability to do so (4, 345-348).

Since much of colonization resistance revolves around microbial metabolism, host dietary inputs play an important role in modulating this phenotype. As previous studies have demonstrated, both macronutrients (e.g., proteins and polysaccharides) and cofactors (e.g., vitamins and minerals) can modulate *C. difficile* colonization resistance by affecting the resident microbiota and host immune system (31, 184, 349). Much like "macroorganisms" adapt to the food available to them, microbes alter their metabolism to capitalize on the nutrient sources in their surroundings. These metabolic shifts lead to different downstream products with which other organisms in the ecosystem interact.

While previous work has characterized forced effects (e.g., antibiotic use) on microbiota post-establishment, limited work has characterized the stochastic processes of community establishment in the context of *C. difficile* colonization resistance (344, 350, 351). To manipulate the microbiota to treat infections, a fuller grasp of the ecological rules underlying community physiology is needed. Specifically, further work is required to accurately describe how random and specific effects alter community establishment and ability to resist the colonization of non-indigenous microbes. Here we describe how stochastic effects, as induced by community dilution, and directed effects, as induced by supplementation with additional carbohydrates, influence the establishment of a microbial community. We also characterize how the functional effects of this variation alter metabolic output and colonization resistance to *Clostridioides difficile.*

4.2 Methods

4.2.1 Stool collection

This study was approved by the University of Michigan's Institutional Review Board (IRB: HUM00141992). We recruited individuals over the age of 18 and who had no history of gastrointestinal disease, including IBD, IBS, Crohn's Disease and cancer. Individuals also had no history of antibiotic use or intestinal infection (bacterial or viral) in the previous six months. Exclusion criteria included immunocompromised status and immunosuppressant use. Following informed consent, we provided enrolled subjects with a commode specimen collection hat and conical tubes for collection. We then instructed them to store their stool sample at -20^{o}C after collection. Upon receipt of each sample, we compensated subjects, and stored the sample at -80^{o}C until use. For the experiments in this manuscript, we recruited two male individuals, aged 29 and 32.

4.2.2 Bioreactor set-up and operation

Minibioreactor array operation has been previously described (344). Briefly, we submitted designs for bioreactors to be constructed through stereolithography by ProtoLabs, Inc. (Maple Plain, MN). Bioreactors were composed a thermostable resin per designs shared with us through a collaboration with Robert Britton (Baylor University, Houston, TX) (344). We filled reactors with 15 mL of bioreactor media (BRM) prepared as previously described except that we sterilized bovine bile (Sigma, St. Louis, MO) by filtering at 0.22 µm. Throughout the experiments, we used a reactor volume of 15 mL BRM. Once we established continuous flow, multichannel Watson Marlow peristaltic

pumps (Falmouth, UK) individually maintained media flow to each reactor (1 rpm, 0.89 mm bore tubing) at a rate of 0.13 mL/hr.

4.2.3 Bioreactor dilution experiment

To prepare the fecal inoculum, we suspended fecal content from Subject A in sterile, pre-reduced phosphate-buffered saline (PBS; Thermo Fisher) at a ratio of 1:2. Feces were serially diluted by 10-fold to 10^{-3}, 10^{-5}, 10^{-7}, and 10^{-9} in sterile, pre-reduced PBS and established in reactors in sextuplicate (N = 4 for 10^{-3}). After 24 hrs of static culture, we initiated continuous flow and allowed to grow for 6 days before challenging with vegetative *Clostridioides difficile* str. 630 (Fig. 4.1A). Immediately before *C. difficile* challenge, we screened all reactors for possible contamination by plating on cycloserine-cefoxitin-fructose agar containing 0.1% taurocholate (TCCFA), which we prepared as previously described (173). To prepare *C. difficile* for challenge, we streaked spores onto agar plates containing taurocholate. After 1 day of anaerobic incubation at 37^{o}C, we inoculated *C. difficile* into 10 mL of sterile, pre-reduced BRM. After approximately 16 hrs, we back-diluted 1 mL of the culture in BRM by 10-fold and monitored to ensure *C. difficile* was in a log-phase of growth. Upon reaching OD 0.1, we again back-diluted the *C. difficile* culture in BRM and then inoculated into each reactor. We took 1 mL samples from the reactors at days 0 (i.e., the start of flow), 2, 3, 6, 7, 9 and 10. We immediately pelleted cells, and transferred the supernatant to be stored separately at -80^{o}C. To assess *C. difficile* colonization, we enumerated colony-forming units (CFU) by serial dilution and plating on TCCFA.

4.2.4 Bioreactor carbohydrate experiment

To prepare the fecal inoculum, we suspended fecal content from Subject B in PBS as described above and then serially diluted to 10^{-3}, 10^{-4}, 10^{-5} and 10^{-6}. We established fecal dilutions into the bioreactors in triplicate. After 24 hrs of static culture, we established continuous flow using BRM (Fig. 4.4A). After 48 hrs of continuous flow, we switched source media for the reactors in each dilution group to BRM containing 10-fold higher inulin than standard BRM, increasing inulin concentrations from the 0.02% present in basal media to 0.2%. We gave reactor communities 5 days under these conditions before challenging with *C. difficile* on day 7 as described above. We took 1 mL samples at days 0, 2, 5, 6, 7, 8, 10 and 11. During sampling, we pelleted cells and transferred the supernatant to store at -80^{o}C. We then resuspended the pellet in RNAprotect Bacteria Reagent (Qiagen, Germantown, MD). We measured pH on day 10 of the experiment using MColorpHast pH test strips (Sigma).

4.2.5 DNA extraction and 16S rRNA-gene sequencing

We followed a detailed protocol for DNA extraction and Illumina MiSeq sequencing as previously described in previous publications with modifications (173). For the dilution bioreactor experiment, we pelleted cells and froze them at -80^{o}C. In preparation for sequencing, cells were bead beaten in molecular grade water using 0.1 mm silica beads for 2 minutes. We then submitted cell extracts to the University of Michigan Microbiome Core for sequencing. For the carbohydrate bioreactor experiment, we pelleted cells and resuspended in Qiagen RNAProtect Bacteria Reagent before storing at -80^{o}C. In preparation for sequencing, we submitted samples to the University of Michigan

Microbiome Core for extraction using the Qiagen MagAttract PowerMicrobiome DNA/RNA Isolation Kit. For both experiments, we randomized samples into each extraction plate. To amplify the DNA, we used barcoded dual-index primers specific to the V4 region of the 16S rRNA-gene, and ran negative and positive controls in each sequencing plate (233). We prepared and sequenced libraries using the 500-cycle MiSeq V2 reagent kit (Illumina, San Diego, CA). Contact the author for raw FASTQ files, including the appropriate controls.

4.2.6 Data processing and microbiota analysis

We performed 16S rRNA-gene sequencing as previously described using the V4 variable region and analyzed using mothur (234). Detailed methods, processed read data and the data analysis are described on GitHub (https://github.com/mschnizlein/cdiff_foundereffects). Briefly, after initial steps, such as assembly and quality control, we aligned contigs to the Silva v. 138 16S rRNA database (235). We removed chimeras using UCHIME and excluded samples with less than 1000 sequences (236). We binned contigs into operational taxonomic units (OTUs) by 97% percent similarity using Opticlust and used the Silva rRNA sequence database to classify those sequences (235, 237). Alpha and beta diversity metrics were calculated from unfiltered OTU samples. After subsampling to 2000 sequences, we used Dirichlet Multinomial Modelling (DMM) to identify bacterial enterotypes based on genus-level classification and then used LEfSe to identify taxa that significantly associate with each of these community types (311, 352). We performed all statistical analyses in R (v. 4.1.1)

using the following packages: ggplot2, reshape2, plyr, tidyverse, ComplexHeatmap, and scales (240-243, 353, 354).

4.2.7 16S rRNA-gene qPCR

Using dilutions of *Escherichia coli* ECOR2 genomic DNA as standards, we performed qPCR using PrimeTime gene expression master mix (IDT, Coralville, IA) and a set of broad-range 16S rRNA gene primers on a Thermo Fisher QuantStudio 3 (310). The DNA samples, standards, and negative controls were all amplified in triplicate. The qPCR reaction conditions were as follows: 95°C for 3 min, followed by 40 cycles of two-step amplification at 95°C for 15 s and 60°C for 60 s. The quantification cycle (Cq) values for each reaction were determined by using the Thermo Fisher Cloud software, and sample DNA concentrations were determined by comparing Cq values to the standards in each plate.

4.2.8 **C. difficile** ***growth curves***

We isolated *C. difficile* strain 630g from a spore stock by growing overnight on BHI agar (BD) supplemented with 0.01% L-cysteine hydrochloride monohydrate (BHI; Sigma) and 0.1% taurocholate (Sigma). Growth curves were conducted with two biological replicates grown from two unique colonies. After growing overnight in BHI, we back-diluted cultures in fresh BHI with the overnight sample, and optical density was monitored to ensure cultures were in log-phase growth. Prior to the growth assay, we pelleted the culture, and then resuspended it in fresh 2x concentration BHI. We mixed this bacterial suspension into sodium butyrate solutions buffered at pH 7 with PBS ranging from 160mM

to 2.5mM (2x final concentrations). The cultures were then placed in a 96-well plate optical density reader (Tecan, Switzerland) and monitored for 24 hours. All conditions were run with three technical replicates. Optical density measurements at 600 nm were automatically taken every 15 min, with 60 s of shaking immediately prior to measurement. We repeated this protocol in a follow-up experiment but substituted BHI for BRM in all steps following *C. difficile* colony isolation.

4.2.9 Short-chain fatty acid analysis

100 uL of fecal supernatants were filtered using 0.22 micron 96-well filter plates and stored at -20^{o}C until analysis. We transferred the filtrate to 1.5 mL screw cap vials with 100 uL inserts for high performance liquid chromatography (HPLC) analysis and then randomized them. We quantified acetate, propionate, and butyrate concentrations using a refractive index detector as part of a Shimadzu HPLC system (Shimadzu Scientific Instruments, Columbia, MD) as previously described (297). Briefly, we used a 0.01 N H_2SO_4 mobile phase in filtered, Milli-Q water through an Aminex HPX87H column (Bio-Rad Laboratories, Hercules, CA). Sample areas under the curve were compared to volatile fatty acid standards with concentrations of 40, 20, 10, 5, 2.5, 1, 0.5, 0.25, and 0.1 mM. Through blinded curation, we assessed baseline and peak quality and excluded poor quality data if necessary.

4.3 Results

4.3.1 Dilution of starting inoculum alters establishment dynamics of continuous flow cultures

Using a bioreactor system initially developed by Auchtung et al., we extended studies on how dilution impacts the membership and variability of microbial communities (344, 351). We established communities in bioreactors from serially diluted stool samples taken from a healthy human donor (10^{-3}, N=4; 10^{-5}, 10^{-7}, and 10^{-9}, N=6). Following inoculation of the reactors, communities were given one day to equilibrate in static culture before initiating continuous flow. The subsequent 6 days in continuous flow allowed communities time to adjust before testing their external stability with a model invasive bacterium, *C. difficile* (Fig. 4.1A).

Dilution increased the variability of communities and lowered the number of taxa that became established. By day 6, 16S rRNA-gene sequencing analysis showed that 93±6 and 60±15 operational taxonomic units (OTUs) became established in those communities diluted 10^{-3} and 10^{-5}, respectively (Fig. 4.1B & Fig. S4.1A). Communities from these stool dilutions consisted mainly of Bacteroidota and Bacillota (Fig. 4.1D-E). Reactors established with more diluted fecal inocula had fewer OTUs established by day 6 (i.e., 10^{-7} and 10^{-9} dilutions had 45±20 and 40±23 OTUs, respectively) and also more varied phyla abundance, with some being dominated by Actinomycetota and others by Pseudomonadota (Fig. 4.1B & Fig. 4.1F-G). More diluted inocula established in individualized community structures in each reactor replicate (Fig. S4.1C-F). Dissimilarity between replicate reactors in each group increased as the dilution factor increased, as

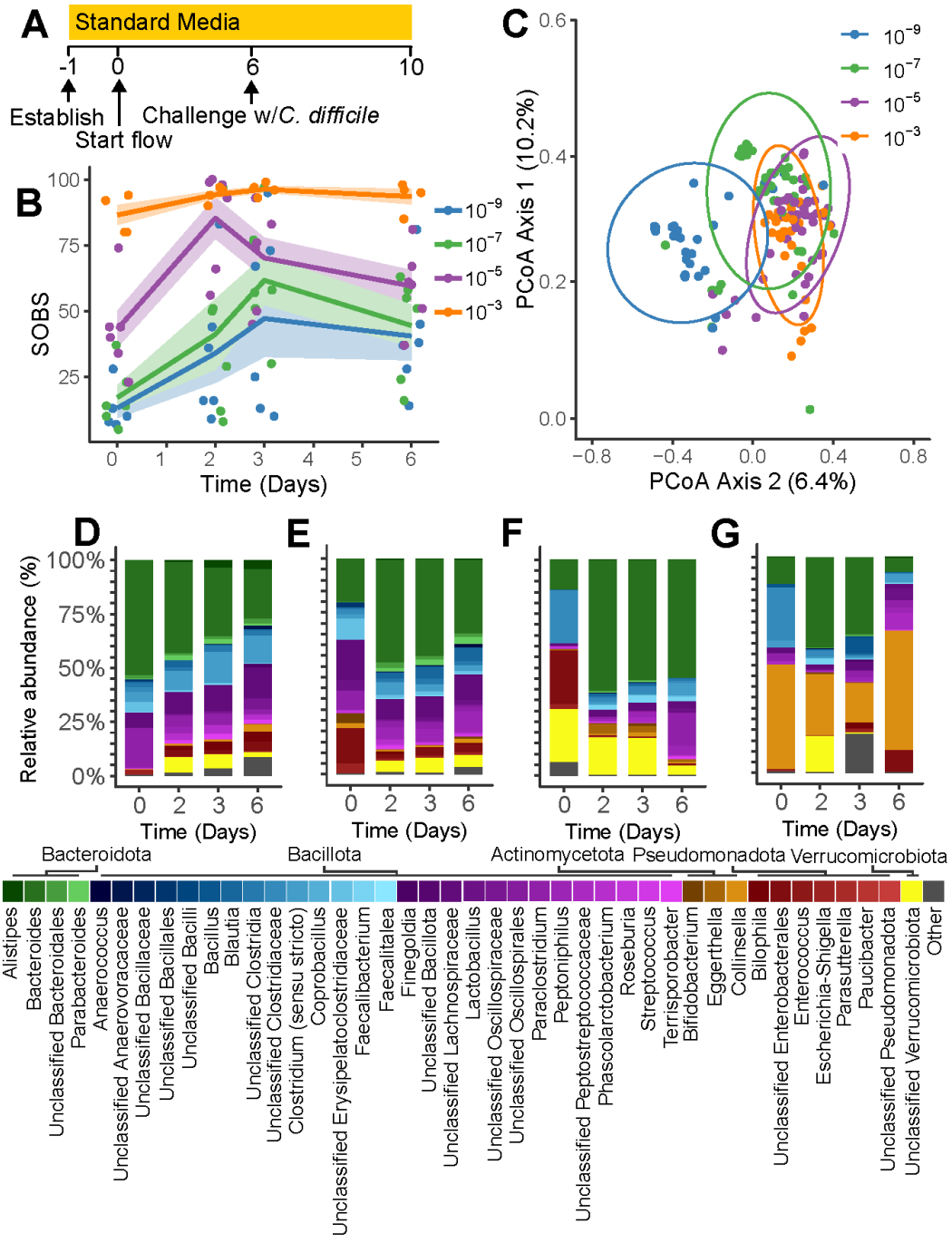

Figure 4.1: Establishment dynamics of diluted microbial communities
A) Experimental timeline of the bioreactor dilution experiment. **B)** Observed species (SOBS) is plotted by dilution from day 0 to the day of *C. difficile* challenge. **C)** Principal coordinate analysis of all timepoints in each community dilution (ellipses represent the 95% confidence interval of a multivariate t-distribution for datapoints in each dilution). **D-G)** Averaged relative abundance at each indicated timepoint for the communities diluted **D)** 10^{-3}, **E)** 10^{-5}, **F)** 10^{-7}, and **G)** 10^{-9}. Taxa are color coded and ordered by phylum (Bacteroidota = green, Bacillota = blue/purple, Actinomycetota = orange, Pseudomonadota = red and Verrucomicrobiota = yellow. Other phyla, low abundance taxa and unclassified bacteria are colored as grey).

measured by Bray-Curtis and Jaccard Dissimilarity Indexes, which capture the abundance and the presence/absence of taxa, respectively (Fig. 4.2A-B). This variability trend was also observed when comparing multiple timepoints within each individual reactor (Fig. S4.2A-B). This variability is also captured by principal coordinate analysis, which shows that dilution altered the dynamics of each community's establishment so that they cluster separately (Fig. 4.1C). While dilution greatly reduced the initial biomass of microbes, after 6 days of growing in continuous culture, communities had reached similar levels of abundance as measured by qPCR of the 16S rRNA-gene (Fig. S4.1B).

4.3.2 Dilution decreases resistance to a model invasive organism

C. difficile is a model organism that can generally not invade communities unless they have been perturbed. Since dilution increased community variability, which is a marker of external stability, we hypothesized that this would result in reduced ability to prevent *C. difficile* colonization. 7 days after establishment of bioreactor communities, they were challenged with 10^4 vegetative *C. difficile* cells. As measured by colony-forming units (CFU), communities possessed varying capabilities to resist colonization with *C. difficile* (Fig. 4.3A). 3 of 4 communities diluted 10^{-3} cleared *C. difficile* colonization within 24 hrs while communities diluted 10^{-9} showed colonization levels around 10^7 CFU/mL in all six replicates. The largest intra-group variation in colonization was observed in the 10^{-5}, where all six reactors had intermediate levels of colonization, and 10^{-7} dilutions, which had three reactors colonize at 10^7 and three fully resist. Since *C. difficile* colonizes at 10^7 CFU/mL when it grows by itself in a reactor (data not shown), our data suggest that

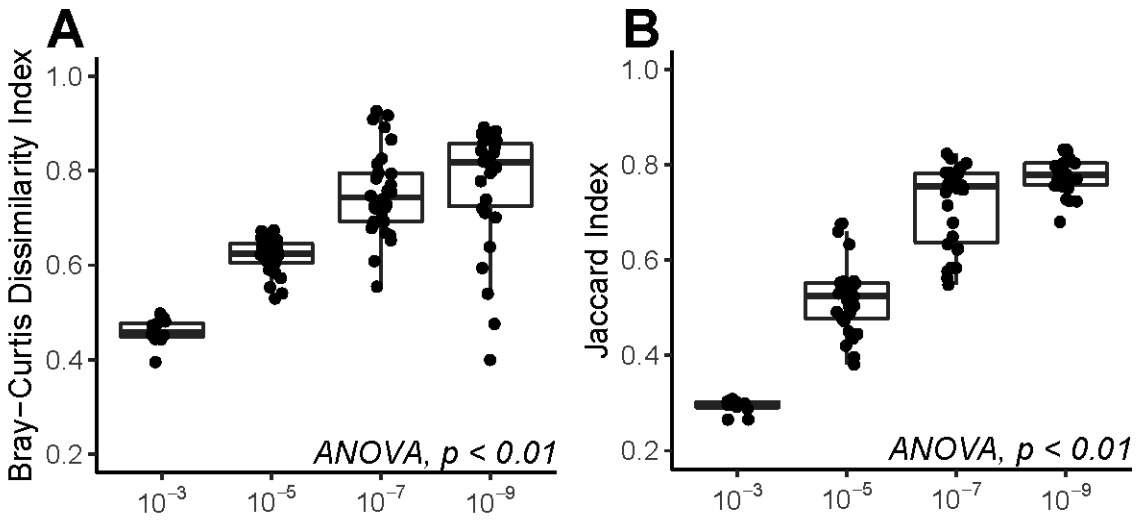

Figure 4.2: Intra-group community variability by dilution
Intra-group β-diversity was compared across samples for each of the four community dilution groups using the **A)** Bray-Curtis Dissimilarity Index and the **B)** Jaccard Dissimilarity Index (statistical analysis: one-way ANOVA).

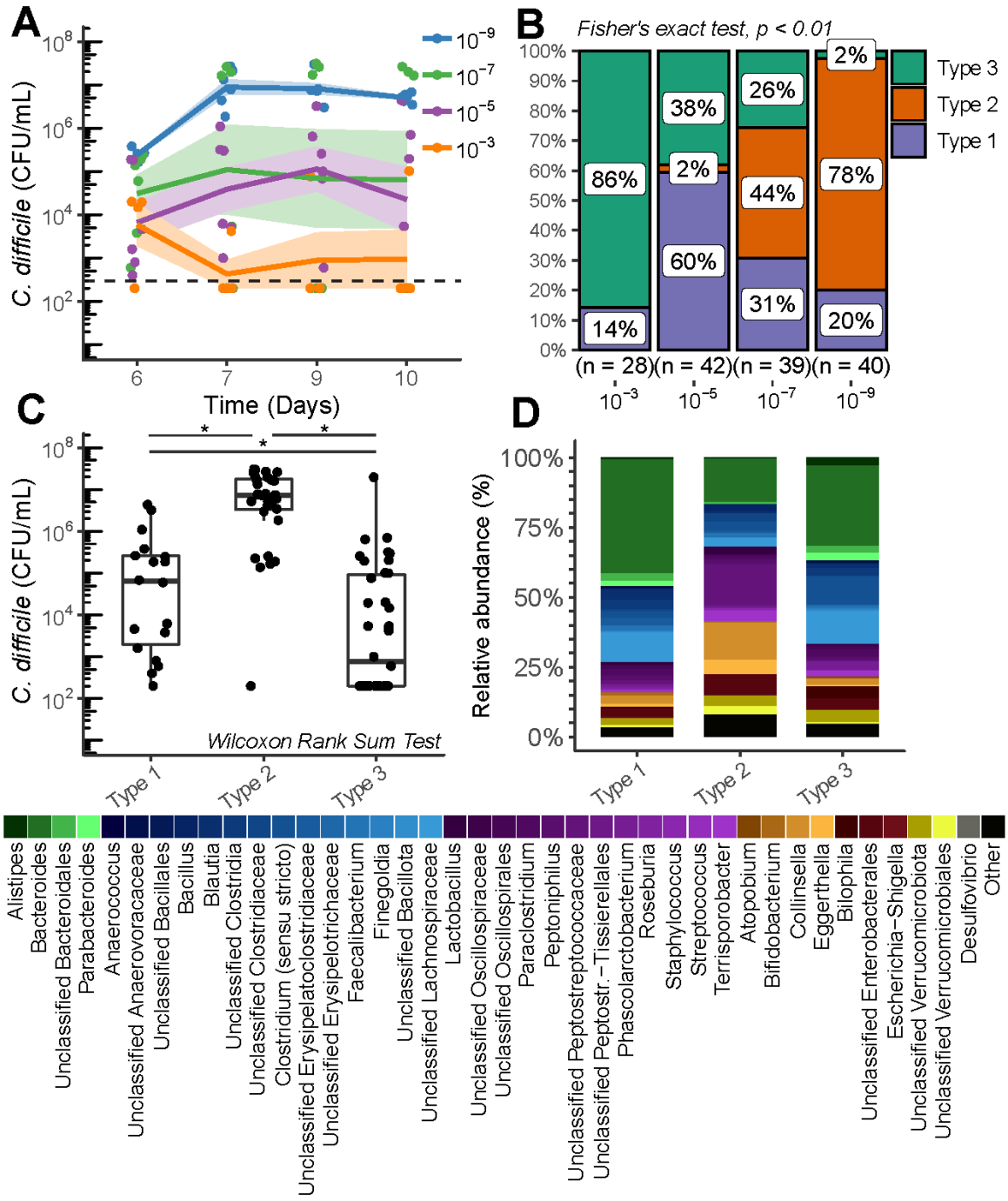

Figure 4.3: Associations between *C. difficile* colonization and microbiota community type
A) *C. difficile* colonization on each day following challenge measured in CFU/mL. **B)** All samples were categorized into three unique community types by Dirichlet Multinomial Modelling (DMM). Their relative abundance in each dilution group is plotted with the total number of samples in each dilution listed on the x-axis (statistical analysis: Fisher's Exact Test). **C)** *C. difficile* abundance in each sample is compared to that samples associated community type (statistical analysis: Wilcoxon Rank Sum Test, * indicates $p < 0.01$). **D)** Average relative abundance of bacterial taxa in each community type (Peptostreptococcales is abbreviated as Peptostr.; Bacteroidota = green, Bacillota = blue/purple, Actinomycetota = orange, Pseudomonadota = red, Verrucomicrobiota = yellow and Desulfovibrio = grey. Other phyla, low abundance taxa and unclassified bacteria are colored as black).

reactor communities that reached this level had no colonization resistance. Furthermore, 24 hrs after *C. difficile* challenge, those communities experienced a loss of resident taxa (37±21 on day 6 to 14±4 on day 7; Wilcoxon Rank Sum Test, $p < 0.01$), demonstrating that these microbial communities had both no ability to resist a non-indigenous microbe or remain intact (Fig. S4.3A-C).

Using Dirichlet Multinomial Modelling (DMM), we identified 3 community types across the established communities, which associated with dilution (Fig. 4.3B). Of these, type 3 supported significantly lower colonization than enterotypes 1 and 2, with type 1 supporting a middle level of colonization (Fig. 4.3C). Through LEfSe, we identified 19 taxa associated with the more resistant enterotypes (i.e., enterotypes 1 & 3; Fig. S4.3D) and five associated with enterotype 2 (Fig. S4.3E). We noted several commonly associated with metabolic functions known to increase resistance to *C. difficile*, such as short-chain fatty acid (SCFA) production. These taxa included *Bifidobacterium, Bacteroides*, *Blautia, Faecalibacterium,* Unclassified Lachnospiraceae and *Clostridium* (sensu stricto) (Fig. 4.3D & Fig. S4.3D-E).

4.3.3 Diluted communities respond uniquely to a change in carbohydrate concentrations

The dilution experiments above indicated that colonization resistance against *C. difficile* was associated with the presence of taxa that could degrade dietary polysaccharides and produce SCFAs (31, 170). Other work has indicated that SCFAs are able to limit the growth of *C. difficile* (31). Therefore, we characterized how a change to higher carbohydrate concentrations affected the formation of communities and their ability

to resist *C. difficile* colonization following a bottleneck event. We chose to increase the availability of the carbohydrate inulin due to its ability to induce the production of SCFAs by the gut microbiota (355-357). We also chose this polysaccharide due to the association of microbes with inulin catabolic potential and colonization resistance in the dilution experiment. Using a second fecal donor, we established reactor communities using feces diluted 10^{-3}, 10^{-4}, 10^{-5} and 10^{-6}. Based on our work above we hypothesized that these dilutions would result in communities that might support moderate levels of *C. difficile* colonization. After growing communities for two days on standard BRM, which contains 0.02% inulin, we increased inulin concentrations to 0.2% (Fig. 4.4A). Despite the narrower range of dilution, communities established in these reactors again differed in the number of OTUs that became established, with less diluted communities having a significantly higher number of resident OTUs (Fig. 4.4B). While we observed a shift in the Bray-Curtis distance relative to baseline in the community diluted 10^{-3} when comparing days 2 and 5, we did not observe a statistically significant change in the number of OTUs (Fig. 4.4B & Fig. S4.4A). There was no shift in ecologic distance in the other dilution groups. Despite the minimal changes in community structure, there was a significant shift in metabolic activity of these communities in terms of carbohydrate metabolism with a drop in acetate and a 3-fold increase in butyrate concentrations (Fig. 4.4C). There was no change in propionate concentrations (Fig. 4.4C). Interestingly, butyrate production prior to the shift in inulin (i.e., day 2) was predictive of concentrations afterward (i.e., day 7), with only communities diluted 10^{-3} and 10^{-4} responding to higher inulin (Fig. 4.4D & Fig. S4.4C). Despite this variation in metabolic output, pH did not differ across dilutions when

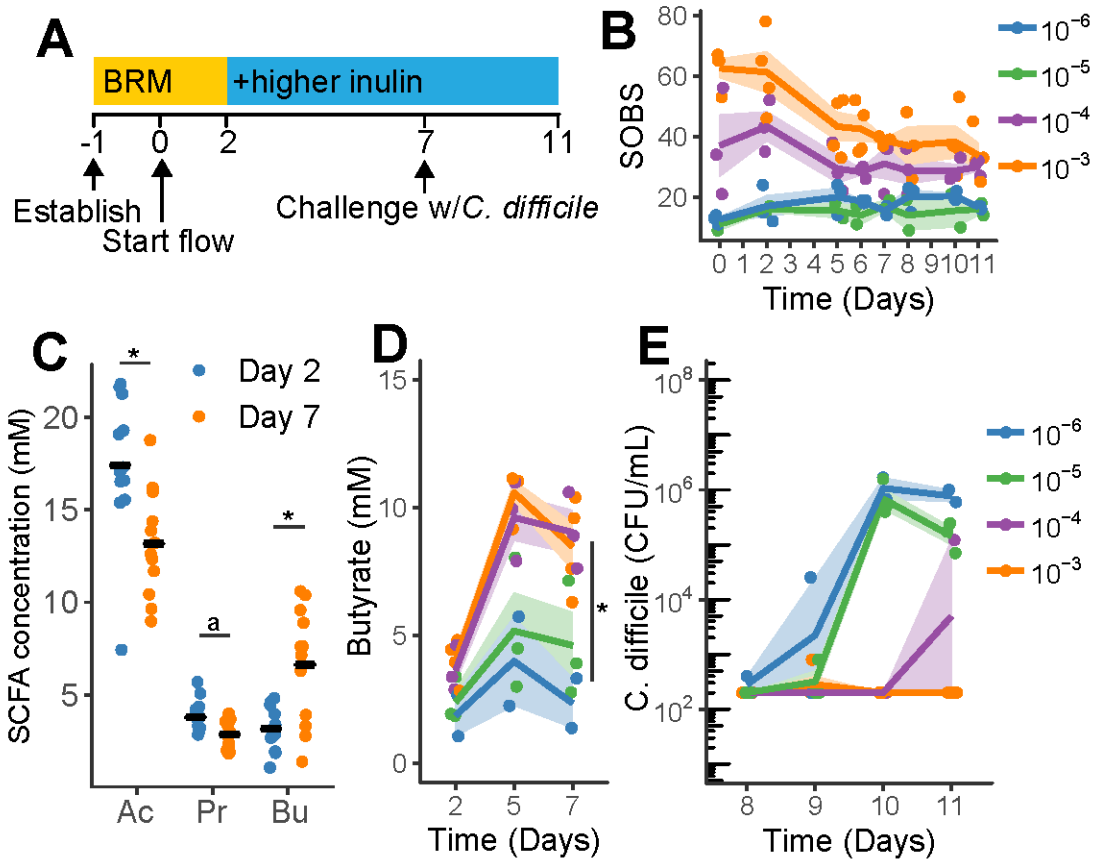

Figure 4.4: Effect of inulin on microbial community function
A) Experimental timeline of the bioreactor carbohydrate experiment. **B)** Observed species (SOBS) over time colored by dilution group (statistical analysis: Kruskal-Wallis Test comparing SOBS at all timepoints with dilution group, $p < 0.01$; Wilcoxon Rank Sum Test comparing OTUs in each group at day 2 and day 5, p = not significant). **C)** Short chain fatty acid concentrations in the 0.2% inulin group as measured by HPLC from day 2 (pre-media switch) and day 7 (5 days post-media switch; Ac = acetate, Pr = propionate, Bu = butyrate; statistical analysis: Wilcoxon Rank Sum Test, * indicates $p < 0.01$ and a indicates $p = 0.033$). **D)** Butyrate response 3 and 5 days following the shift to higher inulin, with communities being colored by dilution (statistical analysis: at day 7, 10^{-3} and 10^{-4} compared to 10^{-5} and 10^{-6} using the Wilcoxon Rank Sum Test, * indicates $p < 0.01$). **E)** *C. difficile* colonization in the reactors treated with 0.2% inulin, colored by community dilution.

measured at day 10 (Fig. S4.4B). Our data suggest that in our bioreactor system a 10-fold inulin increase altered the functional output of the community with minimal effect on its composition, with more diluted communities not responding to that change. Four days after challenging with 10^5 vegetative *C. difficile* cells, reactors colonized to an average density of 10^6 CFU/mL *C. difficile* in the 10^{-5} and 10^{-6} groups (Fig. 4.4E). While all reactors had low initial levels of *C. difficile* colonization, only the communities in the 10^{-3} and 10^{-4} groups were able to ultimately prevent *C. difficile* invasion, suggesting that communities still able to respond to inulin also had the metabolic functions required to mediate colonization resistance (Fig. 4.4E). While we observed a correlation between butyrate concentrations at day 0 and *C. difficile* colonization at day 4, butyrate did not affect *C. difficile* at the concentrations measured in our reactors in *in vitro* curves at pH 7 (Fig. S4.4D-F).

4.4 Discussion

The ability of an ecosystem to resist invasion by a non-indigenous species is tied to the diversity and temporal variability of community membership, an observation noted throughout the animal kingdom (358-360). Whether at the “macro” or “micro” levels of biology, environments provide a given set of nutrients to resident organisms, creating multi-dimensional niches comprised of biotic (e.g., nutrients, predators, etc.) and abiotic (eg., space, gas gradients, etc.) factors (139, 142, 143, 361-363). The diversity and variability of a resident community determines how efficiently niches in the surrounding environment are utilized (363). In our study, we demonstrated that dilution of a community increases the variability of the established community, and those shifts are associated

with *C. difficile* colonization resistance. However, this variability is only a marker of underlying metabolic interactions of colonization resistance as evidenced by an increase in resistance when we altered nutrient inputs into that environment.

These metabolic interactions manifest externally through greater competition with invaders as well as internally through limits placed on opportunistic taxa already present in that environment. Thus, we observed dilution having a two-fold disruptive effect on establishing communities, each tied to niche availability. First, while diversity is not strictly a metric of external stability, greater diversity allows for higher numbers of unique interactions, both mutualistic and antagonistic, among community members (358, 364). These interactions increase the likelihood that spaces within a given niche become occupied through stronger cross-feeding interactions between resident members, which limits the invasion of foreign microbes (365, 366). By removing rarer taxa, the stochastic nature of dilution weakened these interactions by destabilizing how the remaining microbes co-adapted to their new environment. The resulting changes decreased niche coverage by the resident microbiota (365). The resulting gaps reward microbes like *C. difficile*, which can adapt to use distinct niches depending on what is available in an environment (186). Additionally, networks of mutualistic and antagonistic interactions between microbes increase the likelihood of a microbial community's long-term survival (367). As observed in the communities that fully colonized with *C. difficile*, invasion by a foreign microbe triggered a collapse in the networks between resident organisms, resulting in their extinction (367).

Second, in addition to removing rarer taxa, dilution decreased the biomass of microbes starting off in each reactor. Since microbial abundance had recovered by the

time of *C. difficile* challenge, we do not think that low microbial density played a direct role in the niches available to *C. difficile*. However, low microbial density left large open niches at the outset, which altered the early dynamics of community establishment. Microbes arrived in an environment absent of the competitors that previously had limited their expansion. This founder effect allowed opportunistic taxa within the resident community to take on outsized proportions due to their ability to use surrounding resources more efficiently (368, 369). Since the density of a seeding community regulates how they establish, it is inherently tied to how environmental niches become occupied (370). For example, broad-spectrum antibiotic treatment induces significant gaps in niche coverage by reducing microbial abundance (19, 371). The downstream effects of these perturbations can linger for years, particularly if the event occurs early in the stages of microbial community development (e.g., in human infancy) (372). While perturbations that occur after a community reaches “maturity” have persistent effects, microbial communities tend to be impacted to a lesser extent (373, 374).

In our study, we also investigated the role of carbohydrates and microbial short-chain fatty acid metabolism in revealing the nature of altered community assembly affected by founder effects. While the metabolic nature of colonization resistance is multifactorial, several studies have characterized the role of SCFAs in limiting *C. difficile* establishment in the gut by altering the physiology of both microbe and host (30, 170, 375). While all SCFAs we measured can be products of inulin degradation, butyrate is relevant due to its toxicity to *C. difficile* as well as its ability to limit toxin-associated damage on the colonic epithelium (30, 31). While higher inulin concentrations induced an increase in butyrate, *C. difficile* tolerated those butyrate concentrations as measured by

in vitro growth curves. Previous work suggests that SCFAs affect bacterial cells in a pH-dependent mechanism, with higher toxicity at lower pH due to the protonated acid form passing more easily through cellular membranes (169, 376). Our *in vitro* assays were balanced at pH 7, which limited toxicity that might be present in areas of the gut with lower pH and higher fermentative metabolic activity (142). Further research could disentangle the effects of butyrate on *C. difficile* physiology at unique pH levels (142).

Several studies have observed the presence of butyrogenic pathways in *C. difficile*, which may use butyrate as a terminal electron acceptor in the absence of other options, such as Stickland amino acids (197, 377, 378). Due to unique toxicity patterns among the types of media used in our study as well as a previous study, we hypothesize that butyrate may have unique effects on *C. difficile* depending on which metabolic pathways are in use at the time of exposure (31, 379). This may be due in part to pressure from a build-up of downstream metabolic by-products as has been observed in *E. coli's* response to high concentrations of acetate and formate (380). Further work is required to characterize the specific effects of SCFAs on *C. difficile* physiology and potential impacts on virulence (169). In summary, if butyrate is one of the mediators of increased colonization resistance in the inulin-treated communities, our data suggest that it is acting in concert with other unknown mechanisms.

Understanding the establishment of microbes in a new environment is essential as we seek to develop defined consortia to treat microbiota-related gut conditions, such as *C. difficile* infection. Some of the limited success of certain consortia may be due in part to low seeding densities as well as the inadequacy of smaller consortia to cover the

appropriate niche spaces. Keeping these ecological dynamics in mind will assist in creating reliable treatments with broader efficacy across a population.

4.5 Supplemental Figures

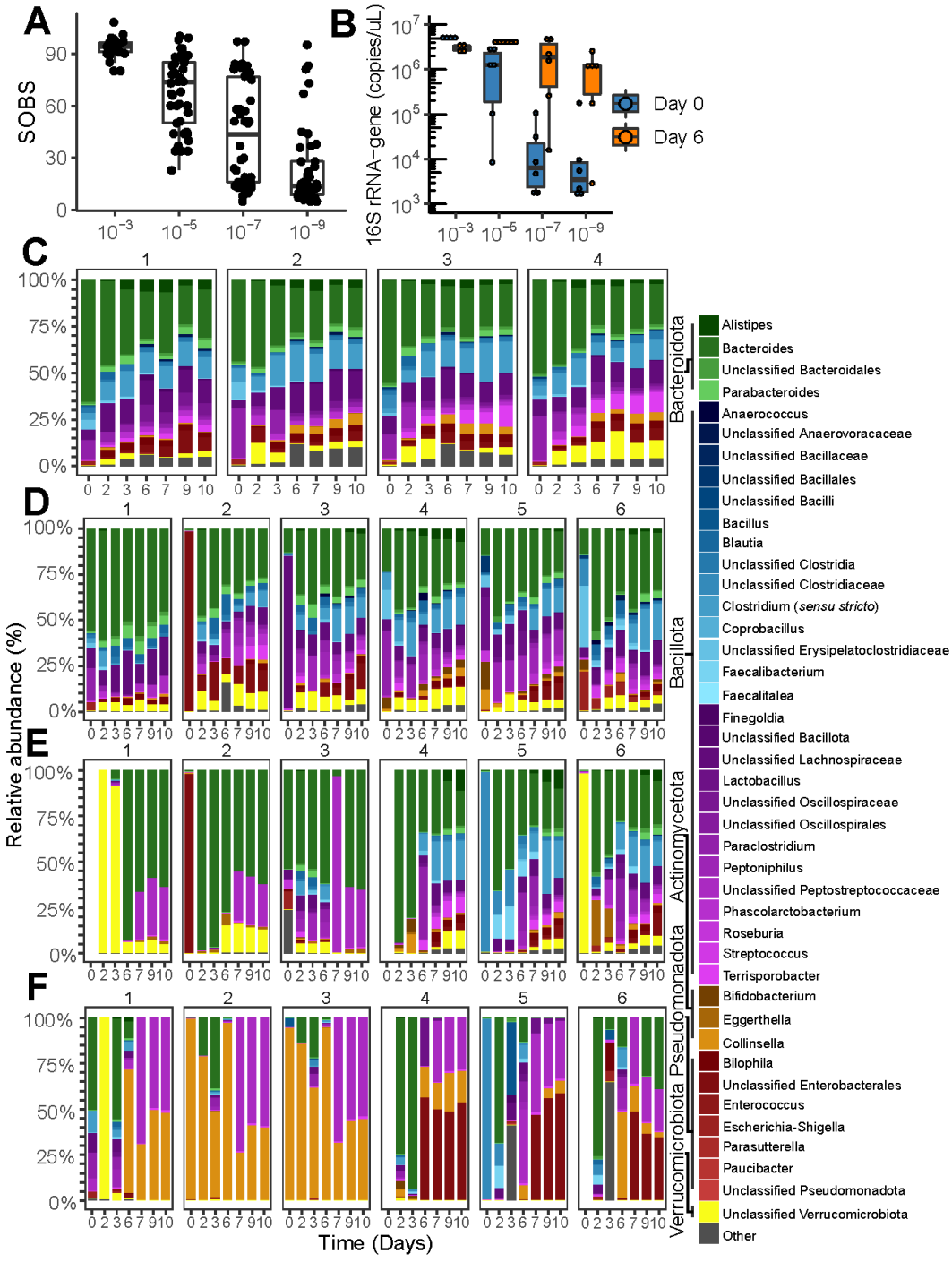

Supplemental Figure 4.1: Individualized establishment dynamics of diluted microbial communities **A)** Observed species (SOBS) from all timepoints are plotted by community dilution. **B)** 16S rRNA-gene copies on days 0 and 6 are plotted by dilution. **C-F)** Relative abundance of 16S rRNA gene sequences is plotted for each individual reactor in the communities diluted **C)** 10^{-3}, **D)** 10^{-5}, **E)** 10^{-7}, and **F)** 10^{-9} (Bacteroidota = green, Bacillota = blue/purple, Actinomycetota = orange, Pseudomonadota = red and Verrucomicrobiota = yellow. Other phyla, low abundance taxa and unclassified bacteria are colored as grey).

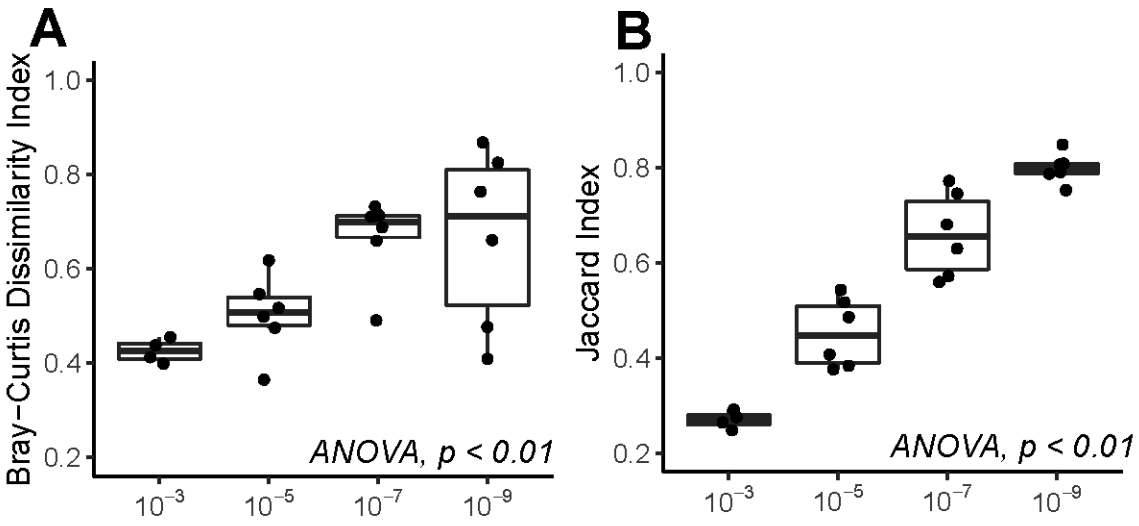

Supplemental Figure 4.2: Intra-reactor community variability by dilution
Intra-reactor β-diversity was compared across samples within each reactor for the four community dilution groups using the **A)** Bray-Curtis Dissimilarity Index and the **B)** Jaccard Dissimilarity Index (statistical analysis: one-way ANOVA).

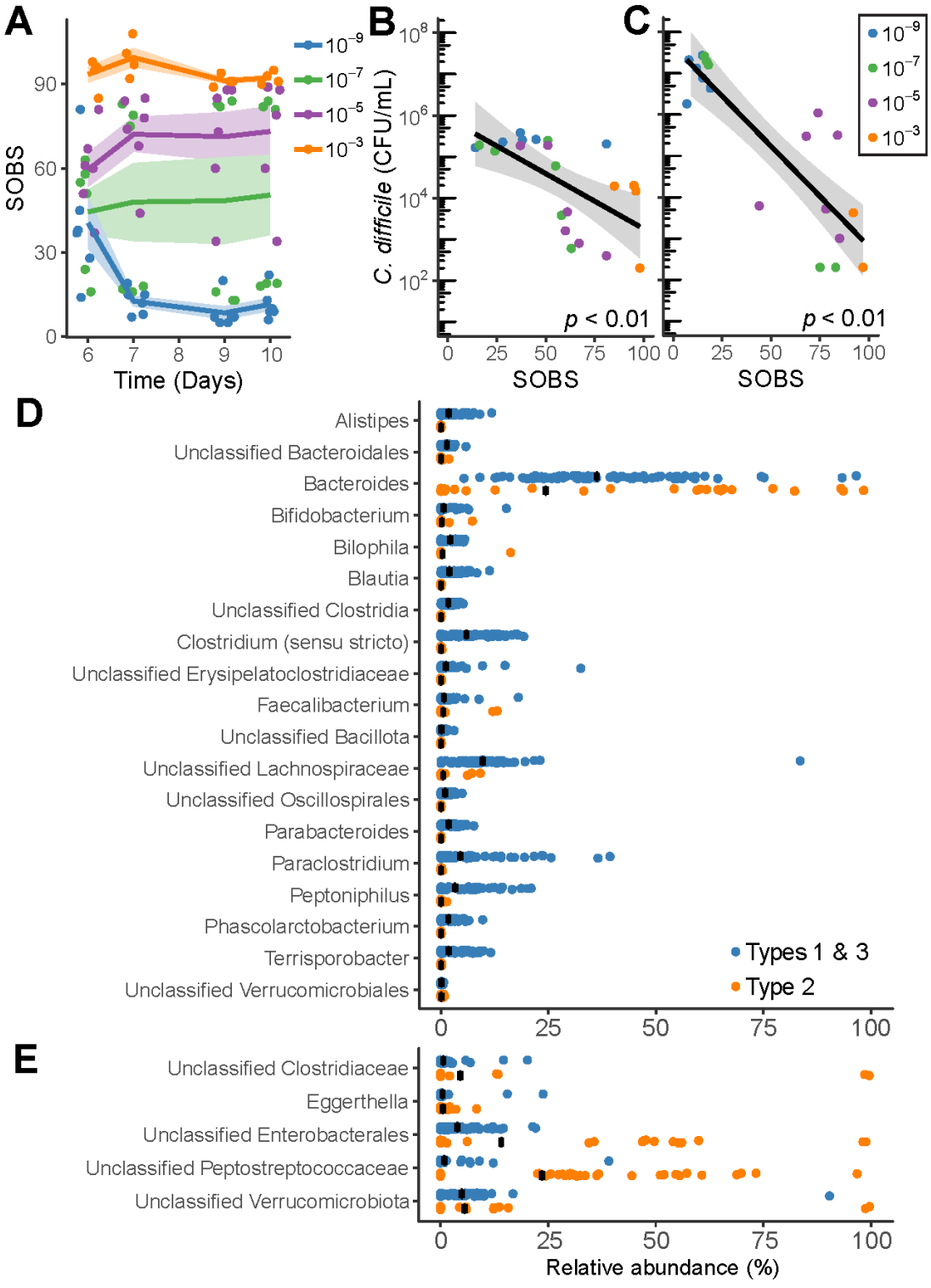

Supplemental Figure 4.3: Associations between *C. difficile* and resident microbes
A) Observed species (SOBS) in each community dilution following *C. difficile* challenge. *C. difficile* abundance compared to the SOBS on **B)** day 6 and **C)** day 7 (statistical analysis: linear regression). LEfSe analysis comparing bacterial taxa in community types 1 & 3 with those in type 2. Certain taxa were more abundant in **D)** types 1 & 3 and others in **E)** type 2.

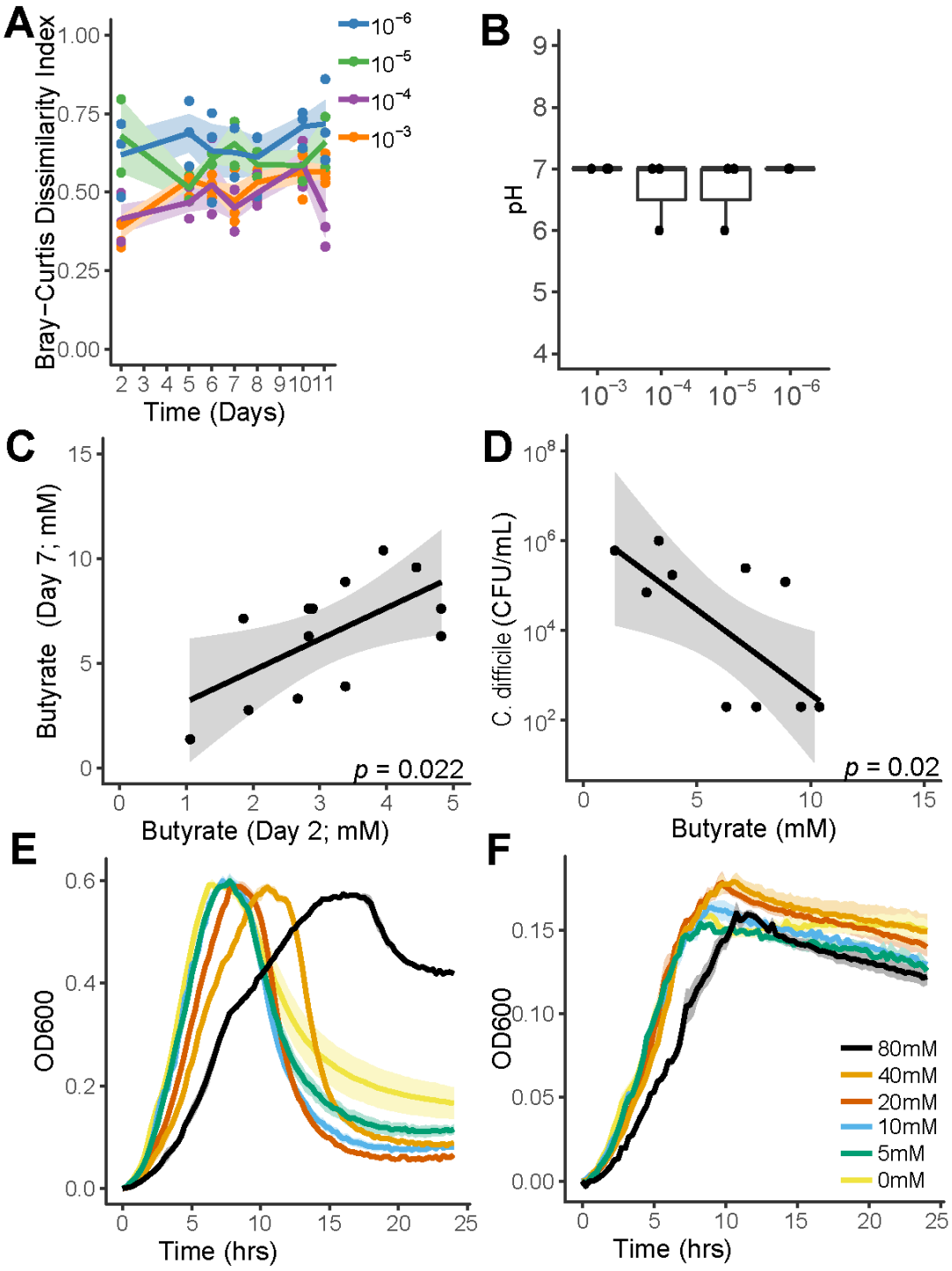

Supplemental Figure 4.4: Effects of inulin on microbial community function
A) Bray-Curtis Dissimilarity index of communities in the 0.2% inulin treated reactor groups colored by dilution. Each point represents the distance of each reactor community relative to its baseline at day 0 (statistical analysis: Wilcoxon Rank Sum Test comparing distance to baseline at day 2 and day 5; for 10^{-3}, $p = 0.016$; for 10^{-4}, 10^{-5} and 10^{-6}, p = not significant). **B)** pH of each reactor by dilution group at day 10. **C)** Butyrate concentrations at day 2 (pre-inulin shift) compared to concentrations at day 7 (statistical analysis: linear regression). **D)** Butyrate concentrations at day 7 compared to *C. difficile* colonization on day 11. *C. difficile* growth curves in assessing butyrate toxicity in **E)** BHI and **F)** BRM, each buffered at pH 7.

Chapter 5: Discussion

A portion of this chapter was published as:

Schnizlein MK & Young VB. Capturing the environment of the *Clostridioides difficile* infection cycle. Nature Reviews: Gastroenterology & Hepatology. 2022. *Accepted*.

5.1 Introduction

The work described in this dissertation tested the central hypothesis that the gut environment plays an integral role in affecting *C. difficile*'s ability to successfully colonize the mammalian gastrointestinal tract. The major findings from these chapters are as follows: 1) gut regions differently affect *C. difficile* physiology, with the small intestine facilitating the transition from dormant spore to actively growing vegetative cell; 2) dietary nutrients play an integral role in shaping the physiology of microbes residing in the gut and the nature of their interactions with non-indigenous microbes; 3) a critical microbial mass is required to maintain external stability (i.e., resistance to invasive microbes), which is closely tied to a microbial community's ability to utilize nutrients. This chapter includes a summary discussion of this dissertation's main findings as well as next steps to understand how ecological dynamics of the mammalian gut can be leveraged to treat *C. difficile* infection.

5.2 Exploring microbiota-environment interactions in the small intestine and their effects on *C. difficile* germination.

In chapter 2, I characterized microbiota dynamics in the human upper gut using a novel catheter design that allowed me to sample multiple gut sites simultaneously over a short period of time (i.e., <7 hrs). Since these samples were collected in conjunction with two studies investigating the pharmacokinetics of mesalamine and ibuprofen, part of this study characterized how drug administration affected microbial taxa. While I observed a limited effect by these drugs on the dynamic microbial community that resides in the small intestine, I observed much larger associations between those microbes and environmental variables, such as pH and bile acid concentrations.

This work is the first to characterize the microbiota of several upper gut regions over time simultaneously. Previous work has characterized the upper gut microbiota over time using ileostoma effluent or across multiple regions but at singular timepoints (90, 211-221). Similarities between the microbiota of the upper gut and the oral cavity suggest that the latter plays a prominent role in shaping the community of the former. For example, recent research shows that characteristics of the oral microbiota associate with diseased states in the stomach and small intestine (381). Due to the toxic acidity the stomach and limitations of sequencing all DNA (i.e., not just that from live microbes), more research is required to understand how microbes from the mouth tolerate transit of the stomach (382). While culture-dependent approaches provide a picture of organisms that are capable of growing outside the gut, previous research has demonstrated that many organisms are either dead at the point of sampling or have difficulty growing under *in vitro* conditions

(383, 384). Future work should use a synergy of sequencing- and culture-dependent approaches to accurately characterize the upper gut microbiota (382).

Due to the importance of bile acids in *C. difficile* physiology, one of the interests in looking at bile acid concentrations is to characterize how the human small intestine affects the germination of *C. difficile* spores. Bile acids are one of several signals required for *C. difficile* to germinate into vegetative cells, which can produce disease-causing toxins. Therefore, understanding how the environmental conditions of early gut regions affect spores in healthy individuals is important for understanding how deviations from a healthy state might lead to disease. This knowledge could also be leveraged for targeted treatments. For example, studies have characterized how inhibitors of germination, usually bile acid analogues, prevent *C. difficile*-associated disease in murine and hamster models (26, 385, 386). Several other studies have characterized *C. difficile* germination in the upper gut, but these are limited to murine models (86, 289). Thus, this work is the first to characterize *C. difficile* germination in gut fluid taken from the human small intestinal tract. I demonstrate that, due to minimal bile acid metabolism by the resident microbiota, those bile acids are mostly conjugated forms that tend to promote germination. Furthermore, using *in vitro* germination assays, those spores can germinate in response to bile acids present in healthy individuals. These data, combined with knowledge that most healthy individuals will resist colonization, suggest that a failure to colonize is not likely due to limiting germination, but rather may be due instead to preventing the establishment of a vegetative cell population. Since lower propagule size (i.e., infectious dose) can limit a microbe's ability to colonize an environment, more research is required to understand whether germination inhibitors would sufficiently lower

the infectious dose to a level that would prevent colonization in individuals that have a microbiota that is permissive of *C. difficile* establishment (364, 387).

5.3 Exploring the impact of diet on the maintenance of colonization resistance

The association of microbial short-chain fatty acid production with resistance to *C. difficile* infection is indicative of its role in microbiota community integrity. In chapter 3, I discussed my findings on the effect of the dietary polysaccharide xanthan gum on the murine microbiota using a murine antibiotic model of *C. difficile* colonization. Changes in the microbiota and its production of SCFAs were observed within 48 hours of starting xanthan gum administration. While mice with 5% xanthan gum in their diet were protected from *C. difficile* colonization, xanthan gum also affected the ability of antibiotics to target the resident microbiota, limiting the reduction of colonization resistance through an alternative mechanism.

Diet as a microbiota-modulating mechanism has been widely explored, especially as probiotics only generally only provide benefits for as long as they are taken (90, 388-390). Thus, providing prebiotic nutrients that can alter the behavior of resident microbes already established in the gut is advantageous (391). Dietary components introduced into human diets alter microbial functions, particularly as processed foods expose microbes to novel energy sources. For example, the dietary additive trehalose may play a role in regulating *C. difficile* fitness in the gut (199-201). Other dietary components, such as zinc, iron and calcium, also can modulate the microbiota and play roles in regulating aspects of *C. difficile* physiology (181-185). Given the prevalence of xanthan gum-degrading taxa in humans, microbes find ways to utilize compounds presented to them (392). As dietary

components are evaluated for incorporation into human diet, research should be extended to understand not only the direct effects on human physiology but also possible indirect outcomes, such as modulating the microbiota, in both health and disease.

5.4 Exploring the dynamics of microbiota establishment and formation of colonization resistance following a bottleneck

In chapter 4, I leverage a bioreactor model to study the formation of microbial colonization resistance following a bottleneck event. The resulting founder effects increased the variability of each established community and in turn altered their ability to resist invasion by the non-indigenous microbe *C. difficile*. While community variability is an indicator of colonization resistance, it only broadly characterizes the possible metabolic interactions capable of its members (393). For example, a community that is less variable will have more stable metabolic interactions that fill environmental niches (365, 366). In turn, a more variable, less diverse community will have more difficulty successfully using surrounding resources efficiently enough to prevent non-indigenous microbes from invading (365, 366). This was evident when bioreactors were treated with higher inulin. Reactor communities that resisted *C. difficile* also retained the ability to respond to the additional carbohydrates by producing more SCFAs. However, those that had been diluted more lost the ability to produce additional SCFAs and prevent *C. difficile* from becoming established.

Understanding these ecological dynamics are important for developing microbe-based treatments to restore colonization resistance. If the goal is to provide sufficient metabolic competition, microbe-based treatments need to not only fulfill specific functions

but provide a broader metabolic support network to limit generalist organisms, such as *C. difficile*, from circumventing resistance to find available niche space.

5.5 Conclusions

As a prominent human pathogen, *C. difficile* has developed diverse means to successfully colonize the gut. The advances described in this thesis have detailed how the microbiota and host work together to prevent *C. difficile* colonization in otherwise healthy individuals. The resulting intersection between clinical and environmental sciences has opened new doors for systems biology approaches as researchers incorporate multiple dimensions of biology to answer research questions.

In this dissertation, I used a synergy of human, murine and *in vitro* models to understand unique aspects of the biology of *C. difficile* infection. By using a human study, I was able to examine the microbiota in its native environment, giving a better picture of how these dynamics play out in the host of interest. While this provides important detail on human physiology, it is difficult to modify the environment for controlled experimental questions. This is where the strengths of the murine and *in vitro* models become valuable. Murine models provide a parallel system for studying the gut as it contains both host and microbial variables. Due to the homogeneity of mouse colonies, scientific questions can be asked in a more controlled environment. I used this model to characterize the microbiota in the context of *C. difficile*-associated disease. However, the differences in physiology between the murine and human guts (e.g. nutrient profile, bile acid metabolism, etc.) can limit the translatability of findings from research done in mice back into humans. Due to the complex interactions between host and microbes in the gut, it

can be difficult to understand relationships among microbes themselves. Therefore, using *in vitro* models, such as bioreactors, improves one's ability to investigate the physiology of gut microbes without host dynamics at play. In this dissertation, I leveraged bioreactors to study community-level metabolism or ecological dynamics. Since each model has their own particular value, using them in concert provides unique insight into the multilayered system of the gut environment.

The gut environment contains a wide variety of mechanisms that alter *C. difficile* physiology. Future treatment options should leverage methods of gut defense already in use by the host (Table 5.1). Furthermore, shifts in microbiota-related research from identifying bacterial community membership to characterizing community function will result in the development of more effective treatment options that incorporate interindividual variability into personalized medicine.

Treatment	Definition	Mode of action
Untargeted microbiota change		
Antibiotics	Broad-spectrum (vancomycin)	Targets *C. difficile* and induces microbiota disruptions
	Narrower-spectrum (fidaxomicin)	Targets *C. difficile* but reduces microbiota disruptions
Microbial	Fecal microbiota transfer	Replaces lost microbial diversity
Targeted microbiota change		
Antimicrobials	Lantibiotics, antimicrobial peptides	Directly targets *C. difficile*
Bacteriophage	Phage cocktails	Directly targets *C. difficile*
Bacteria and/or Fungi	Defined bacterial and/or fungal consortia	Restores specific microbiota functions*
Other mechanisms		
Immunity	Anti-toxin vaccines	Prevents toxin-associated damage
	Anti-toxin monoclonal antibodies	Prevents toxin-associated damage
Diet	Diet composition modification	Enhances microbiota functions through selection

*such as the metabolism of bile acids & short chain fatty acids as well as nutrient competition

Table 5.1 Leveraging the environment for *C. difficile* treatment

References

1. Crobach MJT, Ducarmon QR, Terveer EM, Harmanus C, Sanders IMJG, Verduin KM, Kuijper EJ, Zwittink RD. 2020. The bacterial gut microbiota of adult patients infected, colonized or noncolonized by *Clostridioides difficile*. Microorganisms 8:677.
2. He X, McLean JS, Guo L, Lux R, Shi W. 2014. The social structure of microbial community involved in colonization resistance. ISME J 8:564-574.
3. Baumgartner M, Pfrunder-Cardozo KR, Hall AR. 2021. Microbial community composition interacts with local abiotic conditions to drive colonization resistance in human gut microbiome samples. Proceedings of the Royal Society B: Biological Sciences 288:20203106.
4. Theriot CM, Koenigsknecht MJ, Carlson PE, Jr., Hatton GE, Nelson AM, Li B, Huffnagle GB, J ZL, Young VB. 2014. Antibiotic-induced shifts in the mouse gut microbiome and metabolome increase susceptibility to *Clostridium difficile* infection. Nat Commun 5:3114.
5. Knight DR, Elliott B, Chang BJ, Perkins TT, Riley TV. 2015. Diversity and evolution in the genome of *Clostridium difficile*. Clinical Microbiology Reviews 28:721-741.
6. Moore RJ, Lacey JA. 2019. Genomics of the pathogenic clostridia. Microbiology Spectrum 7.
7. Janezic S, Rupnik M. 2015. Genomic diversity of *Clostridium difficile* strains. Res Microbiol 166:353-60.
8. Janvilisri T, Scaria J, Thompson AD, Nicholson A, Limbago BM, Arroyo LG, Songer JG, Gröhn YT, Chang YF. 2009. Microarray identification of *Clostridium difficile* core components and divergent regions associated with host origin. J Bacteriol 191:3881-91.
9. Stabler RA, Gerding DN, Songer JG, Drudy D, Brazier JS, Trinh HT, Witney AA, Hinds J, Wren BW. 2006. Comparative phylogenomics of *Clostridium difficile* reveals clade specificity and microevolution of hypervirulent strains. J Bacteriol 188:7297-305.
10. Kato H, Hagihara M, Asai N, Shibata Y, Yamagishi Y, Iwamoto T, Mikamo H. 2021. A systematic review and meta-analysis of decontamination methods to prevent hospital environmental contamination and transmission of *Clostridioides difficile*. Anaerobe 73:102478.
11. Brown K, Valenta K, Fisman D, Simor A, Daneman N. 2015. Hospital ward antibiotic prescribing and the risks of *Clostridium difficile* infection. JAMA Internal Medicine 175:626-633.
12. Weese JS. 2020. *Clostridium* (*Clostridioides*) *difficile* in animals. J Vet Diagn Invest 32:213-221.

13. Hernandez BG, Vinithakumari AA, Sponseller B, Tangudu C, Mooyottu S. 2020. Prevalence, colonization, epidemiology, and public health significance of *Clostridioides difficile* in companion animals. Front Vet Sci 7:512551.
14. Rodriguez Diaz C, Seyboldt C, Rupnik M. 2018. Non-human *C. difficile* reservoirs and sources: Animals, food, environment. Adv Exp Med Biol 1050:227-243.
15. Lim SC, Collins DA, Imwattana K, Knight DR, Perumalsamy S, Hain-Saunders NMR, Putsathit P, Speers D, Riley TV. 2021. Whole-genome sequencing links *Clostridium* (*Clostridioides*) *difficile* in a single hospital to diverse environmental sources in the community. J Appl Microbiol doi:10.1111/jam.15408.
16. Paredes-Sabja D, Shen A, Sorg JA. 2014. *Clostridium difficile* spore biology: Sporulation, germination, and spore structural proteins. Trends Microbiol 22:406-16.
17. Janoir C. 2016. Virulence factors of *Clostridium difficile* and their role during infection. Anaerobe 37:13-24.
18. Brown KA, Langford B, Schwartz KL, Diong C, Garber G, Daneman N. 2021. Antibiotic prescribing choices and their comparative *C. difficile* infection risks: A longitudinal case-cohort study. Clin Infect Dis 72:836-844.
19. Schubert AM, Sinani H, Schloss PD. 2015. Antibiotic-induced alterations of the murine gut microbiota and subsequent effects on colonization resistance against *Clostridium difficile*. mBio 6:e00974-15.
20. Antunes A, Camiade E, Monot M, Courtois E, Barbut F, Sernova NV, Rodionov DA, Martin-Verstraete I, Dupuy B. 2012. Global transcriptional control by glucose and carbon regulator CcpA in *Clostridium difficile*. Nucleic Acids Res 40:10701-10718.
21. Girinathan BP, Ou J, Dupuy B, Govind R. 2018. Pleiotropic roles of *Clostridium difficile sin* locus. PLOS Pathogens 14:e1006940.
22. Nawrocki KL, Edwards AN, Daou N, Bouillaut L, McBride SM. 2016. CodY-Dependent Regulation of Sporulation in *Clostridium difficile*. J Bacteriol 198:2113-30.
23. Girinathan BP, DiBenedetto N, Worley JN, Peltier J, Arrieta-Ortiz ML, Immanuel SRC, Lavin R, Delaney ML, Cummins CK, Hoffman M, Luo Y, Gonzalez-Escalona N, Allard M, Onderdonk AB, Gerber GK, Sonenshein AL, Baliga NS, Dupuy B, Bry L. 2021. *In vivo* commensal control of *Clostridioides difficile* virulence. Cell Host Microbe 29:1693-1708.e7.
24. Ali S, Yui S, Muzslay M, Wilson APR. 2017. Comparison of two whole-room ultraviolet irradiation systems for enhanced disinfection of contaminated hospital patient rooms. J Hosp Infect 97:180-184.
25. Yui S, Ali S, Muzslay M, Jeanes A, Wilson APR. 2017. Identification of *Clostridium difficile* reservoirs in the patient environment and efficacy of aerial hydrogen peroxide decontamination. Infect Control Hosp Epidemiol 38:1487-1492.
26. Sharma SK, Yip C, Esposito EX, Sharma PV, Simon MP, Abel-Santos E, Firestine SM. 2018. The design, synthesis, and characterizations of spore germination inhibitors effective against an epidemic strain of *Clostridium difficile*. J of Medicinal Chemistry 61:6759-6778.
27. Weingarden AR, Chen C, Zhang N, Graiziger CT, Dosa PI, Steer CJ, Shaughnessy MK, Johnson JR, Sadowsky MJ, Khoruts A. 2016. Ursodeoxycholic acid inhibits

Clostridium difficile spore germination and vegetative growth, and prevents the recurrence of ileal pouchitis associated with the infection. J Clin Gastroenterol 50:624-30.
28. Webb BJ, Brunner A, Lewis J, Ford CD, Lopansri BK. 2019. Repurposing an old drug for a new epidemic: Ursodeoxycholic acid to prevent recurrent *Clostridioides difficile* infection. Clin Infect Dis 68:498-500.
29. Winston JA, Rivera AJ, Cai J, Thanissery R, Montgomery SA, Patterson AD, Theriot CM. 2020. Ursodeoxycholic acid (UDCA) mitigates the host inflammatory response during *Clostridioides difficile* infection by altering gut bile acids. Infect Immun 88.
30. Fachi JL, Felipe JdS, Pral LP, da Silva BK, Corrêa RO, de Andrade MCP, da Fonseca DM, Basso PJ, Câmara NOS, de Sales e Souza ÉL, dos Santos Martins F, Guima SES, Thomas AM, Setubal JC, Magalhães YT, Forti FL, Candreva T, Rodrigues HG, de Jesus MB, Consonni SR, Farias AdS, Varga-Weisz P, Vinolo MAR. 2019. Butyrate protects mice from *Clostridium difficile*-induced colitis through an HIF-1-dependent mechanism. Cell Reports 27:750-761.e7.
31. Hryckowian AJ, Van Treuren W, Smits SA, Davis NM, Gardner JO, Bouley DM, Sonnenburg JL. 2018. Microbiota-accessible carbohydrates suppress *Clostridium difficile* infection in a murine model. Nat Microbiol 3:662-669.
32. van Prehn J, Reigadas E, Vogelzang EH, Bouza E, Hristea A, Guery B, Krutova M, Norén T, Allerberger F, Coia JE, Goorhuis A, van Rossen TM, Ooijevaar RE, Burns K, Scharvik Olesen BR, Tschudin-Sutter S, Wilcox MH, Vehreschild M, Fitzpatrick F, Kuijper EJ. 2021. European Society of Clinical Microbiology and Infectious Diseases: 2021 update on the treatment guidance document for Clostridioides difficile infection in adults. Clin Microbiol Infect 27 Suppl 2:S1-s21.
33. Park H, Laffin MR, Jovel J, Millan B, Hyun JE, Hotte N, Kao D, Madsen KL. 2019. The success of fecal microbial transplantation in *Clostridium difficile* infection correlates with bacteriophage relative abundance in the donor: A retrospective cohort study. Gut Microbes doi:10.1080/19490976.2019.1586037:1-12.
34. Draper LA, Ryan FJ, Smith MK, Jalanka J, Mattila E, Arkkila PA, Ross RP, Satokari R, Hill C. 2018. Long-term colonisation with donor bacteriophages following successful faecal microbial transplantation. Microbiome 6:220.
35. Zuo T, Wong SH, Lam K, Lui R, Cheung K, Tang W, Ching JYL, Chan PKS, Chan MCW, Wu JCY, Chan FKL, Yu J, Sung JJY, Ng SC. 2018. Bacteriophage transfer during faecal microbiota transplantation in *Clostridium difficile* infection is associated with treatment outcome. Gut 67:634-643.
36. Kers JA, DeFusco AW, Park JH, Xu J, Pulse ME, Weiss WJ, Handfield M. 2018. OG716: Designing a fit-for-purpose lantibiotic for the treatment of *Clostridium difficile* infections. PLOS ONE 13:e0197467.
37. Cebrián R, Macia-Valero A, Jati AP, Kuipers OP. 2019. Design and expression of specific hybrid lantibiotics active against pathogenic *Clostridium* spp. Front Microbiol 10:2154.
38. Woodworth MH, Hayden MK, Young VB, Kwon JH. 2019. The role of fecal microbiota transplantation in reducing intestinal colonization with antibiotic-resistant organisms: The current landscape and future directions. Open Forum Infect Dis 6.

39. Wilson BC, Vatanen T, Cutfield WS, O'Sullivan JM. 2019. The super-donor phenomenon in fecal microbiota transplantation. Frontiers in cellular and infection microbiology 9:2-2.
40. Tariq R, Pardi DS, Bartlett MG, Khanna S. 2018. Low cure rates in controlled trials of fecal microbiota transplantation for recurrent *Clostridium difficile* infection: A systematic review and meta-analysis. Clinical Infectious Diseases 68:1351-1358.
41. Ott SJ, Waetzig GH, Rehman A, Moltzau-Anderson J, Bharti R, Grasis JA, Cassidy L, Tholey A, Fickenscher H, Seegert D, Rosenstiel P, Schreiber S. 2017. Efficacy of sterile fecal filtrate transfer for treating patients with *Clostridium difficile* infection. Gastroenterology 152:799-811.e7.
42. Hui W, Li T, Liu W, Zhou C, Gao F. 2019. Fecal microbiota transplantation for treatment of recurrent *C. difficile* infection: An updated randomized controlled trial meta-analysis. PLOS ONE 14:e0210016.
43. Madoff SE, Urquiaga M, Alonso CD, Kelly CP. 2019. Prevention of recurrent *Clostridioides difficile* infection: A systematic review of randomized controlled trials. Anaerobe doi:10.1016/j.anaerobe.2019.102098:102098.
44. Tan X, Johnson S. 2019. Fecal microbiota transplantation (FMT) for *C. difficile* infection, just say 'No'. Anaerobe 60:102092.
45. Yang Z, Ramsey J, Hamza T, Zhang Y, Li S, Yfantis HG, Lee D, Hernandez LD, Seghezzi W, Furneisen JM, Davis NM, Therien AG, Feng H. 2015. Mechanisms of protection against *Clostridium difficile* infection by the monoclonal antitoxin antibodies actoxumab and bezlotoxumab. Infect Immun 83:822-31.
46. Garland M, Hryckowian AJ, Tholen M, Oresic Bender K, Van Treuren WW, Loscher S, Sonnenburg JL, Bogyo M. 2020. The clinical drug ebselen attenuates inflammation and promotes microbiome recovery in mice after antibiotic treatment for CDI. Cell Reports Medicine 1:100005.
47. Marreddy RKR, Olaitan AO, May JN, Dong M, Hurdle JG, Khursigara CM. 2021. Ebselen not only inhibits *Clostridioides difficile* toxins but displays redox-associated cellular killing. Microbiology Spectrum 9:e00448-21.
48. Tam J, Icho S, Utama E, Orrell KE, Gómez-Biagi RF, Theriot CM, Kroh HK, Rutherford SA, Lacy DB, Melnyk RA. 2020. Intestinal bile acids directly modulate the structure and function of *C. difficile* TcdB toxin. Proc Natl Acad Sci USA 117:6792-6800.
49. Desai K, Gupta SB, Dubberke ER, Prabhu VS, Browne C, Mast TC. 2016. Epidemiological and economic burden of *Clostridium difficile* in the United States: Estimates from a modeling approach. BMC Infectious Diseases 16:303.
50. Reigadas Ramírez E, Bouza ES. 2018. Economic burden of *Clostridium difficile* infection in European countries, p 1-12. *In* Mastrantonio P, Rupnik M (ed), Updates on *Clostridium difficile* in Europe: Advances in microbiology, infectious diseases and public health, vol 8. Springer International Publishing, Cham.
51. Freeman J, Vernon J, Pilling S, Morris K, Nicolson S, Shearman S, Clark E, Palacios-Fabrega JA, Wilcox M. 2020. Five-year pan-European, longitudinal surveillance of *Clostridium difficile* ribotype prevalence and antimicrobial resistance: The extended ClosER study. Eur J Clin Microbiol Infect Dis 39:169-177.

52. Kuijper EJ, Coignard B, Tüll P. 2006. Emergence of *Clostridium difficile*-associated disease in North America and Europe. Clinical Microbiology and Infection 12:2-18.
53. Finn E, Andersson FL, Madin-Warburton M. 2021. Burden of *Clostridioides difficile* infection (CDI) - A systematic review of the epidemiology of primary and recurrent CDI. BMC Infectious Diseases 21:456.
54. Guh AY, Mu Y, Winston LG, Johnston H, Olson D, Farley MM, Wilson LE, Holzbauer SM, Phipps EC, Dumyati GK, Beldavs ZG, Kainer MA, Karlsson M, Gerding DN, McDonald LC. 2020. Trends in U.S. burden of *Clostridioides difficile* infection and outcomes. New England Journal of Medicine 382:1320-1330.
55. Burke KE, Lamont JT. 2014. *Clostridium difficile* infection: A worldwide disease. Gut and Liver 8:1-6.
56. Abad CLR, Safdar N. 2021. A review of *Clostridioides difficile* infection and antibiotic-associated diarrhea. Gastroenterology Clinics of North America 50:323-340.
57. Lessa FC, Mu Y, Bamberg WM, Beldavs ZG, Dumyati GK, Dunn JR, Farley MM, Holzbauer SM, Meek JI, Phipps EC, Wilson LE, Winston LG, Cohen JA, Limbago BM, Fridkin SK, Gerding DN, McDonald LC. 2015. Burden of *Clostridium difficile* infection in the United States. New England Journal of Medicine 372:825-834.
58. Chiang H-Y, Huang H-C, Chung C-W, Yeh Y-C, Chen Y-C, Tien N, Lin H-S, Ho M-W, Kuo C-C. 2019. Risk prediction for 30-day mortality among patients with *Clostridium difficile* infections: A retrospective cohort study. Antimicrobial Resistance & Infection Control 8:175.
59. Czepiel J, Krutova M, Mizrahi A, Khanafer N, Enoch DA, Patyi M, Deptuła A, Agodi A, Nuvials X, Pituch H, Wójcik-Bugajska M, Filipczak-Bryniarska I, Brzozowski B, Krzanowski M, Konturek K, Fedewicz M, Michalak M, Monpierre L, Vanhems P, Gouliouris T, Jurczyszyn A, Goldman-Mazur S, Wultańska D, Kuijper EJ, Skupień J, Biesiada G, Garlicki A. 2021. Mortality following *Clostridioides difficile* infection in Europe: A retrospective multicenter case-control study. Antibiotics (Basel) 10.
60. Parlet CP, Brown MM, Horswill AR. 2019. Commensal staphylococci influence *Staphylococcus aureus* skin colonization and disease. Trends Microbiol 27:497-507.
61. Crouzet L, Rigottier-Gois L, Serror P. 2015. Potential use of probiotic and commensal bacteria as non-antibiotic strategies against vancomycin-resistant enterococci. FEMS Microbiol Letters 362:fnv012.
62. Ducarmon QR, Zwittink RD, Hornung BVH, van Schaik W, Young VB, Kuijper EJ. 2019. Gut microbiota and colonization resistance against bacterial enteric infection. Microbiol Mol Biol Rev 83.
63. Johnson S, Lavergne V, Skinner AM, Gonzales-Luna AJ, Garey KW, Kelly CP, Wilcox MH. 2021. Clinical practice guideline by the Infectious Diseases Society of America (IDSA) and Society for Healthcare Epidemiology of America (SHEA): 2021 focused update guidelines on management of *Clostridioides difficile* infection in adults. Clin Infect Dis 73:755-757.
64. McDonald LC, Gerding DN, Johnson S, Bakken JS, Carroll KC, Coffin SE, Dubberke ER, Garey KW, Gould CV, Kelly C, Loo V, Shaklee Sammons J, Sandora TJ, Wilcox MH. 2018. Clinical practice guidelines for *Clostridium difficile* infection in adults and children: 2017 update by the Infectious Diseases Society of

America (IDSA) and Society for Healthcare Epidemiology of America (SHEA). Clinical Infectious Diseases 66:e1-e48.
65. Song JH, Kim YS. 2019. Recurrent *Clostridium difficile* infection: Risk factors, treatment, and prevention. Gut and Liver 13:16-24.
66. Barbut F, Richard A, Hamadi K, Chomette V, Burghoffer B, Petit J-C. 2000. Epidemiology of recurrences or reinfections of *Clostridium difficile*-associated diarrhea. J of Clinical Microbiology 38:2386-2388.
67. Seekatz AM, Wolfrum E, DeWald CM, Putler RKB, Vendrov KC, Rao K, Young VB. 2018. Presence of multiple *Clostridium difficile* strains at primary infection is associated with development of recurrent disease. Anaerobe 53:74-81.
68. Dayananda P, Wilcox MH. 2019. A review of mixed strain *Clostridium difficile* colonization and infection. Frontiers in Microbiology 10.
69. Leslie JL, Jenior ML, Vendrov KC, Standke AK, Barron MR, O'Brien TJ, Unverdorben L, Thaprawat P, Bergin IL, Schloss PD, Young VB. 2021. Protection from lethal *Clostridioides difficile* infection via intraspecies competition for cogerminant. mBio 12.
70. Merrigan MM, Sambol SP, Johnson S, Gerding DN. 2009. New approach to the management of *Clostridium difficile* infection: Colonisation with non-toxigenic *C. difficile* during daily ampicillin or ceftriaxone administration. Int J of Antimicrobial Agents 33:S46-S50.
71. Zuo T, Wong SH, Cheung CP, Lam K, Lui R, Cheung K, Zhang F, Tang W, Ching JYL, Wu JCY, Chan PKS, Sung JJY, Yu J, Chan FKL, Ng SC. 2018. Gut fungal dysbiosis correlates with reduced efficacy of fecal microbiota transplantation in *Clostridium difficile* infection. Nat Commun 9:3663.
72. Shrestha R, Sorg JA. 2018. Hierarchical recognition of amino acid co-germinants during *Clostridioides difficile* spore germination. Anaerobe 49:41-47.
73. Kochan TJ, Somers MJ, Kaiser AM, Shoshiev MS, Hagan AK, Hastie JL, Giordano NP, Smith AD, Schubert AM, Carlson PE, Jr., Hanna PC. 2017. Intestinal calcium and bile salts facilitate germination of *Clostridium difficile* spores. PLOS Pathogens 13:e1006443.
74. Wheeldon LJ, Worthington T, Hilton AC, Elliott TSJ, Lambert PA. 2008. Physical and chemical factors influencing the germination of *Clostridium difficile* spores. J of Applied Microbiology 105:2223-2230.
75. Sorg JA, Sonenshein AL. 2008. Bile salts and glycine as cogerminants for *Clostridium difficile* spores. J Bacteriol 190:2505-12.
76. Rohlfing AE, Eckenroth BE, Forster ER, Kevorkian Y, Donnelly ML, Benito de la Puebla H, Doublié S, Shen A. 2019. The CspC pseudoprotease regulates germination of *Clostridioides difficile* spores in response to multiple environmental signals. PLOS Genetics 15:e1008224.
77. Shrestha R, Cochran AM, Sorg JA. 2019. The requirement for co-germinants during *Clostridium difficile* spore germination is influenced by mutations in *yabG* and *cspA*. PLOS Pathogens 15:e1007681.
78. Kevorkian Y, Shen A. 2017. Revisiting the role of Csp family proteins in regulating *Clostridium difficile* spore germination. J of Bacteriology 199.
79. Theriot CM, Bowman AA, Young VB. 2015. Antibiotic-induced alterations of the gut microbiota alter secondary bile acid production and allow for *Clostridium*

difficile spore germination and outgrowth in the large intestine. mSphere 1:e00045-15.
80. Thanissery R, Winston JA, Theriot CM. 2017. Inhibition of spore germination, growth, and toxin activity of clinically relevant *C. difficile* strains by gut microbiota derived secondary bile acids. Anaerobe 45:86-100.
81. Winston JA, Theriot CM. 2019. Diversification of host bile acids by members of the gut microbiota. Gut Microbes doi:10.1080/19490976.2019.1674124:1-14.
82. Ridlon JM, Kang D-J, Hylemon PB. 2006. Bile salt biotransformations by human intestinal bacteria. J of Lipid Research 47:241-59.
83. Francis MB, Sorg JA. 2016. Dipicolinic acid release by germinating *Clostridium difficile* spores occurs through a mechanosensing mechanism. mSphere 1.
84. Browne HP, Forster SC, Anonye BO, Kumar N, Neville BA, Stares MD, Goulding D, Lawley TD. 2016. Culturing of 'unculturable' human microbiota reveals novel taxa and extensive sporulation. Nature 533:543.
85. Awad MM, Hutton ML, Quek AJ, Klare WP, Mileto SJ, Mackin K, Ly D, Oorschot V, Bosnjak M, Jenkin G, Conroy PJ, West N, Fulcher A, Costin A, Day CJ, Jennings MP, Medcalf RL, Sanderson-Smith M, Cordwell SJ, Law RHP, Whisstock JC, Lyras D. 2020. Human plasminogen exacerbates *Clostridioides difficile* enteric disease and alters the spore surface. Gastroenterology 159:1431-1443.e6.
86. Kochan TJ, Shoshiev MS, Hastie JL, Somers MJ, Plotnick YM, Gutierrez-Munoz DF, Foss ED, Schubert AM, Smith AD, Zimmerman SK, Carlson PE, Hanna PC. 2018. Germinant synergy facilitates *Clostridium difficile* spore germination under physiological conditions. mSphere 3.
87. Heeg D, Burns DA, Cartman ST, Minton NP. 2012. Spores of *Clostridium difficile* clinical isolates display a diverse germination response to bile salts. PLOS ONE 7:e32381.
88. Bhattacharjee D, Francis MB, Ding X, McAllister KN, Shrestha R, Sorg JA. 2016. Reexamining the germination phenotypes of several *Clostridium difficile* strains suggests another role for the CspC germinant receptor. J of Bacteriology 198:777-786.
89. Sankar SA, Lagier J-C, Pontarotti P, Raoult D, Fournier P-E. 2015. The human gut microbiome, a taxonomic conundrum. Systematic and Applied Microbiology 38:276-286.
90. Zmora N, Zilberman-Schapira G, Suez J, Mor U, Dori-Bachash M, Bashiardes S, Kotler E, Zur M, Regev-Lehavi D, Brik RB-Z, Federici S, Cohen Y, Linevsky R, Rothschild D, Moor AE, Ben-Moshe S, Harmelin A, Itzkovitz S, Maharshak N, Shibolet O, Shapiro H, Pevsner-Fischer M, Sharon I, Halpern Z, Segal E, Elinav E. 2018. Personalized gut mucosal colonization resistance to empiric probiotics is associated with unique host and microbiome features. Cell 174:1388-1405.e21.
91. Wiles TJ, Guillemin K. 2019. The other side of the coin: What beneficial microbes can teach us about pathogenic potential. J Mol Biol 431:2946-2956.
92. Garrett EM, Sekulovic O, Wetzel D, Jones JB, Edwards AN, Vargas-Cuebas G, McBride SM, Tamayo R. 2019. Phase variation of a signal transduction system controls *Clostridioides difficile* colony morphology, motility, and virulence. PLOS Biology 17:e3000379.

93. Reyes Ruiz LM, Williams CL, Tamayo R. 2020. Enhancing bacterial survival through phenotypic heterogeneity. PLOS Pathogens 16:e1008439.
94. Crobach MJT, Vernon JJ, Loo VG, Kong LY, Péchiné S, Wilcox MH, Kuijper EJ. 2018. Understanding *Clostridium difficile* colonization. Clinical Microbiology Reviews 31.
95. Anjewierden S, Han Z, Brown AM, Donskey CJ, Deshpande A. 2021. Risk factors for *Clostridioides difficile* colonization among hospitalized adults: A meta-analysis and systematic review. Infect Control Hosp Epidemiol 42:565-572.
96. Cao Y, Wang L, Ke S, Villafuerte Gálvez JA, Pollock NR, Barrett C, Sprague R, Daugherty K, Xu H, Lin Q, Yao J, Chen Y, Kelly CP, Liu YY, Chen X. 2021. Fecal mycobiota combined with host immune factors distinguish *Clostridioides difficile* infection from asymptomatic carriage. Gastroenterology 160:2328-2339.e6.
97. Dubois T, Tremblay YDN, Hamiot A, Martin-Verstraete I, Deschamps J, Monot M, Briandet R, Dupuy B. 2019. A microbiota-generated bile salt induces biofilm formation in *Clostridium difficile*. NPJ Biofilms Microbiomes 5:14.
98. Semenyuk EG, Poroyko VA, Johnston PF, Jones SE, Knight KL, Gerding DN, Driks A. 2015. Analysis of bacterial communities during *Clostridium difficile* infection in the mouse. Infect Immun 83:4383-91.
99. Brauer M, Lassek C, Hinze C, Hoyer J, Becher D, Jahn D, Sievers S, Riedel K. 2021. What's a biofilm?—How the choice of the biofilm model impacts the protein inventory of *Clostridioides difficile*. Front Microbiol 12:682111.
100. Ahmed UKB, Shadid TM, Larabee JL, Ballard JD, Gilmore MS. 2020. Combined and distinct roles of Agr proteins in *Clostridioides difficile* 630 sporulation, motility, and toxin production. mBio 11:e03190-20.
101. Edwards AN, Nawrocki KL, McBride SM. 2014. Conserved oligopeptide permeases modulate sporulation initiation in *Clostridium difficile*. Infect Immun 82:4276-91.
102. Chen KY, Rathod J, Chiu YC, Chen JW, Tsai PJ, Huang IH. 2019. The transcriptional regulator Lrp contributes to toxin expression, sporulation, and swimming motility in *Clostridium difficile*. Front Cell Infect Microbiol 9:356.
103. Edwards AN, Tamayo R, McBride SM. 2016. A novel regulator controls *Clostridium difficile* sporulation, motility and toxin production. Mol Microbiol 100:954-71.
104. El Meouche I, Peltier J. 2018. Toxin release mediated by the novel autolysin Cwp19 in *Clostridium difficile*. Microb Cell 5:421-423.
105. Govind R, Dupuy B. 2012. Secretion of *Clostridium difficile* toxins A and B requires the holin-like protein TcdE. PLOS Pathogens 8.
106. Govind R, Fitzwater L, Nichols R. 2015. Observations on the Role of TcdE isoforms in *Clostridium difficile* toxin secretion. J of Bacteriology 197:2600-2609.
107. Olling A, Seehase S, Minton NP, Tatge H, Schröter S, Kohlscheen S, Pich A, Just I, Gerhard R. 2012. Release of TcdA and TcdB from *Clostridium difficile* cdi 630 is not affected by functional inactivation of the *tcdE* gene. Microb Pathog 52:92-100.
108. Tan KS, Wee BY, Song KP. 2001. Evidence for holin function of *tcdE* gene in the pathogenicity of *Clostridium difficile*. J Med Microbiol 50:613-619.
109. Ransom EM, Kaus GM, Tran PM, Ellermeier CD, Weiss DS. 2018. Multiple factors contribute to bimodal toxin gene expression in *Clostridioides* (*Clostridium*) *difficile*. Molecular Microbiology 110:533-549.

110. Aktories K, Schwan C, Jank T. 2017. *Clostridium difficile* toxin biology. Annu Rev Microbiol 71:281-307.
111. Bouillaut L, Dubois T, Sonenshein AL, Dupuy B. 2015. Integration of metabolism and virulence in *Clostridium difficile*. Res Microbiol 166:375-383.
112. Natarajan M, Walk ST, Young VB, Aronoff DM. 2013. A clinical and epidemiological review of non-toxigenic *Clostridium difficile*. Anaerobe 22:1-5.
113. Janezic S, Dingle K, Alvin J, Accetto T, Didelot X, Crook DW, Lacy DB, Rupnik M. 2020. Comparative genomics of *Clostridioides difficile* toxinotypes identifies module-based toxin gene evolution. Microb Genom 6.
114. Tao L, Tian S, Zhang J, Liu Z, Robinson-McCarthy L, Miyashita SI, Breault DT, Gerhard R, Oottamasathien S, Whelan SPJ, Dong M. 2019. Sulfated glycosaminoglycans and low-density lipoprotein receptor contribute to *Clostridium difficile* toxin A entry into cells. Nat Microbiol 4:1760-1769.
115. Tao L, Zhang J, Meraner P, Tovaglieri A, Wu X, Gerhard R, Zhang X, Stallcup WB, Miao J, He X, Hurdle JG, Breault DT, Brass AL, Dong M. 2016. Frizzled proteins are colonic epithelial receptors for *C. difficile* toxin B. Nature 538:350-355.
116. Schöttelndreier D, Langejürgen A, Lindner R, Genth H. 2020. Low density lipoprotein receptor-related protein-1 (LRP1) is involved in the uptake of *Clostridioides difficile* toxin A and serves as an internalizing receptor. Front Cell Infect Microbiol 10:565465.
117. LaFrance ME, Farrow MA, Chandrasekaran R, Sheng J, Rubin DH, Lacy DB. 2015. Identification of an epithelial cell receptor responsible for *Clostridium difficile* TcdB-induced cytotoxicity. Proc Natl Acad Sci USA 112:7073-8.
118. López-Ureña D, Orozco-Aguilar J, Chaves-Madrigal Y, Ramírez-Mata A, Villalobos-Jimenez A, Ost S, Quesada-Gómez C, Rodríguez C, Papatheodorou P, Chaves-Olarte E. 2019. Toxin B variants from *Clostridium difficile* strains VPI 10463 and NAP1/027 share similar substrate profile and cellular intoxication kinetics but use different host cell entry factors. Toxins 11.
119. Zhao H, Nickle DC, Zeng Z, Law PYT, Wilcox MH, Chen L, Peng Y, Meng J, Deng Z, Albright A, Zhong H, Xu X, Zhu S, Shen J, Blanchard RL, Dorr MB, Shaw PM, Li J. 2021. Global landscape of *Clostridioides difficile* phylogeography, antibiotic susceptibility, and toxin polymorphisms by post-hoc whole-genome sequencing from the MODIFY I/II Studies. Infect Dis Ther 10:853-870.
120. Papatheodorou P, Barth H, Minton N, Aktories K. 2018. Cellular uptake and mode-of-action of *Clostridium difficile* toxins. Adv Exp Med Biol 1050:77-96.
121. Chandrasekaran R, Kenworthy AK, Lacy DB. 2016. *Clostridium difficile* toxin A undergoes clathrin-independent, PACSIN2-dependent endocytosis. PLOS Pathogens 12:e1006070.
122. Gerhard R, Frenzel E, Goy S, Olling A. 2013. Cellular uptake of *Clostridium difficile* TcdA and truncated TcdA lacking the receptor binding domain. J Med Microbiol 62:1414-1422.
123. Pan Z, Zhang Y, Luo J, Li D, Zhou Y, He L, Yang Q, Dong M, Tao L. 2021. Functional analyses of epidemic *Clostridioides difficile* toxin B variants reveal their divergence in utilizing receptors and inducing pathology. PLOS Pathogens 17:e1009197.

124. Abernathy-Close L, Barron Madeline R, George James M, Dieterle Michael G, Vendrov Kimberly C, Bergin Ingrid L, Young Vincent B, Ballard Jimmy D. Intestinal inflammation and altered gut microbiota associated with inflammatory bowel disease render mice susceptible to *Clostridioides difficile* colonization and infection. mBio 12:e02733-20.
125. Fletcher JR, Pike CM, Parsons RJ, Rivera AJ, Foley MH, McLaren MR, Montgomery SA, Theriot CM. 2021. *Clostridioides difficile* exploits toxin-mediated inflammation to alter the host nutritional landscape and exclude competitors from the gut microbiota. Nat Commun 12:462.
126. Sehgal K, Khanna S. 2021. Immune response against *Clostridioides difficile* and translation to therapy. Therap Adv Gastroenterol 14:17562848211014817.
127. Kelly CP, Poxton IR, Shen J, Wilcox MH, Gerding DN, Zhao X, Laterza OF, Railkar R, Guris D, Dorr MB. 2020. Effect of endogenous *Clostridioides difficile* toxin antibodies on recurrence of *C. difficile* infection. Clin Infect Dis 71:81-86.
128. Akiyama S, Yamada A, Komaki Y, Komaki F, Micic D, Sakuraba A. 2021. Efficacy and safety of monoclonal antibodies against *Clostridioides difficile* toxins for prevention of recurrent *Clostridioides difficile* infection: A systematic review and meta-analysis. J Clin Gastroenterol 55:43-51.
129. Kyne L, Warny M, Qamar A, Kelly CP. 2001. Association between antibody response to toxin A and protection against recurrent *Clostridium difficile* diarrhoea. The Lancet 357:189-193.
130. Segev E, Smith Y, Ben-Yehuda S. 2012. RNA dynamics in aging bacterial spores. Cell 148:139-149.
131. Shen A. 2020. *Clostridioides difficile* spore formation and germination: New insights and opportunities for intervention. Annu Rev Microbiol 74:545-566.
132. Castro-Córdova P, Mora-Uribe P, Reyes-Ramírez R, Cofré-Araneda G, Orozco-Aguilar J, Brito-Silva C, Mendoza-León MJ, Kuehne SA, Minton NP, Pizarro-Guajardo M, Paredes-Sabja D. 2021. Entry of spores into intestinal epithelial cells contributes to recurrence of *Clostridioides difficile* infection. Nat Commun 12:1140.
133. de Cena JA, Zhang J, Deng D, Damé-Teixeira N, Do T. 2021. Low-abundant microorganisms: The human microbiome's dark matter, a scoping review. Front Cell Infect Microbiol 11:689197.
134. Shortt C, Hasselwander O, Meynier A, Nauta A, Fernández EN, Putz P, Rowland I, Swann J, Türk J, Vermeiren J, Antoine J-M. 2018. Systematic review of the effects of the intestinal microbiota on selected nutrients and non-nutrients. European Journal of Nutrition 57:25-49.
135. Kern L, Abdeen SK, Kolodziejczyk AA, Elinav E. 2021. Commensal inter-bacterial interactions shaping the microbiota. Current Opinion in Microbiology 63:158-171.
136. Runge S, Rosshart SP. 2021. The mammalian metaorganism: A holistic view on how microbes of all kingdoms and niches shape local and systemic immunity. Frontiers in Immunology 12.
137. Suez J, Zmora N, Zilberman-Schapira G, Mor U, Dori-Bachash M, Bashiardes S, Zur M, Regev-Lehavi D, Ben-Zeev Brik R, Federici S, Horn M, Cohen Y, Moor AE, Zeevi D, Korem T, Kotler E, Harmelin A, Itzkovitz S, Maharshak N, Shibolet O, Pevsner-Fischer M, Shapiro H, Sharon I, Halpern Z, Segal E, Elinav E. 2018. Post-

antibiotic gut mucosal microbiome reconstitution is impaired by probiotics and improved by autologous FMT. Cell 174:1406-1423.e16.
138. Islam W, Noman A, Naveed H, Huang Z, Chen HYH. 2020. Role of environmental factors in shaping the soil microbiome. Environ Sci Pollut Res Int 27:41225-41247.
139. Konjar Š, Pavšič M, Veldhoen M. 2021. Regulation of oxygen homeostasis at the intestinal epithelial barrier site. Int J Mol Sci 22.
140. Kint N, Alves Feliciano C, Martins MC, Morvan C, Fernandes SF, Folgosa F, Dupuy B, Texeira M, Martin-Verstraete I. 2020. How the anaerobic enteropathogen *Clostridioides difficile* tolerates low O_2 Tensions. mBio 11.
141. Morvan C, Folgosa F, Kint N, Teixeira M, Martin-Verstraete I. 2021. Responses of clostridia to oxygen: from detoxification to adaptive strategies. Environ Microbiol 23:4112-4125.
142. Wetzel D, McBride SM. 2020. The impact of pH on *Clostridioides difficile* sporulation and physiology. Appl Environ Microbiol 86.
143. Djemai K, Drancourt M, Tidjani Alou M. 2021. Bacteria and methanogens in the human microbiome: A review of syntrophic interactions. Microb Ecol doi:10.1007/s00248-021-01796-7.
144. Magrone T, Russo MA, Jirillo E. 2018. Antimicrobial peptides: Phylogenic sources and biological activities. First of two parts. Curr Pharm Des 24:1043-1053.
145. Moravej H, Moravej Z, Yazdanparast M, Heiat M, Mirhosseini A, Moosazadeh Moghaddam M, Mirnejad R. 2018. Antimicrobial peptides: Features, action, and their resistance mechanisms in bacteria. Microb Drug Resist 24:747-767.
146. Barreto-Santamaría A, Arévalo-Pinzón G, Patarroyo MA, Patarroyo ME. 2021. How to combat Gram-negative bacteria using antimicrobial peptides: A challenge or an unattainable goal? Antibiotics 10.
147. Sandiford SK. 2019. Current developments in lantibiotic discovery for treating *Clostridium difficile* infection. Expert Opin Drug Discov 14:71-79.
148. Suárez JM, Edwards AN, McBride SM. 2013. The *Clostridium difficile cpr* locus is regulated by a noncontiguous two-component system in response to type A and B lantibiotics. J Bacteriol 195:2621-31.
149. Townsend EM, Kelly L, Muscatt G, Box JD, Hargraves N, Lilley D, Jameson E. 2021. The human gut phageome: Origins and roles in the human gut microbiome. Front Cell Infect Microbiol 11:643214.
150. Naureen Z, Dautaj A, Anpilogov K, Camilleri G, Dhuli K, Tanzi B, Maltese PE, Cristofoli F, De Antoni L, Beccari T, Dundar M, Bertelli M. 2020. Bacteriophages presence in nature and their role in the natural selection of bacterial populations. Acta Biomed 91:e2020024.
151. Baugher JL, Durmaz E, Klaenhammer TR. 2014. Spontaneously induced prophages in *Lactobacillus gasseri* contribute to horizontal gene transfer. Appl Environ Microbiol 80:3508-17.
152. Oladeinde A, Cook K, Lakin SM, Woyda R, Abdo Z, Looft T, Herrington K, Zock G, Lawrence JP, Thomas JCt, Beaudry MS, Glenn T. 2019. Horizontal gene transfer and acquired antibiotic resistance in *Salmonella enterica* serovar Heidelberg following *in vitro* incubation in broiler ceca. Appl Environ Microbiol 85.
153. Zünd M, Ruscheweyh HJ, Field CM, Meyer N, Cuenca M, Hoces D, Hardt WD, Sunagawa S. 2021. High throughput sequencing provides exact genomic locations

of inducible prophages and accurate phage-to-host ratios in gut microbial strains. Microbiome 9:77.
154. Roux S, Brum JR, Dutilh BE, Sunagawa S, Duhaime MB, Loy A, Poulos BT, Solonenko N, Lara E, Poulain J, Pesant S, Kandels-Lewis S, Dimier C, Picheral M, Searson S, Cruaud C, Alberti A, Duarte CM, Gasol JM, Vaqué D, Bork P, Acinas SG, Wincker P, Sullivan MB, Tara Oceans C. 2016. Ecogenomics and potential biogeochemical impacts of globally abundant ocean viruses. Nature 537:689-693.
155. de Jonge PA, Nobrega FL, Brouns SJJ, Dutilh BE. 2019. Molecular and evolutionary determinants of bacteriophage host range. Trends Microbiol 27:51-63.
156. Riedel T, Wittmann J, Bunk B, Schober I, Spröer C, Gronow S, Overmann J. 2017. A *Clostridioides difficile* bacteriophage genome encodes functional binary toxin-associated genes. J of Biotechnology 250:23-28.
157. Nale JY, Spencer J, Hargreaves KR, Buckley AM, Trzepiński P, Douce GR, Clokie MRJ. 2016. Bacteriophage combinations significantly reduce *Clostridium difficile* growth *in vitro* and proliferation *in vivo*. Antimicrob Agents Chemother 60:968-981.
158. Nale JY, Redgwell TA, Millard A, Clokie MRJ. 2018. Efficacy of an optimised bacteriophage cocktail to clear *Clostridium difficile* in a batch fermentation model. Antibiotics 7:13.
159. Usui Y, Ayibieke A, Kamiichi Y, Okugawa S, Moriya K, Tohda S, Saito R. 2020. Impact of deoxycholate on *Clostridioides difficile* growth, toxin production, and sporulation. Heliyon 6:e03717.
160. Buffie CG, Bucci V, Stein RR, McKenney PT, Ling L, Gobourne A, No D, Liu H, Kinnebrew M, Viale A, Littmann E, van den Brink MRM, Jenq RR, Taur Y, Sander C, Cross JR, Toussaint NC, Xavier JB, Pamer EG. 2015. Precision microbiome reconstitution restores bile acid mediated resistance to *Clostridium difficile*. Nature 517:205-208.
161. Reed AD, Nethery MA, Stewart A, Barrangou R, Theriot CM, Comstock LE. 2020. Strain-dependent inhibition of *Clostridioides difficile* by commensal *Clostridia* carrying the bile acid-inducible (*bai*) operon. J of Bacteriology 202:e00039-20.
162. Quinn RA, Melnik AV, Vrbanac A, Fu T, Patras KA, Christy MP, Bodai Z, Belda-Ferre P, Tripathi A, Chung LK, Downes M, Welch RD, Quinn M, Humphrey G, Panitchpakdi M, Weldon KC, Aksenov A, da Silva R, Avila-Pacheco J, Clish C, Bae S, Mallick H, Franzosa EA, Lloyd-Price J, Bussell R, Thron T, Nelson AT, Wang M, Leszczynski E, Vargas F, Gauglitz JM, Meehan MJ, Gentry E, Arthur TD, Komor AC, Poulsen O, Boland BS, Chang JT, Sandborn WJ, Lim M, Garg N, Lumeng JC, Xavier RJ, Kazmierczak BI, Jain R, Egan M, Rhee KE, Ferguson D, Raffatellu M, Vlamakis H, et al. 2020. Global chemical effects of the microbiome include new bile-acid conjugations. Nature 579:123-129.
163. Sievers S, Metzendorf NG, Dittmann S, Troitzsch D, Gast V, Tröger SM, Wolff C, Zühlke D, Hirschfeld C, Schlüter R, Riedel K. 2019. Differential view on the bile acid stress response of *Clostridioides difficile*. Frontiers in Microbiology 10.
164. Koropatkin NM, Cameron EA, Martens EC. 2012. How glycan metabolism shapes the human gut microbiota. Nature Reviews Microbiology 10:323-323.
165. van der Hee B, Wells JM. 2021. Microbial regulation of host physiology by short-chain fatty acids. Trends Microbiol 29:700-712.

166. Weiner N, Draskóczy P. 1961. The effects of organic acids on the oxidative metabolism of intact and disrupted *E. coli*. J of Pharmacology and Experimental Therapeutics 132:299-305.
167. Repaske DR, Adler J. 1981. Change in intracellular pH of *Escherichia coli* mediates the chemotactic response to certain attractants and repellents. J Bacteriol 145:1196-208.
168. Fischbach MA, Sonnenburg JL. 2011. Eating for two: How metabolism establishes interspecies interactions in the gut. Cell Host Microbe 10:336-47.
169. Sun Y, O'Riordan MXD. 2013. Regulation of bacterial pathogenesis by intestinal short-chain fatty acids. Advances in Applied Microbiology 85:93-118.
170. Seekatz AM, Theriot CM, Rao K, Chang Y-M, Freeman AE, Kao JY, Young VB. 2018. Restoration of short chain fatty acid and bile acid metabolism following fecal microbiota transplantation in patients with recurrent *Clostridium difficile* infection. Anaerobe doi:10.1016/j.anaerobe.2018.04.001.
171. Pettit LJ, Browne HP, Yu L, Smits WK, Fagan RP, Barquist L, Martin MJ, Goulding D, Duncan SH, Flint HJ, Dougan G, Choudhary JS, Lawley TD. 2014. Functional genomics reveals that *Clostridium difficile* Spo0A coordinates sporulation, virulence and metabolism. BMC Genomics 15:160.
172. Buckel W. 2021. Energy conservation in fermentations of anaerobic bacteria. Front Microbiol 12:703525.
173. Leslie JL, Vendrov KC, Jenior ML, Young VB. 2019. The gut microbiota is associated with clearance of *Clostridium difficile* infection independent of adaptive immunity. mSphere 4:e00698-18.
174. Frisbee AL, Saleh MM, Young MK, Leslie JL, Simpson ME, Abhyankar MM, Cowardin CA, Ma JZ, Pramoonjago P, Turner SD, Liou AP, Buonomo EL, Petri WA, Jr. 2019. IL-33 drives group 2 innate lymphoid cell-mediated protection during *Clostridium difficile* infection. Nat Commun 10:2712.
175. Freter R, Brickner H, Botney M, Cleven D, Aranki A. 1983. Mechanisms that control bacterial populations in continuous-flow culture models of mouse large intestinal flora. Infect Immun 39:676-685.
176. Marcobal A, Southwick AM, Earle KA, Sonnenburg JL. 2013. A refined palate: Bacterial consumption of host glycans in the gut. Glycobiology 23:1038-46.
177. Wittung-Stafshede P. 2002. Role of cofactors in protein folding. Accounts of Chemical Research 35:201-208.
178. Faber F, Bäumler AJ. 2014. The impact of intestinal inflammation on the nutritional environment of the gut microbiota. Immunol Lett 162:48-53.
179. Berger T, Togawa A, Duncan GS, Elia AJ, You-Ten A, Wakeham A, Fong HEH, Cheung CC, Mak TW. 2006. Lipocalin 2-deficient mice exhibit increased sensitivity to *Escherichia coli* infection but not to ischemia-reperfusion injury. Proc Natl Acad Sci USA 103:1834-1839.
180. Fischbach MA, Lin H, Zhou L, Yu Y, Abergel RJ, Liu DR, Raymond KN, Wanner BL, Strong RK, Walsh CT, Aderem A, Smith KD. 2006. The pathogen-associated *iroA* gene cluster mediates bacterial evasion of lipocalin 2. Proc Natl Acad Sci USA 103:16502-16507.
181. Knippel RJ, Wexler AG, Miller JM, Beavers WN, Weiss A, de Crécy-Lagard V, Edmonds KA, Giedroc DP, Skaar EP. 2020. *Clostridioides difficile* senses and

hijacks host heme for incorporation into an oxidative stress defense system. Cell Host Microbe 28:411-421.e6.
182. Knippel RJ, Zackular JP, Moore JL, Celis AI, Weiss A, Washington MK, DuBois JL, Caprioli RM, Skaar EP. 2018. Heme sensing and detoxification by HatRT contributes to pathogenesis during *Clostridium difficile* infection. PLOS Pathogens 14:e1007486.
183. Zackular JP, Knippel RJ, Lopez CA, Beavers WN, Maxwell CN, Chazin WJ, Skaar EP. 2020. ZupT facilitates *Clostridioides difficile* resistance to host-mediated nutritional immunity. mSphere 5.
184. Zackular JP, Moore JL, Jordan AT, Juttukonda LJ, Noto MJ, Nicholson MR, Crews JD, Semler MW, Zhang Y, Ware LB, Washington MK, Chazin WJ, Caprioli RM, Skaar EP. 2016. Dietary zinc alters the microbiota and decreases resistance to *Clostridium difficile* infection. Nat Med 22:1330-1334.
185. Lopez CA, Beavers WN, Weiss A, Knippel RJ, Zackular JP, Chazin W, Skaar EP. 2019. The immune protein calprotectin impacts *Clostridioides difficile* metabolism through zinc limitation. mBio 10.
186. Jenior ML, Leslie JL, Young VB, Schloss PD. 2017. *Clostridium difficile* colonizes alternative nutrient niches during infection across distinct murine gut microbiomes. mSystems 2.
187. Darkoh C, Plants-Paris K, Bishoff D, DuPont HL. 2019. *Clostridium difficile* modulates the gut microbiota by inducing the production of indole, an interkingdom signaling and antimicrobial molecule. mSystems 4.
188. Dawson LF, Donahue EH, Cartman ST, Barton RH, Bundy J, McNerney R, Minton NP, Wren BW. 2011. The analysis of para-cresol production and tolerance in *Clostridium difficile* 027 and 012 strains. BMC Microbiology 11:86.
189. Passmore IJ, Letertre MPM, Preston MD, Bianconi I, Harrison MA, Nasher F, Kaur H, Hong HA, Baines SD, Cutting SM, Swann JR, Wren BW, Dawson LF. 2018. *Para*-cresol production by *Clostridium difficile* affects microbial diversity and membrane integrity of Gram-negative bacteria. PLOS Pathogens 14:e1007191.
190. Hansson GC. 2020. Mucins and the microbiome. Annual Review of Biochemistry 89:769-793.
191. Engevik MA, Engevik AC, Engevik KA, Auchtung JM, Chang-Graham AL, Ruan W, Luna RA, Hyser JM, Spinler JK, Versalovic J. 2021. Mucin-degrading microbes release monosaccharides that chemoattract *Clostridioides difficile* and facilitate colonization of the human intestinal mucus layer. ACS Infectious Diseases 7:1126-1142.
192. Engevik MA, Yacyshyn MB, Engevik KA, Wang J, Darien B, Hassett DJ, Yacyshyn BR, Worrell RT. 2015. Human *Clostridium difficile* infection: altered mucus production and composition. American Journal of Physiology-Gastrointestinal and Liver Physiology 308:G510-G524.
193. Pereira FC, Wasmund K, Cobankovic I, Jehmlich N, Herbold CW, Lee KS, Sziranyi B, Vesely C, Decker T, Stocker R, Warth B, von Bergen M, Wagner M, Berry D. 2020. Rational design of a microbial consortium of mucosal sugar utilizers reduces *Clostridiodes difficile* colonization. Nat Commun 11:5104.
194. Ng KM, Ferreyra JA, Higginbottom SK, Lynch JB, Kashyap PC, Gopinath S, Naidu N, Choudhury B, Weimer BC, Monack DM, Sonnenburg JL. 2013. Microbiota-

liberated host sugars facilitate post-antibiotic expansion of enteric pathogens. Nature 502:96-9.
195. Neumann-Schaal M, Jahn D, Schmidt-Hohagen K. 2019. Metabolism the difficile way: The key to the success of the pathogen *Clostridioides difficile*. Front Microbiol 10:219.
196. Robinson JI, Weir WH, Crowley JR, Hink T, Reske KA, Kwon JH, Burnham CD, Dubberke ER, Mucha PJ, Henderson JP. 2019. Metabolomic networks connect host-microbiome processes to human *Clostridioides difficile* infections. J Clin Invest 129:3792-3806.
197. Gencic S, Grahame DA. 2020. Diverse energy-conserving pathways in *Clostridium difficile*: Growth in the absence of amino acid Stickland acceptors and the role of the Wood-Ljungdahl Pathway. J Bacteriol 202.
198. Aguirre AM, Yalcinkaya N, Wu Q, Swennes A, Tessier ME, Roberts P, Miyajima F, Savidge T, Sorg JA. 2021. Bile acid-independent protection against *Clostridioides difficile* infection. PLOS Pathogens 17:e1010015.
199. Collins J, Robinson C, Danhof H, Knetsch CW, van Leeuwen HC, Lawley TD, Auchtung JM, Britton RA. 2018. Dietary trehalose enhances virulence of epidemic *Clostridium difficile*. Nature 553:291.
200. Eyre DW, Didelot X, Buckley AM, Freeman J, Moura IB, Crook DW, Peto TEA, Walker AS, Wilcox MH, Dingle KE. 2019. *Clostridium difficile* trehalose metabolism variants are common and not associated with adverse patient outcomes when variably present in the same lineage. EBioMedicine 43:347-355.
201. Saund K, Rao K, Young VB, Snitkin ES. 2020. Genetic determinants of trehalose utilization are not associated with severe *Clostridium difficile* infection outcome. Open Forum Infect Dis 7:ofz548.
202. El Aidy S, van den Bogert B, Kleerebezem M. 2015. The small intestine microbiota, nutritional modulation and relevance for health. Current Opinion in Biotechnology 32:14-20.
203. Poulakos L, Kent TH. 1973. Gastric emptying and small intestinal propulsion in fed and fasted rats. Gastroenterology 64:962-967.
204. Ridlon JM, Kang DJ, Hylemon PB, Bajaj JS. 2014. Bile acids and the gut microbiome. Current Opinion in Gastroenterology 30:332-8.
205. Araújo JR, Tomas J, Brenner C, Sansonetti PJ. 2017. Impact of high-fat diet on the intestinal microbiota and small intestinal physiology before and after the onset of obesity. Biochimie 141:97-106.
206. Martinez-Guryn K, Hubert N, Frazier K, Urlass S, Musch MW, Ojeda P, Pierre JF, Miyoshi J, Sontag TJ, Cham CM, Reardon CA, Leone V, Chang EB. 2018. Small intestine microbiota regulate host digestive and absorptive adaptive responses to dietary lipids. Cell Host Microbe 23:458-469.e5.
207. Flynn KJ, Ruffin MT, Turgeon DK, Schloss PD. 2018. Spatial variation of the native colon microbiota in healthy adults. Cancer Prevention Research 11:393-402.
208. Falony G, Vieira-Silva S, Raes J. 2018. Richness and ecosystem development across faecal snapshots of the gut microbiota. Nat Microbiol 3:526-528.
209. Sekirov I, Russell SL, Antunes LCM, Finlay BB. 2010. Gut microbiota in health and disease. Physiological Reviews 90:859-904.

210. Donaldson GP, Lee SM, Mazmanian SK. 2015. Gut biogeography of the bacterial microbiota. Nature Reviews Microbiology 14:20.
211. Hayashi H, Takahashi R, Nishi T, Sakamoto M, Benno Y. 2005. Molecular analysis of jejunal, ileal, caecal and recto-sigmoidal human colonic microbiota using 16S rRNA gene libraries and terminal restriction fragment length polymorphism. J of Medical Microbiology 54:1093-1101.
212. Wang M, Ahrné S, Jeppsson B, Molin G. 2005. Comparison of bacterial diversity along the human intestinal tract by direct cloning and sequencing of 16S rRNA genes. FEMS Microbiology Ecology 54:219-231.
213. Wang X, Heazlewood SP, Krause DO, Florin THJ. 2003. Molecular characterization of the microbial species that colonize human ileal and colonic mucosa by using 16S rDNA sequence analysis. J of Applied Microbiology 95:508-520.
214. Dey N, Soergel DA, Repo S, Brenner SE. 2013. Association of gut microbiota with post-operative clinical course in Crohn's disease. BMC Gastroenterol 13:131.
215. Barrett E, Guinane CM, Ryan CA, Dempsey EM, Murphy BP, O'Toole PW, Fitzgerald GF, Cotter PD, Ross RP, Stanton C. 2013. Microbiota diversity and stability of the preterm neonatal ileum and colon of two infants. MicrobiologyOpen 2:215-225.
216. Di Pilato V, Freschi G, Ringressi MN, Pallecchi L, Rossolini GM, Bechi P. 2016. The esophageal microbiota in health and disease. Annals of the New York Academy of Sciences 1381:21-33.
217. Verma D, Garg PK, Dubey AK. 2018. Insights into the human oral microbiome. Archives of Microbiology 200:525-540.
218. Booijink CCGM, El-Aidy S, Rajilić-Stojanović M, Heilig HGHJ, Troost FJ, Smidt H, Kleerebezem M, Vos WMD, Zoetendal EG. 2010. High temporal and inter-individual variation detected in the human ileal microbiota. Environ Microbiol 12:3213-3227.
219. den Bogert Bv, Erkus O, Boekhorst J, Goffau Md, Smid EJ, Zoetendal EG, Kleerebezem M. 2013. Diversity of human small intestinal *Streptococcus* and *Veillonella* populations. FEMS Microbiology Ecology 85:376-388.
220. Angelakis E, Armougom F, Carrière F, Bachar D, Laugier R, Lagier J-C, Robert C, Michelle C, Henrissat B, Raoult D. 2015. A metagenomic investigation of the duodenal microbiota reveals links with obesity. PLOS ONE 10:e0137784.
221. Zoetendal EG, Raes J, van den Bogert B, Arumugam M, Booijink CCGM, Troost FJ, Bork P, Wels M, de Vos WM, Kleerebezem M. 2012. The human small intestinal microbiota is driven by rapid uptake and conversion of simple carbohydrates. ISME J 6:1415.
222. Hauso Ø, Martinsen TC, Waldum H. 2015. 5-Aminosalicylic acid, a specific drug for ulcerative colitis. Scandinavian Journal of Gastroenterology 50:933-941.
223. Dahl J-U, Gray MJ, Bazopoulou D, Beaufay F, Lempart J, Koenigsknecht MJ, Wang Y, Baker JR, Hasler WL, Young VB, Sun D, Jakob U. 2017. The anti-inflammatory drug mesalamine targets bacterial polyphosphate accumulation. Nat Microbiol 2:16267.
224. Silva AR, Gomes JC, Salvador AF, Martins G, Alves MM, Pereira L. 2020. Ciprofloxacin, diclofenac, ibuprofen and 17α-ethinylestradiol differentially affect

the activity of acetogens and methanogens in anaerobic communities. Ecotoxicology 29:866-875.
225. Rogers MAM, Aronoff DM. 2016. The influence of non-steroidal anti-inflammatory drugs on the gut microbiome. Clinical Microbiology and Infection 22:178.e1-178.e9.
226. Liu S, Chen D, Wang Z, Zhang M, Zhu M, Yin M, Zhang T, Wang X. 2022. Shifts of bacterial community and molecular ecological network in activated sludge system under ibuprofen stress. Chemosphere 295:133888.
227. Zhu M, Zhang M, Yuan Y, Zhang P, Du S, Ya T, Chen D, Wang X, Zhang T. 2021. Responses of microbial communities and their interactions to ibuprofen in a bio-electrochemical system. J of Environmental Management 289:112473.
228. Zhou G, Li N, Rene ER, Liu Q, Dai M, Kong Q. 2019. Chemical composition of extracellular polymeric substances and evolution of microbial community in activated sludge exposed to ibuprofen. J of Environmental Management 246:267-274.
229. Yu A, Baker JR, Fioritto AF, Wang Y, Luo R, Li S, Wen B, Bly M, Tsume Y, Koenigsknecht MJ, Zhang X, Lionberger R, Amidon GL, Hasler WL, Sun D. 2017. Measurement of *in vivo* gastrointestinal release and dissolution of three locally acting mesalamine formulations in regions of the human gastrointestinal tract. Molecular Pharmaceutics 14:345-358.
230. Koenigsknecht MJ, Baker JR, Wen B, Frances A, Zhang H, Yu A, Zhao T, Tsume Y, Pai MP, Bleske BE, Zhang X, Lionberger R, Lee A, Amidon GL, Hasler WL, Sun D. 2017. *In vivo* dissolution and systemic absorption of immediate release ibuprofen in human gastrointestinal tract under fed and fasted conditions. Molecular Pharmaceutics 14:4295-4304.
231. Committee AQAIE, Petersen BT, Chennat J, Cohen J, Cotton PB, Greenwald DA, Kowalski TE, Krinsky ML, Park WG, Pike IM, Romagnuolo J, Society for Healthcare Epidemiology of A, Rutala WA. 2011. Multisociety guideline on reprocessing flexible gastrointestinal endoscopes: 2011. Gastrointest Endosc 73:1075-84.
232. Seekatz AM, Theriot CM, Molloy CT, Wozniak KL, Bergin IL, Young VB. 2015. Fecal microbiota transplantation eliminates *Clostridium difficile* in a murine model of relapsing disease. Infect Immun 83:3838-46.
233. Kozich JJ, Westcott SL, Baxter NT, Highlander SK, Schloss PD. 2013. Development of a dual-index sequencing strategy and curation pipeline for analyzing amplicon sequence data on the MiSeq Illumina sequencing platform. Appl Environ Microbiol 79.
234. Schloss PD, Westcott SL, Ryabin T, Hall JR, Hartmann M, Hollister EB, Lesniewski RA, Oakley BB, Parks DH, Robinson CJ, Sahl JW, Stres B, Thallinger GG, Van Horn DJ, Weber CF. 2009. Introducing mothur: Open-source, platform-independent, community-supported software for describing and comparing microbial communities. Appl Environ Microbiol 75:7537-41.
235. Pruesse E, Quast C, Knittel K, Fuchs BM, Ludwig W, Peplies J, Glockner FO. 2007. SILVA: a comprehensive online resource for quality checked and aligned ribosomal RNA sequence data compatible with ARB. Nucleic Acids Res 35:7188-96.

236. Edgar RC, Haas BJ, Clemente JC, Quince C, Knight R. 2011. UCHIME improves sensitivity and speed of chimera detection. Bioinformatics 27:2194-200.
237. Westcott SL, Schloss PD. 2017. OptiClust, an improved method for assigning amplicon-based sequence data to operational taxonomic units. mSphere 2.
238. Cole JR, Wang Q, Cardenas E, Fish J, Chai B, Farris RJ, Kulam-Syed-Mohideen AS, McGarrell DM, Marsh T, Garrity GM, Tiedje JM. 2009. The ribosomal database project: Improved alignments and new tools for rRNA analysis. Nucleic Acids Res 37:D141-5.
239. Yue JC, Clayton MK. 2005. A similarity measure based on species proportions. Communications in Statistics - Theory and Methods 34:2123-2131.
240. Wickham H. 2016. ggplot2: Elegant graphics for data analysis. Springer-Verlag, New York.
241. Wickham H, Averick M, Bryan J, Chang W, McGowan LDA, François R, Grolemund G, Hayes A, Henry L, Hester J, Kuhn M, Pedersen TL, Miller E, Bache SM, Müller K, Ooms J, Robinson D, Seidel DP, Spinu V, Takahashi K, Vaughan D, Wilke C, Woo K, Yutani H. 2019. Welcome to the Tidyverse. J of Open Source Software 4.
242. Team RC. 2013. R: A language and environment for statistical computing. R Foundation for Statistical Computing.
243. Wickham H. 2011. The split-apply-combine strategy for data analysis. J of Statistical Software 40:1 - 29.
244. Gu Z, Gu L, Eils R, Schlesner M, Brors B. 2014. circlize implements and enhances circular visualization in R. Bioinformatics 30:2811-2.
245. Moritz S. 2017. imputeTS: Time series missing value imputation in R. The R Journal 9:207-2018.
246. Bates D, Mächler M, Bolker B, Walker S. 2015. Fitting linear mixed-effects models using lme4. J of Statistical Software 1.
247. Kuznetsova A, Brockhoff PB, Christensen RHB. 2017. lmerTest package: Tests in linear mixed effects models. J of Statistical Software 1.
248. Xia Y, Sun J. 2017. Hypothesis testing and statistical analysis of microbiome. Genes & Diseases 4:138-148.
249. Gajer P, Brotman RM, Bai G, Sakamoto J, Schutte UM, Zhong X, Koenig SS, Fu L, Ma ZS, Zhou X, Abdo Z, Forney LJ, Ravel J. 2012. Temporal dynamics of the human vaginal microbiota. Sci Transl Med 4:132ra52.
250. Mehta SD, Donovan B, Weber KM, Cohen M, Ravel J, Gajer P, Gilbert D, Burgad D, Spear GT. 2015. The vaginal microbiota over an 8- to 10-year period in a cohort of HIV-infected and HIV-uninfected women. PLOS ONE 10:e0116894.
251. Heimesaat MM, Boelke S, Fischer A, Haag L-M, Loddenkemper C, Kühl AA, Göbel UB, Bereswill S. 2012. Comprehensive postmortem analyses of intestinal microbiota changes and bacterial translocation in human flora associated mice. PLOS ONE 7:e40758.
252. DeBruyn JM, Hauther KA. 2017. Postmortem succession of gut microbial communities in deceased human subjects. PeerJ 5:e3437.
253. Fukuyama J, Rumker L, Sankaran K, Jeganathan P, Dethlefsen L, Relman DA, Holmes SP. 2017. Multidomain analyses of a longitudinal human microbiome

intestinal cleanout perturbation experiment. PLOS Computational Biology 13:e1005706.
254. Young VB, Raffals LH, Huse SM, Vital M, Dai D, Schloss PD, Brulc JM, Antonopoulos DA, Arrieta RL, Kwon JH, Reddy KG, Hubert NA, Grim SL, Vineis JH, Dalal S, Morrison HG, Eren AM, Meyer F, Schmidt TM, Tiedje JM, Chang EB, Sogin ML. 2013. Multiphasic analysis of the temporal development of the distal gut microbiota in patients following ileal pouch anal anastomosis. Microbiome 1:9.
255. Muller-Lissner SA, Fimmel CJ, Will N, Muller-Duysing W, Heinzel F, Blum AL. 1982. Effect of gastric and transpyloric tubes on gastric emptying and duodenogastric reflux. Gastroenterology 83:1276.
256. Onishi JC, Campbell S, Moreau M, Patel F, Brooks AI, Zhou YX, Häggblom MM, Storch J. 2017. Bacterial communities in the small intestine respond differently to those in the caecum and colon in mice fed low- and high-fat diets. Microbiology 163:1189-1197.
257. Hartman AL, Lough DM, Barupal DK, Fiehn O, Fishbein T, Zasloff M, Eisen JA. 2009. Human gut microbiome adopts an alternative state following small bowel transplantation. Proc Natl Acad Sci USA 106:17187-17192.
258. Caporaso JG, Lauber CL, Costello EK, Berg-Lyons D, Gonzalez A, Stombaugh J, Knights D, Gajer P, Ravel J, Fierer N, Gordon JI, Knight R. 2011. Moving pictures of the human microbiome. Genome Biology 12:R50.
259. Dethlefsen L, Relman DA. 2011. Incomplete recovery and individualized responses of the human distal gut microbiota to repeated antibiotic perturbation. Proc Natl Acad Sci USA 108:4554-4561.
260. Villmones HC, Haug ES, Ulvestad E, Grude N, Stenstad T, Halland A, Kommedal Ø. 2018. Species level description of the human ileal bacterial microbiota. Sci Rep 8:4736.
261. Hinata M, Kohyama A, Ogawa H, Haneda S, Watanabe K, Suzuki H, Shibata C, Funayama Y, Takahashi K-i, Sasaki I, Fukushima K. 2012. A shift from colon- to ileum-predominant bacteria in ileal-pouch feces following total proctocolectomy. Digestive Diseases and Sciences 57:2965-2974.
262. Maharshak N, Cohen NA, Reshef L, Tulchinsky H, Gophna U, Dotan I. 2017. Alterations of enteric microbiota in patients with a normal ileal pouch are predictive of pouchitis. J of Crohn's and Colitis 11:314-320.
263. Harris KG, Chang EB. 2018. The intestinal microbiota in the pathogenesis of inflammatory bowel diseases: new insights into complex disease. Clin Sci 132:2013-2028.
264. De Cruz P, Kang S, Wagner J, Buckley M, Sim WH, Prideaux L, Lockett T, McSweeney C, Morrison M, Kirkwood CD, Kamm MA. 2015. Association between specific mucosa-associated microbiota in Crohn's disease at the time of resection and subsequent disease recurrence: A pilot study. J Gastroenterol Hepatol 30:268-78.
265. Gevers D, Kugathasan S, Denson LA, Vazquez-Baeza Y, Van Treuren W, Ren B, Schwager E, Knights D, Song SJ, Yassour M, Morgan XC, Kostic AD, Luo C, Gonzalez A, McDonald D, Haberman Y, Walters T, Baker S, Rosh J, Stephens M, Heyman M, Markowitz J, Baldassano R, Griffiths A, Sylvester F, Mack D, Kim S,

Crandall W, Hyams J, Huttenhower C, Knight R, Xavier RJ. 2014. The treatment-naive microbiome in new-onset Crohn's disease. Cell Host Microbe 15:382-392.
266. Pancholi V, Caparon C. 2016. *Streptococcus pyogenes* Metabolism. *In* Ferretti JJ, Stevens DL, Fischetti VA (ed), *Streptococcus pyogenes*: Basic biology to clinical manifestations. University of Oklahoma Health Sciences Center, The University of Oklahoma Health Sciences Center., Oklahoma City, OK.
267. Scott KP, Gratz SW, Sheridan PO, Flint HJ, Duncan SH. 2013. The influence of diet on the gut microbiota. Pharmacological Research 69:52-60.
268. Abuhelwa AY, Williams DB, Upton RN, Foster DJR. 2017. Food, gastrointestinal pH, and models of oral drug absorption. European Journal of Pharmaceutics and Biopharmaceutics 112:234-248.
269. Lund P, Tramonti A, De Biase D. 2014. Coping with low pH: molecular strategies in neutralophilic bacteria. FEMS Microbiology Reviews 38:1091-1125.
270. Bradshaw D, Marsh PD. 1998. Analysis of pH–driven disruption of oral microbial communities *in vitro*. Caries Research 32:456-462.
271. Wright EK, Kamm MA, Teo SM, Inouye M, Wagner J, Kirkwood CD. 2015. Recent advances in characterizing the gastrointestinal microbiome in Crohn's disease: A systematic review. Inflammatory Bowel Diseases 21:1219-1228.
272. Lim WC, Wang Y, MacDonald JK, Hanauer S. 2016. Aminosalicylates for induction of remission or response in Crohn's disease. Cochrane Database Syst Rev 7:Cd008870.
273. Allocca M, Landi R, Bonovas S, Fiorino G, Papa A, Spinelli A, Furfaro F, Peyrin-Biroulet L, Armuzzi A, Danese S. 2017. Effectiveness of mesalazine, thiopurines and tumour necrosis factor antagonists in preventing post-operative Crohn's disease recurrence in a real-life setting. Digestion 96:166-172.
274. Hanauer SB, Korelitz BI, Rutgeerts P, Peppercorn MA, Thisted RA, Cohen RD, Present DH. 2004. Postoperative maintenance of Crohn’s disease remission with 6-mercaptopurine, mesalamine, or placebo: A 2-year trial. Gastroenterology 127:723-729.
275. Singh S, Nguyen GC. 2017. Management of Crohn's disease after surgical resection. Gastroenterology Clinics of North America 46:563-575.
276. Tian Y, Gui W, Koo I, Smith PB, Allman EL, Nichols RG, Rimal B, Cai J, Liu Q, Patterson AD. 2020. The microbiome modulating activity of bile acids. Gut Microbes 11:979-996.
277. Floch MH, Binder HJ, Filburn B, Gershengoren W. 1972. The effect of bile acids on intestinal microflora. The American Journal of Clinical Nutrition 25:1418-1426.
278. Islam KBMS, Fukiya S, Hagio M, Fujii N, Ishizuka S, Ooka T, Ogura Y, Hayashi T, Yokota A. 2011. Bile acid is a host factor that regulates the composition of the cecal microbiota in rats. Gastroenterology 141:1773-1781.
279. Turnbaugh PJ, Ridaura VK, Faith JJ, Rey FE, Knight R, Gordon JI. 2009. The effect of diet on the human gut microbiome: A metagenomic analysis in humanized gnotobiotic mice. Science Translational Medicine 1:6ra14-6ra14.
280. Kakiyama G, Pandak WM, Gillevet PM, Hylemon PB, Heuman DM, Daita K, Takei H, Muto A, Nittono H, Ridlon JM, White MB, Noble NA, Monteith P, Fuchs M, Thacker LR, Sikaroodi M, Bajaj JS. 2013. Modulation of the fecal bile acid profile by gut microbiota in cirrhosis. J of Hepatology 58:949-955.

281. Duboc H, Nguyen CC, Cavin JB, Ribeiro-Parenti L, Jarry AC, Rainteau D, Humbert L, Coffin B, Le Gall M, Bado A, Sokol H. 2019. Roux-en-Y gastric-bypass and sleeve gastrectomy induces specific shifts of the gut microbiota without altering the metabolism of bile acids in the intestinal lumen. Int J Obes (Lond) 43:428-431.
282. Marion S, Desharnais L, Studer N, Dong Y, Notter MD, Poudel S, Menin L, Janowczyk A, Hettich RL, Hapfelmeier S, Bernier-Latmani R. 2020. Biogeography of microbial bile acid transformations along the murine gut. J of Lipid Research 61:1450-1463.
283. Tannock GW, Tangerman A, Van Schaik A, McConnell MA. 1994. Deconjugation of bile acids by lactobacilli in the mouse small bowel. Appl Environ Microbiol 60:3419-20.
284. Bogatyrev SR, Rolando JC, Ismagilov RF. 2020. Self-reinoculation with fecal flora changes microbiota density and composition leading to an altered bile-acid profile in the mouse small intestine. Microbiome 8:19.
285. Theisen J, Nehra D, Citron D, Johansson J, Hagen JA, Crookes PF, DeMeester SR, Bremner CG, DeMeester TR, Peters JH. 2000. Suppression of gastric acid secretion in patients with gastroesophageal reflux disease results in gastric bacterial overgrowth and deconjugation of bile acids. J Gastrointest Surg 4:50-4.
286. Shindo K, Machida M, Koide K, Fukumura M, Yamazaki R. 1998. Deconjugation ability of bacteria isolated from the jejunal fluid of patients with progressive systemic sclerosis and its gastric pH. Hepatogastroenterology 45:1643-50.
287. Chinda D, Takada T, Mikami T, Shimizu K, Oana K, Arai T, Akitaya K, Sakuraba H, Katto M, Nagara Y, Makino H, Fujii D, Oishi K, Fukuda S. 2022. Spatial distribution of live gut microbiota and bile acid metabolism in various parts of human large intestine. Sci Rep 12:3593.
288. Thomas LA, Veysey MJ, French G, Hylemon PB, Murphy GM, Dowling RH. 2001. Bile acid metabolism by fresh human colonic contents: a comparison of caecal versus faecal samples. Gut 49:835-42.
289. Koenigsknecht MJ, Theriot CM, Bergin IL, Schumacher CA, Schloss PD, Young VB. 2015. Dynamics and establishment of *Clostridium difficile* infection in the murine gastrointestinal tract. Infect Immun 83:934-41.
290. Smits SA, Leach J, Sonnenburg ED, Gonzalez CG, Lichtman JS, Reid G, Knight R, Manjurano A, Changalucha J, Elias JE, Dominguez-Bello MG, Sonnenburg JL. 2017. Seasonal cycling in the gut microbiome of the Hadza hunter-gatherers of Tanzania. Science 357:802-806.
291. Feng Q, Chen W-D, Wang Y-D. 2018. Gut microbiota: An integral moderator in health and disease. Frontiers in Microbiology 9.
292. Pan W-H, Sommer F, Falk-Paulsen M, Ulas T, Best P, Fazio A, Kachroo P, Luzius A, Jentzsch M, Rehman A, Müller F, Lengauer T, Walter J, Künzel S, Baines JF, Schreiber S, Franke A, Schultze JL, Bäckhed F, Rosenstiel P. 2018. Exposure to the gut microbiota drives distinct methylome and transcriptome changes in intestinal epithelial cells during postnatal development. Genome Medicine 10:27.
293. David LA, Materna AC, Friedman J, Campos-Baptista MI, Blackburn MC, Perrotta A, Erdman SE, Alm EJ. 2014. Host lifestyle affects human microbiota on daily timescales. Genome Biology 15:R89.

294. Desai MS, Seekatz AM, Koropatkin NM, Kamada N, Hickey CA, Wolter M, Pudlo NA, Kitamoto S, Terrapon N, Muller A, Young VB, Henrissat B, Wilmes P, Stappenbeck TS, Nuñez G, Martens EC. 2016. A dietary fiber-deprived gut microbiota degrades the colonic mucus barrier and enhances pathogen susceptibility. Cell 167:1339-1353.e21.
295. Jefferson A, Adolphus K. 2019. The effects of intact cereal grain fibers, including wheat bran on the gut microbiota composition of healthy adults: A systematic review. Frontiers in Nutrition 6.
296. Gong L, Cao W, Chi H, Wang J, Zhang H, Liu J, Sun B. 2018. Whole cereal grains and potential health effects: Involvement of the gut microbiota. Food Research International 103:84-102.
297. Baxter NT, Schmidt AW, Venkataraman A, Kim KS, Waldron C, Schmidt TM. 2019. Dynamics of human gut microbiota and short-chain fatty acids in response to dietary interventions with three fermentable fibers. mBio 10:e02566-18.
298. Venkataraman A, Sieber JR, Schmidt AW, Waldron C, Theis KR, Schmidt TM, Tremaroli V, Backhed F, Flint HJ, Duncan SH, Scott KP, Louis P, Hartstra AV, Bouter KE, Backhed F, Nieuwdorp M, Buffie CG, Bucci V, Stein RR, McKenney PT, Ling L, Gobourne A, Donohoe DR, Garge N, Zhang X, Sun W, O'Connell TM, Bunger MK, Peng L, Li ZR, Green RS, Holzman IR, Lin J, Furusawa Y, Obata Y, Fukuda S, Endo TA, Nakato G, Takahashi D, Ruemmele FM, Schwartz S, Seidman EG, Dionne S, Levy E, Lentze MJ, Mikkelsen KH, Allin KH, Knop FK, Mathewson ND, Jenq R, et al. 2016. Variable responses of human microbiomes to dietary supplementation with resistant starch. Microbiome 4:33-33.
299. Koh A, De Vadder F, Kovatcheva-Datchary P, Backhed F. 2016. From dietary fiber to host pysiology: Short-chain fatty acids as key bacterial metabolites. Cell 165:1332-1345.
300. Warren FJ, Fukuma NM, Mikkelsen D, Flanagan BM, Williams BA, Lisle AT, P OC, Morrison M, Gidley MJ. 2018. Food starch structure impacts gut microbiome composition. mSphere 3.
301. Park CH, Eun CS, Han DS. 2018. Intestinal microbiota, chronic inflammation, and colorectal cancer. Intest Res 16:338-345.
302. Bedford A, Gong J. 2018. Implications of butyrate and its derivatives for gut health and animal production. Animal Nutrition 4:151-159.
303. Bach Knudsen KE, Lærke HN, Hedemann MS, Nielsen TS, Ingerslev AK, Gundelund Nielsen DS, Theil PK, Purup S, Hald S, Schioldan AG, Marco ML, Gregersen S, Hermansen K. 2018. Impact of diet-modulated butyrate production on intestinal barrier function and inflammation. Nutrients 10:1499.
304. Sworn G. 2009. 8 - Xanthan gum, p 186-203. *In* Phillips GO, Williams PA (ed), Handbook of Hydrocolloids (Second Edition) doi:10.1533/9781845695873.186. Woodhead Publishing.
305. Montagne L, Pluske JR, Hampson DJ. 2003. A review of interactions between dietary fibre and the intestinal mucosa, and their consequences on digestive health in young non-ruminant animals. Animal Feed Science and Technology 108:95-117.

306. Jonathan MC, van den Borne JJGC, van Wiechen P, Souza da Silva C, Schols HA, Gruppen H. 2012. *In vitro* fermentation of 12 dietary fibres by faecal inoculum from pigs and humans. Food Chemistry 133:889-897.
307. Theriot CM, Koumpouras CC, Carlson PE, Bergin, II, Aronoff DM, Young VB. 2011. Cefoperazone-treated mice as an experimental platform to assess differential virulence of *Clostridium difficile* strains. Gut Microbes 2:326-34.
308. Reeves AE, Theriot CM, Bergin IL, Huffnagle GB, Schloss PD, Young VB. 2011. The interplay between microbiome dynamics and pathogen dynamics in a murine model of *Clostridium difficile* infection. Gut Microbes 2:145-58.
309. Chen X, Katchar K, Goldsmith JD, Nanthakumar N, Cheknis A, Gerding DN, Kelly CP. 2008. A mouse model of *Clostridium difficile*-associated disease. Gastroenterology 135:1984-92.
310. Nadkarni MA, Martin FE, Jacques NA, Hunter N. 2002. Determination of bacterial load by real-time PCR using a broad-range (universal) probe and primers set. Microbiology 148:257-266.
311. Segata N, Izard J, Waldron L, Gevers D, Miropolsky L, Garrett WS, Huttenhower C. 2011. Metagenomic biomarker discovery and explanation. Genome Biology 12:R60-R60.
312. Zackular JP, Skaar EP. 2018. The role of zinc and nutritional immunity in *Clostridium difficile* infection. Gut Microbes doi:10.1080/19490976.2018.1448354:00-00.
313. Jones RN, Wilson HW, Thornsberry C, Barry AL. 1985. *In vitro* antimicrobial activity of cefoperazone-sulbactam combinations against 554 clinical isolates including a review and β-lactamase studies. Diagnostic Microbiology and Infectious Disease 3:489-499.
314. Williams JD. 1997. β-Lactamase inhibition and *in vitro* activity of sulbactam and sulbactam/cefoperazone. Clinical Infectious Diseases 24:494-497.
315. Antonopoulos DA, Huse SM, Morrison HG, Schmidt TM, Sogin ML, Young VB. 2009. Reproducible community dynamics of the gastrointestinal microbiota following antibiotic perturbation. Infect Immun 77:2367-75.
316. Theriot CM, Young VB. 2015. Interactions between the gastrointestinal microbiome and *Clostridium difficile*. Annu Rev Microbiol 69:445-61.
317. Jarocki P, Targoński Z. 2013. Genetic diversity of bile salt hydrolases among human intestinal bifidobacteria. Current
Microbiology 67:286-292.
318. O'Flaherty S, Briner Crawley A, Theriot CM, Barrangou R. 2018. The *Lactobacillus* bile salt hydrolase repertoire reveals niche-specific adaptation. mSphere 3.
319. Kitahara M, Takamine F, Imamura T, Benno Y. 2001. *Clostridium hiranonis* sp. nov., a human intestinal bacterium with bile acid 7α-dehydroxylating activity. Int J Syst Evol Microbiol 51:39-44.
320. Kang DJ, Ridlon JM, Moore DR, 2nd, Barnes S, Hylemon PB. 2008. *Clostridium scindens baiCD* and *baiH* genes encode stereo-specific 7alpha/7beta-hydroxy-3-oxo-delta4-cholenoic acid oxidoreductases. Biochim Biophys Acta 1781:16-25.
321. Weingarden AR, Chen C, Bobr A, Yao D, Lu Y, Nelson VM, Sadowsky MJ, Khoruts A. 2014. Microbiota transplantation restores normal fecal bile acid composition in

recurrent *Clostridium difficile* infection. Am J Physiol Gastrointest Liver Physiol 306:G310-9.
322. Wilson KH, Perini F. 1988. Role of competition for nutrients in suppression of *Clostridium difficile* by the colonic microflora. Infect Immun 56:2610-4.
323. Reeves AE, Koenigsknecht MJ, Bergin IL, Young VB. 2012. Suppression of *Clostridium difficile* in the gastrointestinal tracts of germfree mice inoculated with a murine isolate from the family Lachnospiraceae. Infect Immun 80:3786-94.
324. Vincent C, Stephens DA, Loo VG, Edens TJ, Behr MA, Dewar K, Manges AR. 2013. Reductions in intestinal Clostridiales precede the development of nosocomial *Clostridium difficile* infection. Microbiome 1:18.
325. Moundras C, Behr SR, Rémésy C, Demigné C. 1997. Fecal losses of sterols and bile acids induced by feeding rats guar gum are due to greater pool size and liver bile acid secretion. The J of Nutrition 127:1068-1076.
326. Demigné C, Rémésy C, Levrat-Verny M-A, Behr S, Mustad V. 2000. Low levels of viscous hydrocolloids lower plasma cholesterol in rats primarily by impairing cholesterol absorption. The J of Nutrition 130:243-248.
327. Cox LM, Cho I, Young SA, Anderson WHK, Waters BJ, Hung S-C, Gao Z, Mahana D, Bihan M, Alekseyenko AV, Methé BA, Blaser MJ. 2013. The nonfermentable dietary fiber hydroxypropyl methylcellulose modulates intestinal microbiota. The FASEB Journal 27:692-702.
328. Hoving LR, Katiraei S, Heijink M, Pronk A, van der Wee-Pals L, Streefland T, Giera M, van Dijk KW, van Harmelen V. 2018. Dietary mannan oligosaccharides modulate gut microbiota, increase fecal bile acid excretion, and decrease plasma cholesterol and atherosclerosis development. Mol Nutr Food Res doi:10.1002/mnfr.201700942:e1700942.
329. Neyrinck AM, Van Hée VF, Piront N, De Backer F, Toussaint O, Cani PD, Delzenne NM. 2012. Wheat-derived arabinoxylan oligosaccharides with prebiotic effect increase satietogenic gut peptides and reduce metabolic endotoxemia in diet-induced obese mice. Nutrition and Diabetes 2:e28.
330. Neyrinck AM, Possemiers S, Verstraete W, De Backer F, Cani PD, Delzenne NM. 2012. Dietary modulation of clostridial cluster XIVa gut bacteria (*Roseburia* spp.) by chitin–glucan fiber improves host metabolic alterations induced by high-fat diet in mice. The J of Nutritional Biochemistry 23:51-59.
331. Suriano F, Bindels LB, Verspreet J, Courtin CM, Verbeke K, Cani PD, Neyrinck AM, Delzenne NM. 2017. Fat binding capacity and modulation of the gut microbiota both determine the effect of wheat bran fractions on adiposity. Sci Rep 7:5621.
332. Talukdar MM, Michoel A, Rombaut P, Kinget R. 1996. Comparative study on xanthan gum and hydroxypropylmethyl cellulose as matrices for controlled-release drug delivery I. Compaction and in vitro drug release behaviour. Int J of Pharmaceutics 129:233-241.
333. Dhopeshwarkar V, Zatz JL. 1993. Evaluation of xanthan gum in the preparation of sustained release matrix tablets. Drug Development and Industrial Pharmacy 19:999-1017.
334. Jackson C, Ofoefule S. 2011. Use of xanthan gum and ethylcellulose in formulation of metronidazole for colon delivery. J Chem Pharm Res 3:11-20.

335. Andreopoulos AG, Tarantili PA. 2001. Xanthan gum as a carrier for controlled release of drugs. J of Biomaterials Applications 16:34-46.
336. Chilton CH, Crowther GS, Baines SD, Todhunter SL, Freeman J, Locher HH, Athanasiou A, Wilcox MH. 2014. *In vitro* activity of cadazolid against clinically relevant *Clostridium difficile* isolates and in an in vitro gut model of *C. difficile* infection. J Antimicrob Chemother 69:697-705.
337. Davies M, Galazzo G, van Hattem JM, Arcilla MS, Melles DC, de Jong MD, Schultsz C, Wolffs P, McNally A, Schaik WV, Penders J. 2022. Enterobacteriaceae and Bacteroidaceae provide resistance to travel-associated intestinal colonization by multi-drug resistant *Escherichia coli*. Gut Microbes 14:2060676.
338. Li Q, Chen S, Zhu K, Huang X, Huang Y, Shen Z, Ding S, Gu D, Yang Q, Sun H, Hu F, Wang H, Cai J, Ma B, Zhang R, Shen J. 2022. Collateral sensitivity to pleuromutilins in vancomycin-resistant *Enterococcus faecium*. Nat Commun 13:1888.
339. Pérez Escriva P, Fuhrer T, Sauer U. 2022. Distinct N and C cross-feeding networks in a synthetic mouse gut consortium. mSystems doi:10.1128/msystems.01484-21:e0148421.
340. Reed AD, Fletcher JR, Huang YY, Thanissery R, Rivera AJ, Parsons RJ, Stewart AK, Kountz DJ, Shen A, Balskus EP, Theriot CM. 2022. The stickland reaction precursor *trans*-4-hydroxy-l-proline differentially impacts the metabolism of *Clostridioides difficile* and commensal clostridia. mSphere doi:10.1128/msphere.00926-21:e0092621.
341. Rajan A, Robertson MJ, Carter HE, Poole NM, Clark JR, Green SI, Criss ZK, Zhao B, Karandikar U, Xing Y, Margalef-Català M, Jain N, Wilson RL, Bai F, Hyser JM, Petrosino J, Shroyer NF, Blutt SE, Coarfa C, Song X, Prasad BV, Amieva MR, Grande-Allen J, Estes MK, Okhuysen PC, Maresso AW. 2020. Enteroaggregative E. coli Adherence to Human Heparan Sulfate Proteoglycans Drives Segment and Host Specific Responses to Infection. PLOS Pathogens 16:e1008851.
342. Engevik MA, Danhof HA, Shrestha R, Chang-Graham AL, Hyser JM, Haag AM, Mohammad MA, Britton RA, Versalovic J, Sorg JA, Spinler JK. 2020. Reuterin disrupts *Clostridioides difficile* metabolism and pathogenicity through reactive oxygen species generation. Gut Microbes 12:1788898.
343. Gonyar LA, Smith RM, Giron JA, Zachos NC, Ruiz-Perez F, Nataro JP. 2020. Aggregative adherence fimbriae II of enteroaggregative *Escherichia coli* are required for adherence and barrier disruption during infection of human colonoids. Infect Immun 88.
344. Auchtung JM, Robinson CD, Farrell K, Britton RA. 2016. MiniBioReactor Arrays (MBRAs) as a tool for studying *C. difficile* physiology in the presence of a complex community. Methods Mol Biol 1476:235-58.
345. Freeman J, O'Neill FJ, Wilcox MH. 2003. Effects of cefotaxime and desacetylcefotaxime upon *Clostridium difficile* proliferation and toxin production in a triple-stage chemostat model of the human gut. J Antimicrob Chemother 52.
346. Freeman J, Baines SD, Jabes D, Wilcox MH. 2005. Comparison of the efficacy of ramoplanin and vancomycin in both *in vitro* and *in vivo* models of clindamycin-induced *Clostridium difficile* infection. J Antimicrob Chemother 56:717-25.

347. Baines SD, Freeman J, Wilcox MH. 2005. Effects of piperacillin/tazobactam on *Clostridium difficile* growth and toxin production in a human gut model. J Antimicrob Chemother 55:974-82.
348. Abbas A, Zackular JP. 2020. Microbe–microbe interactions during *Clostridioides difficile* infection. Current Opinion in Microbiology 53:19-25.
349. Ward P, P. Young G. 1997. Dynamics of *Clostridium difficile* infection: Control using diet, vol 412.
350. Auchtung JM, Robinson CD, Britton RA. 2015. Cultivation of stable, reproducible microbial communities from different fecal donors using minibioreactor arrays (MBRAs). Microbiome 3:42.
351. Auchtung JM, Preisner EC, Collins J, Lerma AI, Britton RA, Young VB. 2020. Identification of simplified microbial communities that inhibit *Clostridioides difficile* infection through dilution/extinction. mSphere 5:e00387-20.
352. Holmes I, Harris K, Quince C. 2012. Dirichlet multinomial mixtures: Generative models for microbial metagenomics. PLOS ONE 7:e30126.
353. Wickham H. 2007. Reshaping data with the reshape package. J of Statistical Software 21:1 - 20.
354. Gu Z, Eils R, Schlesner M. 2016. Complex heatmaps reveal patterns and correlations in multidimensional genomic data. Bioinformatics 32:2847-9.
355. Yang J, Martínez I, Walter J, Keshavarzian A, Rose DJ. 2013. *In vitro* characterization of the impact of selected dietary fibers on fecal microbiota composition and short chain fatty acid production. Anaerobe 23:74-81.
356. Van den Abbeele P, Venema K, Van de Wiele T, Verstraete W, Possemiers S. 2013. Different human gut models reveal the distinct fermentation patterns of arabinoxylan versus inulin. J Agric Food Chem 61:9819-27.
357. Valcheva R, Koleva P, Martínez I, Walter J, Gänzle MG, Dieleman LA. 2019. Inulin-type fructans improve active ulcerative colitis associated with microbiota changes and increased short-chain fatty acids levels. Gut Microbes 10:334-357.
358. Qian JJ, Akçay E. 2020. The balance of interaction types determines the assembly and stability of ecological communities. Nat Ecol Evol 4:356-365.
359. Song C, Uricchio LH, Mordecai EA, Saavedra S. 2021. Understanding the emergence of contingent and deterministic exclusion in multispecies communities. Ecol Lett 24:2155-2168.
360. Morris JR, Allhoff KT, Valdovinos FS. 2021. Strange invaders increase disturbance and promote generalists in an evolving food web. Sci Rep 11:21274.
361. Pereira FC, Berry D. 2017. Microbial nutrient niches in the gut. Environ Microbiol 19:1366-1378.
362. Bono LM, Draghi JA, Turner PE. 2020. Evolvability costs of niche expansion. Trends Genet 36:14-23.
363. Baquero F, Coque TM, Galán JC, Martinez JL. 2021. The origin of niches and species in the bacterial world. Frontiers in Microbiology 12.
364. Vila JCC, Jones ML, Patel M, Bell T, Rosindell J. 2019. Uncovering the rules of microbial community invasions. Nature Ecology & Evolution 3:1162-1171.
365. Badali M, Zilman A. 2020. Effects of niche overlap on coexistence, fixation and invasion in a population of two interacting species. R Soc Open Sci 7:192181.

366. Herren CM. 2020. Disruption of cross-feeding interactions by invading taxa can cause invasional meltdown in microbial communities. Proc Biol Sci 287:20192945.
367. Bascompte J, Stouffer DB. 2009. The assembly and disassembly of ecological networks. Philosophical Transactions of the Royal Society B: Biological Sciences 364:1781-1787.
368. Brown SP, Cornforth DM, Mideo N. 2012. Evolution of virulence in opportunistic pathogens: generalism, plasticity, and control. Trends Microbiol 20:336-342.
369. Sheppard SK. 2022. Strain wars and the evolution of opportunistic pathogens. Current Opinion in Microbiology 67:102138.
370. Waters JM, Fraser CI, Hewitt GM. 2013. Founder takes all: Density-dependent processes structure biodiversity. Trends in Ecology & Evolution 28:78-85.
371. Dethlefsen L, Relman DA. 2011. Incomplete recovery and individualized responses of the human distal gut microbiota to repeated antibiotic perturbation. Proc Natl Acad Sci USA 108 Suppl 1:4554-61.
372. Korpela K, Salonen A, Virta LJ, Kekkonen RA, Forslund K, Bork P, de Vos WM. 2016. Intestinal microbiome is related to lifetime antibiotic use in Finnish pre-school children. Nat Commun 7:10410.
373. Dethlefsen L, Huse S, Sogin ML, Relman DA. 2008. The pervasive effects of an antibiotic on the human gut microbiota, as revealed by deep 16S rRNA sequencing. PLOS Biology 6:e280.
374. Jernberg C, Löfmark S, Edlund C, Jansson JK. 2007. Long-term ecological impacts of antibiotic administration on the human intestinal microbiota. ISME J 1:56-66.
375. Gregory AL, Pensinger DA, Hryckowian AJ. 2021. A short chain fatty acid-centric view of *Clostridioides difficile* pathogenesis. PLOS Pathogens 17:e1009959.
376. Cherrington CA, Hinton M, Mead GC, Chopra I. 1991. Organic acids: Chemistry, antibacterial activity and practical applications, p 87-108. *In* Rose AH, Tempest DW (ed), Advances in Microbial Physiology, vol 32. Academic Press.
377. Mullany P, Clayton CL, Pallen MJ, Slone R, al-Saleh A, Tabaqchali S. 1994. Genes encoding homologues of three consecutive enzymes in the butyrate/butanol-producing pathway of *Clostridium acetobutylicum* are clustered on the *Clostridium difficile* chromosome. FEMS Microbiol Letters 124:61-7.
378. Aboulnaga el H, Pinkenburg O, Schiffels J, El-Refai A, Buckel W, Selmer T. 2013. Effect of an oxygen-tolerant bifurcating butyryl coenzyme A dehydrogenase/electron-transferring flavoprotein complex from *Clostridium difficile* on butyrate production in *Escherichia coli*. J Bacteriol 195:3704-13.
379. Karasawa T, Ikoma S, Yamakawa K, Nakamura S. 1995. A defined growth medium for *Clostridium difficile*. Microbiology 141:371-375.
380. Kirkpatrick C, Maurer LM, Oyelakin NE, Yoncheva YN, Maurer R, Slonczewski JL. 2001. Acetate and formate stress: Opposite responses in the proteome of *Escherichia coli*. J of Bacteriology 183:6466-6477.
381. Chen M, Fan HN, Chen XY, Yi YC, Zhang J, Zhu JS. 2022. Alterations in the saliva microbiome in patients with gastritis and small bowel inflammation. Microb Pathog 165:105491.

382. Villmones HC, Svanevik M, Ulvestad E, Stenstad T, Anthonisen IL, Nygaard RM, Dyrhovden R, Kommedal Ø. 2022. Investigating the human jejunal microbiota. Sci Rep 12:1682.
383. Tidjani Alou M, Naud S, Khelaifia S, Bonnet M, Lagier JC, Raoult D. 2020. State of the art in the culture of the human microbiota: New interests and strategies. Clin Microbiol Rev 34.
384. Bellali S, Lagier JC, Million M, Anani H, Haddad G, Francis R, Kuete Yimagou E, Khelaifia S, Levasseur A, Raoult D, Bou Khalil J. 2021. Running after ghosts: Are dead bacteria the dark matter of the human gut microbiota? Gut Microbes 13:1-12.
385. Howerton A, Seymour CO, Murugapiran SK, Liao Z, Phan JR, Estrada A, Wagner AJ, Mefferd CC, Hedlund BP, Abel-Santos E. 2018. Effect of the synthetic bile salt analog CamSA on the hamster model of *Clostridium difficile* infection. Antimicrob Agents Chemother 62.
386. Howerton A, Patra M, Abel-Santos E. 2013. A new strategy for the prevention of *Clostridium difficile* infection. J Infect Dis 207:1498-504.
387. Phan JR, Do DM, Truong MC, Ngo C, Phan JH, Sharma SK, Schilke A, Mefferd CC, Villarama JV, Lai D, Consul A, Hedlund BP, Firestine SM, Abel-Santos E. 2022. An aniline-substituted bile salt analog protects both mice and hamsters from multiple *Clostridioides difficile* strains. Antimicrob Agents Chemother 66:e0143521.
388. Wu S, Bhat ZF, Gounder RS, Mohamed Ahmed IA, Al-Juhaimi FY, Ding Y, Bekhit AEA. 2022. Effect of dietary protein and processing on gut microbiota-A systematic review. Nutrients 14.
389. Tawfick MM, Xie H, Zhao C, Shao P, Farag MA. 2022. Inulin fructans in diet: Role in gut homeostasis, immunity, health outcomes and potential therapeutics. Int J Biol Macromol doi:10.1016/j.ijbiomac.2022.03.218.
390. Sun CY, Zheng ZL, Chen CW, Lu BW, Liu D. 2022. Targeting gut microbiota with natural polysaccharides: Effective interventions against high-fat diet-induced metabolic diseases. Front Microbiol 13:859206.
391. Druart C, Alligier M, Salazar N, Neyrinck AM, Delzenne NM. 2014. Modulation of the gut microbiota by nutrients with prebiotic and probiotic properties. Adv Nutr 5:624s-633s.
392. Ostrowski MP, La Rosa SL, Kunath BJ, Robertson A, Pereira G, Hagen LH, Varghese NJ, Qiu L, Yao T, Flint G, Li J, McDonald SP, Buttner D, Pudlo NA, Schnizlein MK, Young VB, Brumer H, Schmidt TM, Terrapon N, Lombard V, Henrissat B, Hamaker B, Eloe-Fadrosh EA, Tripathi A, Pope PB, Martens EC. 2022. Mechanistic insights into consumption of the food additive xanthan gum by the human gut microbiota. Nat Microbiol 7:556-569.
393. Shade A. 2017. Diversity is the question, not the answer. ISME J 11:1-6.